AD-A259 742

REPORT DOCUMENTATION PAGE

Form Approved
OMB No. 0704-0188

2. REPORT DATE	3. REPORT TYPE AND DATES COVERED
11/30/1992	~~INTERIM~~ Annual 11/1/1991 to 10/31/1992

4. TITLE AND SUBTITLE
Sensory sensitivities and discriminations and their roles in aviation.

5. FUNDING NUMBERS
Project 61102F
2313/AS
2313/CS

(2)

6. AUTHOR(S)
D. Regan

7. PERFORMING ORGANIZATION NAME(S) AND ADDRESS(ES)
York University (Mrs. N. Swatman)
Room 5415, Ross Building
4700 Keele Street
North York, Ontario, Canada M3J 1P3

AFOSR-TR

8. PERFORMING ORGANIZATION REPORT NUMBER
92 0097

9. SPONSORING/MONITORING AGENCY NAME(S) AND ADDRESS(ES)
AFOSR/NL
Life Sciences Directorate
Bolling AFB, DC 20332, U.S.A.

10. SPONSORING/MONITORING AGENCY REPORT NUMBER
AFOSR-91-0080

11. SUPPLEMENTARY NOTES

DTIC
ELECTE
JAN 27 1993
S B D

12a. DISTRIBUTION/AVAILABILITY STATEMENT
Approved for Public Release
Distribution Unlimited

136
PP

12b. DISTRIBUTION CODE

BEST AVAILABLE COPY

13. ABSTRACT *(Maximum 200 words)*

(1) Evidence that intersubject differences in the ability to process motion-defined (MD) shape are not predicted by the ability to process luminance-defined (LD) shape, that motion is processed by hierarchical manner, that discrimination and detection can be dissociated for MD form, and that spatial discrimination for MD and LD form are not entirely mediated by the same mechanism is as follows. (A) Reducing presentation duration or dot lifetime from 1.0 to 0.1 sec progressively reduced the visibility of a MD bar, but did not reduce orientation discrimination for the bar when visibility was held constant. (B) Detection and/or recognition of MD letters can be degraded by removal of brain tissue underlying prestriate cortex without affecting contrast sensitivity, Snellen acuity, low contrast acuity or sensitivity to motion. (2) Shape discrimination for an MD rectangle can be as low as 2-3%—as good as for an LD rectangle. (3) Evidence for a neural mechanism sensitive to shape independently of size. (4) Evidence for a neural mechanism directly sensitive to time to collision with an approaching object. A method for measuring intersubject differences in discrimination of time to contact. (5) A titration method for uncovering the color-defined form system. (6) The 40 Hz human brain response indexes magnocellular activity. (7) By recording the magnetic field of the brain we have identified an audio-visual integration area in the brain. We have also unconfounded responses to texture-defined form and color-defined form from responses to luminance-defined form. (8) We have developed a technique for measuring intersubject differences in susceptibility to glare, and are using it in a prospective study of flying safety. Also, the test quantifies visual status in cataract patients. (9) Our motion-defined letter test is now freely available, and we are using it in a prospective study of helicopter flying safety. Also, it detects damage hidden to acuity, motion and contrast sensitivity tests in patients with ocular hypertension and amblyopia and multiple sclerosis. (10)Theoretical and experimental analysis of auditory responses to AM tones.

14. SUBJECT TERMS
vision; visual flying skills; intersubject differences; visual navigation; perception of motion & self-motion; stereo; neuromagnetic recording; models of visual & auditory processing; multisensory convergence

15. NUMBER OF PAGES
135

16. PRICE CODE

17. SECURITY CLASSIFICATION OF REPORT	18. SECURITY CLASSIFICATION OF THIS PAGE	19. SECURITY CLASSIFICATION OF ABSTRACT	20. LIMITATION OF ABSTRACT
Unclassified	Unclassified	Unclassified	

Department of Psychology

UNIVERSITÉ YORK UNIVERSITY

FACULTY OF ARTS

4700 KEELE STREET • NORTH YORK • ONTARIO • CANADA • M3J 1P3

1

RESEARCH OBJECTIVES

The research objectives for three years were listed in the grant proposal as follows.

1.1 Long Term Aims

1.1.1 We will further define the roles of the channeling hypothesis in: (a) identifying specific visual processes; (b) understanding visual performance; (c) specifying visual parameters likely to be important in eye-hand coordination especially in aviation, and flight simulator visual displays.

1.1.2 We will use neuromagnetic recording techniques to: (d) identify the brain sites of different kinds of visual processing, auditory processing and multisensory integration, and relate these sites to the organization of visual, auditory and multisensory convergence areas in macaque monkey cortex; (e) relate objective data on visual and auditory processing in human brain to psychophysical models of human vision and hearing.

1.2 Specific Aims: Psychophysics

1.2.1 *Camouflage and the Visual Processing of Objects Defined by Motion Alone*

We will determine the dynamics of the visual processing that mediates spatial discriminations of camouflaged objects that are defined by motion alone. We will investigate interactions between visual processing of objects defined by relative motion, objects defined by luminance contrast and objects defined by chromatic contrast by means of cross-adaptation and cross-masking paradigms. Drawing closer to the real-world visual environment we will investigate visual detection and spatial discriminations for objects that are defined by a combination of relative motion, luminance contrast and chromatic contrast.

1.2.2 *Cyclopean Processing of Motion-in-Depth and Changing-Size*

We will generate targets that are visible in binocular view but invisible monocularly, and compare the sensitivities and dynamic characteristics of the processing of motion-in-depth generated by changing-disparity and changing-size for such cyclopean targets. By comparing these data

Department of Psychology

UNIVERSITÉ YORK UNIVERSITY

FACULTY OF ARTS

4700 KEELE STREET • NORTH YORK • ONTARIO • CANADA • M3J 1P3

with corresponding data for noncyclopean targets we will distinguish between the processing of motion-in-depth and changing-size that occurs before and after convergence of the signals from left and right eyes.

1.2.3 *Monocular Judgments of Trajectory of 3-Dimensional Motion*

We will measure the precision with which subjects can judge the trajectory of motion-in-depth monocularly, and establish quantitative norms and normal intersubject variability.

1.3 Specific Aims: Theoretical

1.3.1 *Multi-Rectifier Model with Dynamics*

We will extend our theoretical work on multi-rectifier models to include dynamics.

1.3.2 *Multi-Rectifier Models of the Auditory Pathway*

We will develop a theoretical approach to characterizing multi-neuron models whose input is the sum of two modulated tones.

1.4 Specific Aims: Experimental neuromagnetic studies

1.4.1 *Visual and Auditory Projections*

We will identify evoked activity in different visual, and auditory projections in human cortex, elucidate the differences between the type of processing occurring in the different areas, and link these data with the known functional neuroanatomy of macaque monkey brain and with human psychophysics.

1.4.2 *Multi-Sensory Areas*

We will identify the cortical sites of interactions between responses to stimuli of different modalities, and compare these sites with the known multi-sensory cortical areas in nonhuman primates.[6]

1.5 Specific Aims: Single-unit electrophysiology

Department of Psychology

UNIVERSITÉ YORK UNIVERSITY

FACULTY OF ARTS

4700 KEELE STREET • NORTH YORK • ONTARIO • CANADA • M3J 1P3

We will find whether the high stability evident in human evoked brain signals exists at the level of single cell firing or whether it is exclusively a population property. We will find whether the theoretical work described in Ref 179 can be used to test multi-stage models of neural processing that takes place between the retina and the cortical cell under investigation.

1.6 Specific Aims: Simple tests of visual function

We will determine intersubject variability among controls for our motion-defined letter test and find whether test results correlate with contrast sensitivity and Snellen acuity in controls. We will determine whether our motion-defined letter test and low contrast acuity test can provide clinically valuable information that is not provided by other tests in patients with Parkinson's disease and glaucoma.

2 STATEMENT OF WORK

The statement of work for three years was set out in the grant proposal as follows.

2.1 Psychophysics: Dynamics of orientation discrimination for MD and LD bars

Using temporal two-alternative forced choice we will measure velocity detection threshold for a perfectly camouflaged motion-defined (MD) dotted bar. This measurement will be carried out for each of 10 values of dot lifetime between 6 msec and 1000 msec, but with presentation time held constant at 1000 msec. A luminance-defined (LD) bar will be created by removing all dots outside the bar, and contrast detection threshold measured for the same 10 values of dot lifetime, presentation duration again held constant at 1000 msec. These detection threshold data will be used in measuring how orientation discrimination threshold for the MD bar depends on dot lifetime, dot velocity being adjusted at each dot lifetime so that it is a constant multiple (N) of bar detection threshold. The experiment will be repeated for different values of N. Then we will find how

Department of Psychology

UNIVERSITÉ YORK UNIVERSITY

FACULTY OF ARTS

4700 KEELE STREET • NORTH YORK • ONTARIO • CANADA • M3J 1P3

orientation discrimination for a LD bar depends on dot lifetime, dot contrast being adjusted at each dot lifetime so that it is a constant multiple (N) of bar detection threshold. This experiment will also be repeated for different values of N.

We will compare plots of orientation discrimination threshold versus dot lifetime for MD and LD bars, the visibilities of the MD and LD bars being matched at N times above their respective velocity and contrast detection thresholds, and attempt to use these data to establish the degree to which the visual processing underlying orientation discrimination for MD bars is separate from the visual processing underlying orientation discrimination for LD bars.

Then we will compare the dot lifetime data for MD and LD bars with the effect of presentation duration on orientation discrimination, dot lifetime being held equal to presentation duration. We will endeavor to relate these data to a model of orientation discrimination for MD bars in which (A) dot velocity within the bar and outside the bar is computed, then (B) the bar is detected (i.e. segregated from its surroundings) and a population of orientation-tuned neurons are excited by the bar, then (C) orientation discrimination is based on the relative activity of these orientation-tuned neurons. (Stage C follows the spirit of opponent process and line element hypotheses of orientation discrimination for contrast-defined bars or gratings [Refs 136, 145]). The first hypothesis to be tested is that, for MD bars that are a constant N times above detection threshold, excitation of stages (A) and (B) are constant, and differences in orientation discrimination is due entirely to stage (C). The second hypothesis to be tested is that the effect of dot lifetime at constant N is restricted to stages (A) and (B) and does not involve stage (C), while the effect of dot presentation time at constant N substantially involves stage (C).

2.2 Experiment 2. Psychophysics: Dynamics of shape discrimination for MD and LD rectangles

This experiment is similar to 2.1 above except that we will measure aspect ratio (i.e. shape)

Department of Psychology

UNIVERSITÉ YORK UNIVERSITY

FACULTY OF ARTS

4700 KEELE STREET • NORTH YORK • ONTARIO • CANADA • M3J 1P3

discrimination for rectangular targets. Aspect ratio discrimination will be defined as the just noticeable (75% correct) difference in the ratio (**a/b**) where **a** and **b** are, respectively, the rectangle's horizontal and vertical side lengths. To ensure that aspect ratio judgements are based on a comparison of side lengths rather than the value of **a** or **b** alone, the area of the stimulus rectangle will be varied randomly between successive presentations. We will attempt to use these data to establish the degree to which the visual processing that underlies shape (aspect ratio) discrimination of MD rectangles is independent of the visual processing that underlies aspect ratio discrimination for LD rectangles. Also, we will endeavor to relate the data to a model of aspect ratio discrimination for MD rectangles in which (A) dot velocity within the bar and outside the bar is computed, then (B) the rectangle is detected (i.e. segregated from its surroundings) and a population of neurons sensitive to the ratio of side lengths (**a/b**) is excited, then (C) orientation discrimination is based on the distribution of activity among these neurons. We hope to distinguish between the dynamic properties of stage (C) and those of earlier stages.

2.3 Experiment 3. Psychophysics: Cross-adaptation between MD, LD and color-defined stimuli

We will display either (A) a dot pattern in which a motion-defined sinewave grating is generated by moving the dots in one direction (e.g. horizontally) at a speed that varies in a perpendicular direction (vertically in this instance) according to a sinusoidal profile; (B) a pattern of stationary dots in which a sinewave grating is produced by varying dot luminance in one direction according to a sinusoidal profile; (C) a solid sinewave luminance grating; (D) an equiluminant color-defined grating. For any given presentation, the kind of grating and its orientation, spatial frequency, dot speed, luminance distribution, and color will be controlled by a PC that runs the psychophysical procedure (2AFC, constant stimuli) using our software. We will compare speed detection thresholds for MD gratings, before and after adapting to a high-speed MD grating, in

Department of Psychology

UNIVERSITÉ YORK UNIVERSITY

FACULTY OF ARTS

4700 KEELE STREET • NORTH YORK • ONTARIO • CANADA • M3J 1P3

order to find whether postadaptation threshold elevations for MD gratings are tuned to orientation and spatial frequency. (This protocol follows the protocols of Blakemore and Nachmias[8] for luminance gratings). Because postadaptation data of this kind cannot be interpreted unequivocally in terms of orientation and spatial frequency channels[32,33] we will obtain complementary evidence on this point by obtaining masking data by analogy with the protocol of De Valois and Switkes.[32] In this experiment we will measure the dot speed for just-detectable MD test gratings (75% correct, temporal 2AFC, method of constant stimuli) with and without MD masker gratings whose spatial frequencies and/or orientations differ from the test gratings. We will use these data to test the hypothesis that there are spatial frequency and orientation channels for MD targets (Ref 203).

Then we will repeat these experiments for all cross-adaptation and cross-masking permutations (e.g. adapt to solid luminance grating, test for MD dotted grating and vice versa). We will use these data to establish the degree to which the orientation and spatial frequency of a MD grating is processed independently of the orientation and spatial frequency of a CD grating and of a color-defined grating.

2.4 Experiment 4. Psychophysics: Interactions between contributions of motion contrast and luminance contrast to detection and discrimination

We will generate dotted gratings that are rendered visible by a combination of relative velocity and luminance contrast. We have developed PC software that allows up to 100 different combinations to be presented in a method of constant stimuli protocol according to a matrix of the following kind. Suppose that parameter x is the contrast of the luminance grating and parameter y is the relative dot speed of the motion-defined grating. The matrix below contains every permutation of 10 values of luminance contrast (1-10 with #1 corresponding to zero contrast) with 10 values of relative dot speed (A-J with A corresponding to stationary dots). The PC selects the 100 stimuli random order and records the subjects button presses. The data can be analyzed by Probit

Department of Psychology

UNIVERSITÉ YORK UNIVERSITY

FACULTY OF ARTS

4700 KEELE STREET • NORTH YORK • ONTARIO • CANADA • M3J 1P3

analysis along any given row (giving contrast threshold in the presence of fixed dot speeds) or columns (giving velocity thresholds in the presence of fixed amounts of luminance contrast). This matrix provides a total of 20 threshold estimates. Collecting the data for a large experiment of this kind will extend over many days, whatever procedure is used. The chief purpose of the matrix method is to ensure that day-to-day variability is spread out among the whole 20 thresholds rather than perturbing individual thresholds as may be the case when individual thresholds are measured on different days. However, the thresholds will be compared with those obtained by the more usual psychophysical procedure when only one parameter is varied systematically (i.e. when the PC selects stimuli from only one row or column), because in the matrix procedure, the subject is exposed to two independently-varying visual parameters, a situation that more closely approximate many real-world situations than the more usual psychophysical procedure where only one parameter is varied systematically. On the basis of findings that stimulus uncertainty affects threshold (e.g. Ball & Sekuler, 1990) it is envisaged that thresholds may differ in the two situations.

MATRIX

INCREASING DOT CONTRAST

A1	**A2**	**A3**	**A4**	**A5**	**A6**	**A7**	**A8**	**A9**	**A10**
B1	**B2**	**B3**	**B4**	**B5**	**B6**	**B7**	**B8**	**B9**	**B10**
C1	**C2**	**C3**	**C4**	**C5**	**C6**	**C7**	**C8**	**C9**	**C10**
D1	**D2**	**D3**	**D4**	**D5**	**D6**	**D7**	**D8**	**D9**	**D10**
E1	**E2**	**E3**	**E4**	**E5**	**E6**	**E7**	**E8**	**E9**	**E10**
F1	**F2**	**F3**	**F4**	**F5**	**F6**	**F7**	**F8**	**F9**	**F10**

Department of Psychology

UNIVERSITÉ YORK UNIVERSITY

FACULTY OF ARTS

4700 KEELE STREET • NORTH YORK • ONTARIO • CANADA • M3J 1P3

G1	G2	G3	G4	G5	G6	G7	G8	G9	G10
H1	H2	H3	H4	H5	H6	H7	H8	H9	H10
I1	I2	I3	I4	I5	I6	I7	I8	I9	I10
J1	J2	J3	J4	J5	J6	J7	J8	J9	J10

In separate experiments we will measure grating detection threshold and discrimination thresholds for orientation and spatial frequency. The subject will have 3 pairs of response buttons and in temporal 2AFC be instructed to respond (A) which interval contained a grating, first or second?, (B) was the grating an MD grating?, (C) was the grating a luminance grating? The subject will be further instructed that the correct answer may be YES to both (B) and (C), NO to both (B) and (C), or YES to either (B) or (C) and NO to the other. The 3 sets of button presses will be analyzed separately. We will use the data to find whether visual responses to contrast and to relative velocity and independently or interact nonlinearly in determining grating detection threshold. In particular, we will find whether the two parameters combine according to probability summation when both parameters are below detection threshold level when presented alone. Also, we will find the combination rules for the two parameters in determining orientation discrimination and spatial frequency discrimination when one or both parameters are above detection threshold level.

2.5 Experiment 5. Psychophysics: Cyclopean and non-cyclopean motion in depth

We will generate two dot patterns, one on each half of the screen, one viewed by the left eye and one by the right eye. A new dot pattern will be generated at 60 Hz frame rate so as to create dynamic random noise and one pattern will be routed optically to the left eye and the other pattern to the right eye. It is necessary to use dynamic rather than static random noise because a moving target in static random noise breaks camouflage and would, therefore, be visible monocularly,

Department of Psychology

UNIVERSITÉ YORK UNIVERSITY

FACULTY OF ARTS

4700 KEELE STREET • NORTH YORK • ONTARIO • CANADA • M3J 1P3

while a moving target in dynamic random noise is not visible monocularly.[1]

A rectangular area within the dot pattern will be rendered visible by a relative displacement of the left and right eye's rectangles so as to create binocular disparity as described by Julesz.[1] The dimensions of the rectangle, its rate of change of size and its rate of change of disparity will all be controlled by instructions to the IRIS from the PC that runs the experiment .

First we will modulate the rectangle's size sinusoidally and using temporal 2AFC, separately measure the oscillation amplitude that gives just-detectable size oscillation and just detectable motion-in-depth for a range of oscillation frequencies from 0.2 Hz upwards. Then we will oscillate disparity at fixed size and use 2AFC to measure the amplitude of disparity oscillation for just-detectable motion-in-depth. These experiments will be repeated at fixed values of mean disparity (crossed and uncrossed).

A pilot experiment using our hardware dot generator (Ref 130) indicates that motion-in-depth sensation generated by changing-disparity can be cancelled by pitting changing-disparity against changing-size stimulation. This pilot result suggests that changing-size and changing-disparity signals converge at a single motion-in-depth stage. For sinusoidally oscillating disparity and changing-size we will use temporal 2AFC to measure the amplitude of size oscillation that cancels the sensation of motion-in-depth produced by a fixed amplitude of disparity oscillation for different oscillation frequencies. This experiment will be repeated for different fixed amplitudes of disparity oscillation. Then we will investigate dynamics in the time domain using transient (ramping) changes of disparity and changing-size. We will use temporal 2AFC to measure formally the ramping rates of change of size that cancels the sensation of motion-in-depth a fixed rate of change of disparity for different ramp durations. This experiment will be repeated for different fixed rates of change of disparity.

The above experimental protocols are the same as these used earlier for monocularly-visible

Department of Psychology

UNIVERSITÉ YORK UNIVERSITY

FACULTY OF ARTS

4700 KEELE STREET • NORTH YORK • ONTARIO • CANADA • M3J 1P3

targets (Ref 85). By comparing our cyclopean data with data for monocularly-visible dotted targets we will endeavor to distinguish between the processing underlying motion-in-depth perception that takes place after and before convergence of the signals from left and right eyes.

2.6 Experiment 6. Psychophysics: Monocular discrimination of time to contact and direction of motion in depth

We will generate a bright solid rectangle on a Tektronix model 608 monitor using our own-design hardware and view the rectangle monocularly. Motion-in-depth along different trajectories will be mimicked by moving the rectangle across the CRT screen at different speeds and at the same time changing the rectangle's size. The resulting stimulus will be quantified in terms of the relative velocity of the rectangle's opposite edges. The rectangle's motion will be controlled by a PC (2AFC, constant stimuli). We will measure the just discriminable change of trajectory for a wide range of trajectories in the horizontal, vertical and the two 45 deg oblique planes for a population of 20 control subjects.

2.7 Experiment 7. Theoretical: Two-sinewave approach to characterizing nonlinear multi-neuron models

We will extend the theoretical work described in the Final Technical Report for 1987–1990 to include dynamics by inserting a linear frequency-dependent filter before and after every rectifier. We aim to build a catalog of families of curves for the following kinds of multi-neuron models with dynamics: (A) a sequence of n cascaded rectifiers, including the case that all rectifiers are different, and (B) two such parallel sequences, converging into a third sequence of cascaded rectifiers (i.e. the dichoptic or the diotic case). The high speed of the IRIS will allow us to obtain numerical solutions for these cases.

2.8 Experiment 8. Theoretical: Amplitude- and frequency-modulated tones

We will develop a procedure for calculating the amplitudes and phases of the frequency

Department of Psychology

UNIVERSITÉ YORK UNIVERSITY

FACULTY OF ARTS

4700 KEELE STREET • NORTH YORK • ONTARIO • CANADA • M3J 1P3

terms in the output of a single rectifier whose input is the sum of two amplitude-modulated (AM) or two frequency-modulated (FM) tones, or one AM plus one FM tone. The rectifier characteristics treated will include compressive, accelerating and mixed, with and without threshold. Then we will go on to consider: (A) a sequence of cascaded rectifiers including the case that all the rectifiers have different characteristics, and (B) two parallel cascaded sequences of rectifiers converging onto a third cascade of rectifiers (i.e. the diotic case). In cases (A) and (B) we will treat dynamic properties by including a linear frequency-dependent stage on either side of every individual rectifier. We will build a catalog of families of curves that characterize multi-rectifier models of the auditory pathway, and will allow these models to be tested against neuromagnetic data.

2.9 Experiment 9. Neuromagnetism: Interactions specific to orientation and spatial frequency

By combining neuromagnetic recording with the two-sinewave techniques described in the Final Technical Report for 1987–90 extended to include dynamics we will identify the sites of interaction between cortical neurons tuned to different orientations and spatial frequencies. We will compare these sites in human brain with known properties of neurons in V1, V2, V3 and other known prestriate areas in macaque cortex. We will relate our conclusions to the processing of complex two-dimensional patterns in human brain.

2.10 Experiment 10. Neuromagnetism: Location and characterization of neural mechanism underlying the 40 Hz response in human

By stimulating with flickering light at frequencies near 40 Hz and with gratings of low spatial frequencies counterphase-modulated at rates near 20 Hz we will find whether the human brain has a 40 Hz neuromagnetic resonant-like response that corresponds to the electrical 40 Hz response we described previously (Ref 4). If so, we will estimate the brain location of the response, then we will stimulate with two flickering lights and with two gratings of F_1 and F_2 Hz

Department of Psychology

UNIVERSITÉ YORK UNIVERSITY

FACULTY OF ARTS

4700 KEELE STREET • NORTH YORK • ONTARIO • CANADA • M3J 1P3

and use our theoretical method described in the Final Report for 1987–90 (Refs 167, 178, 179, 183) to characterize the 40 Hz response. The results will be related to the recently-reported 40 Hz response in single-unit activity.[2]

2.11 Experiment 11. Neuromagnetism: Characterization of brain responses to stereomotion

We will find which areas of human cortex are selectively sensitive to the direction of stereomotion-in-depth and compare their properties with the properties of stereomotion channels (Refs 34, 49) and motion-in-depth neurons (Refs 73, 79, 111, 112). We will use areas of motion-in-depth "blindness" in control subjects to check that neuromagnetic responses to changing disparity are associated with motion-in-depth perception.

2.12 Experiment 12. Neuromagnetism: Characterization of brain responses to motion-defined form

In control subjects we will measure the distribution of evoked magnetic responses to camouflaged objects defined by motion alone, estimate the source location, and compare this location with published estimates (Brodmann areas 19 & 39) of the location of the human equivalent of monkey area MT.[3,4,5] Measurements will also be made on patients with focal cortical lesions that involve the human equivalent of MT (shown by magnetic resonance imaging) and who have abnormal psychophysical scores on our form-from-motion test (see Fig 13 below).

We will also compare our psychophysical findings on spatiotemporal integration for motion-defined objects with corresponding magnetic evoked responses.

2.13 Experiment 13. Neuromagnetism: Characterization of audio-visual convergence areas in human brain

Control subjects will be stimulated simultaneously with a light modulated at F_1 Hz and a sound modulated at F_2 Hz. We will obtain the spectrum of the neuromagnetic response and search for cross-modulation terms of frequency ($nF_1 \pm mF_2$) where neither n nor m is zero. Such terms

Department of Psychology

UNIVERSITÉ YORK UNIVERSITY

FACULTY OF ARTS

4700 KEELE STREET • NORTH YORK • ONTARIO • CANADA • M3J 1P3

must necessarily be generated after convergence of visual and auditory pathways. We will estimate the brain location(s) of at which these terms are generated and compare these sites with the sites of multi-sensory projection areas in monkey cortex described by Van Essen.[6]

2.14 Experiment 14. Neuromagnetism: Interactions of brain responses to AM and FM tones

We will use zoom-FFT to record interactions between responses to two simultaneous modulated tones and in particular we will compare interactions between two AM tones, two FM tones and cross-interactions between AM and FM tones. We will model the data using the theoretical approach proposed in Section 6.2.8 above, and relate the data to the shape of the hair cell transducer function, i.e. we will provide a theoretical treatment for the empirical findings reported in Section 7 of the original grant application (see Refs 177, 188). We will also use the data to test our psychophysically-based hypothesis that the human auditory pathway processes AM and FM information in parallel and almost independently (Refs 80, 87).

2.15 Experiment 15. Single Unit Electrophysiology: Analysis of orientation-specific interactions using the two-sinewave approach

This experiment will be carried jointly with Professor Grasse. He will be responsible for anesthesia, surgery and for recording the single-unit spikes. We will stimulate the eye with a grating counterphase-modulated at F Hz and obtain ultra-high resolution spectra by processing the spike train as described in the Final Technical Report for 1987–90. We will analyze a 500 sec recording so as to obtain 0.002 Hz resolution, and will measure the bandwidth of the 2F Hz and 4F Hz responses. We will simultaneously record local evoked potentials from a wire electrode in contact with the cortex, and analyze these data as described in Section 7 of the original grant application (Ref 179). Then we will compare the bandwidths of the single-unit firing and of the evoked potential.

Department of Psychology

UNIVERSITÉ YORK UNIVERSITY

FACULTY OF ARTS

4700 KEELE STREET • NORTH YORK • ONTARIO • CANADA • M3J 1P3

We will go on to stimulate the eye with two superimposed gratings, one modulated at F_1 Hz, the other at F_2 Hz while recording spike firing and local slow waves, and subject 500-sec records to spectral analysis at 0.002 Hz resolution. With one grating at constant orientation we will repeat the measurement at different orientations of the second grating, and use the theoretical work described in the Final Technical Report for 1987–90 to test multi-neuron models of orientation processing. We will compare these data on orientation processing with orientation tuning data obtained conventionally using a single sinewave for different classes of cell (i.e. simple, complex).

2.16 Experiment 16. Medical Tests: Motion-defined letter test

We will record results for our motion-defined letter test, our low-contrast acuity test, contrast sensitivity for a 3 cycles-deg, 8 Hz sinewave grating and Snellen acuity every 2 months on patients with Parkinson's disease, and correlate test results with the clinical progress of the disease. (Clinical progress will be assessed by Professor A. Lang, M.D. as part of the ongoing U.S./Canadian DATATOP multi-center trial of the drug Deprenyl in Parkinson's disease.) We will compare motion-defined letter test results with deficits in smooth pursuit eye movements that have been measured by Professor J. Sharpe, M.D. in a separate ongoing study. We will record motion-defined letter test results in patients with ocular hypertension and early glaucoma and correlate these results longitudinally with the clinical progress of the disease. (Clinical progress will be assessed by Professor G.E. Trope as part of an ongoing separate study.)

3 STATUS OF THE RESEARCH EFFORT

3.1 Experiment 1 and Specific Aim 1.2.1

This experiment has been completed. A paper has been published in *Vision Research* (Ref 210) and a chapter is in preparation for a book proceedings of the 1991 York International

Department of Psychology

UNIVERSITÉ
YORK
UNIVERSITY

FACULTY OF ARTS

4700 KEELE STREET • NORTH YORK • ONTARIO • CANADA • M3J 1P3

Conference on Spatial Vision (Ref 220).

Our previous finding that orientation discrimination can be as acute for MD bars as for LD bars poses a challenge for models of orientation discrimination. With the aim of providing further data for testing competing models, we extend our previous study of orientation discrimination by measuring dynamic properties of bar detection and orientation discrimination for MD bars. Further, we compare these data with measurements of the corresponding dynamic properties of detection and discrimination for LD bars. We describe below two aspects of these dynamic properties. The first aspect was brought out by varying stimulus duration, and the second by varying dot lifetime.

A pseudo-random pattern of bright dots subtending 2.2 x 2.2 deg was generated by laboratory-built hardware electronics, displayed on a CRT (Tektronix model 608 with green P31 phosphor) and viewed from a distance of 207 cm. Figure 1A shows a photograph of a typical pattern. There were 100 complete frames per sec. Dots subtended about 2.0 min arc, and mean dot separation was 6 min arc (approx. 1000 dots in all). A new dot pattern could be generated every frame. Dots could be moved in any direction by applying an analog voltage to the monitor's x and/or y plates. The motion of dots within a rectangular region of the entire 2.2 x 2.2 deg pattern could be controlled independently of the motion of dots outside this region, and the orientation, x-y dimensions and location of the region were controlled by external voltages independently of dot motion. This rectangular region could not be demarcated visually from the rest of the dot pattern if the dot velocity inside and outside the region were the same.

By means of a beamsplitter, the dot pattern was optically superimposed on a circular, uniformly-illuminated green area of diameter 3.7 deg and luminance 2.1 cd m^{-2}. Dots were switched off except during the pattern presentations. A new pseudo-random dot pattern was generated for each trial.

A 1.5 x 0.22 deg stationary bar-shaped area within the dot pattern was rendered visible by

Department of Psychology

UNIVERSITÉ
YORK
UNIVERSITY

FACULTY OF ARTS

4700 KEELE STREET • NORTH YORK • ONTARIO • CANADA • M3J 1P3

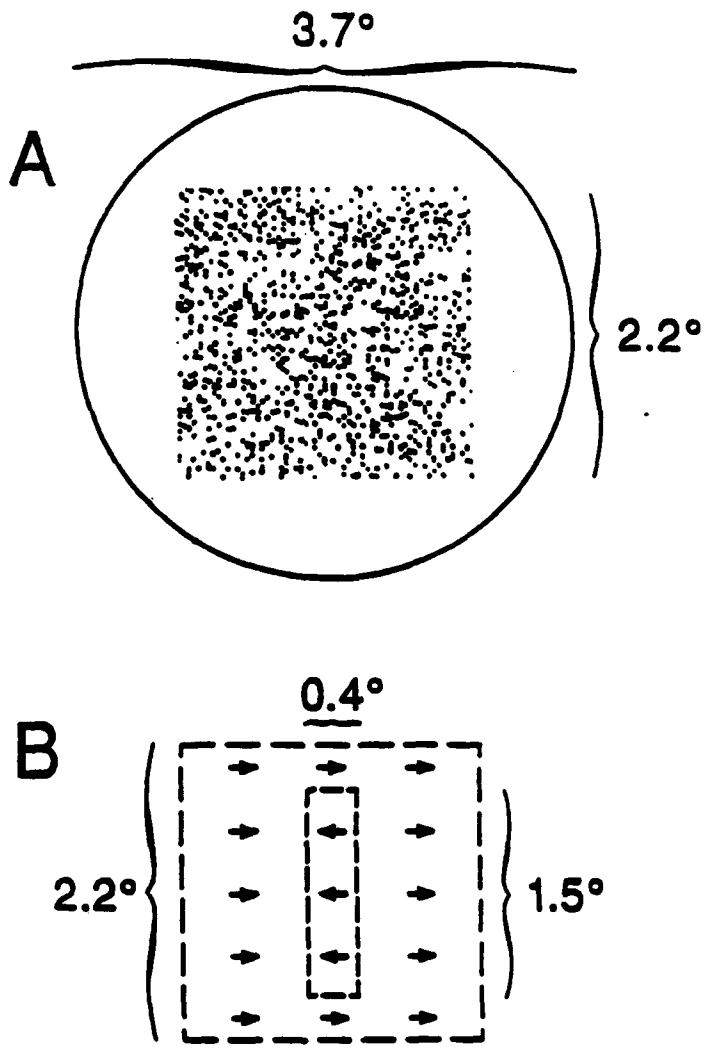

Figure 1. A: Random dot pattern subtending 2.2 deg and containing a perfectly camouflaged bar was superimposed on a homogeneous, circular, uniformly-illuminated area of diameter 3.7 deg. Note that the dots were bright rather than black as shown here. B: The camouflaged bar was revealed by moving dots inside and outside the bar at equal speeds in opposite directions.

Department of Psychology

UNIVERSITÉ YORK UNIVERSITY

FACULTY OF ARTS

4700 KEELE STREET • NORTH YORK • ONTARIO • CANADA • M3J 1P3

moving the dots inside the bar horizontally to the left at a constant speed that was equal and opposite to the speed of the dots in the remainder of the pattern (Ref 157). The reason for choosing type B motion-defined form rather than type A motion-defined form and for using equal and opposite speeds rather than different speeds or different directions of motion was as follows. The bar and its orientation were clearly visible in a photographic time exposure of type A motion-defined form, whether the moving bar was surrounded by stationary dots or by dynamic random noise. The bar was clear to eyeball inspection also, but we cannot necessarily assume that it was detected by using the relative motion cue rather than by texture contrast. A type B motion-defined bar was rendered visible by texture contrast in a photograph when dots within the bar and outside the bar moved at different speeds or in different directions (Ref 157). In principle, the population activity of cortical neurons could signal the presence of such a type B bar or of a type A bar *even in a motion-blind visual system*. The reason is that cortical neurons sensitive to the length and orientation of a line have a finite temporal integration time constant for luminance, and thus could give a similar response to a rapidly-moving spot and a line. However, when the dots inside and outside the bar moved at equal and opposite speeds the bar was almost invisible to the camera, though clearly evident to eyeball inspection (Ref 157), so that we can assume that the texture contrast cue to bar detection was effectively removed. The possibility that subjects might track either the dots within the bar or outside the bar, and thus re-introduce the blurring cue, was discounted by measuring eye movements using an SRI double-Purkinje eye tracker.

In order to measure thresholds of about 0.3 deg, it was necessary to present orientation differences as small as 0.1 deg. A pixel-based system has the disadvantage that the long edges of an inclined bar are stepped rather than being straight, and this limits the smallest change in orientation. For example, a bar 600 pixels in length oriented at 0.1 deg to the vertical would have only a single one-pixel step along its length – whatever the viewing distance. Our display has the

Department of Psychology

UNIVERSITÉ YORK UNIVERSITY

FACULTY OF ARTS

4700 KEELE STREET • NORTH YORK • ONTARIO • CANADA • M3J 1P3

advantage that indefinitely small changes in orientation can be generated.

Effects of presentation duration and dot lifetime on orientation discrimination for MD and LD bars at constant dot speed and contrast

Figure 2 shows that orientation discrimination was approximately the same for MD and LD bars when presentation duration was sufficiently long. The best value of orientation discrimination threshold for an MD bar was 0.4 deg for subject 1, 0.5 deg for subject 2 and 0.7 deg for subject 3 at the longest presentation duration of 1.0 sec, but discrimination worsened rapidly as presentation duration was reduced below 0.10–0.15 sec, and could not be measured at all for durations below 0.04–0.05 sec. For a LD bar, orientation discrimination threshold showed a comparatively small increase as presentation duration was reduced from 1.0 sec to 0.01 sec (from 0.33 deg to 1.0 deg for subject 1, from 0.42 deg to 0.9 deg for subject 2 and from 0.55 deg to 1.6 deg for subject 3).

Figure 3 shows that, for a fixed presentation duration of 1.0 sec, orientation discrimination was approximately the same for MD and LD bars when dot lifetime was sufficiently long. For MD bars, dot lifetime had no appreciable effect on orientation discrimination over a range of long lifetimes, but discrimination degraded rapidly as dot lifetime fell below about 0.15 sec (Fig. 3A) or 0.25 sec (Fig. 3B, C) and could not be measured at all for dot lifetimes less than about 0.04–0.06 sec. For LD bars, dot lifetime had no effect on orientation discrimination over the entire range of lifetimes investigated between 0.01 sec (i.e. one frame) to 1.0 sec.

Effect of presentation duration and dot lifetime on bar detection threshold for MD and LD bars

Solid circles in Fig. 4A, B plot bar detection threshold speed versus presentation duration, for MD bars with dot lifetime always equal to presentation duration. Solid triangles in Fig. 4A, B plot bar detection threshold speed for MD bars versus dot lifetime, presentation duration being constant at 1.0 sec. These data were obtained using procedure 1 (see below). Bar detection threshold speed was approximately 0.006 deg/sec (i.e. relative speed 0.012 deg/sec) for a presentation

Department of Psychology

UNIVERSITÉ YORK UNIVERSITY

FACULTY OF ARTS

4700 KEELE STREET • NORTH YORK • ONTARIO • CANADA • M3J 1P3

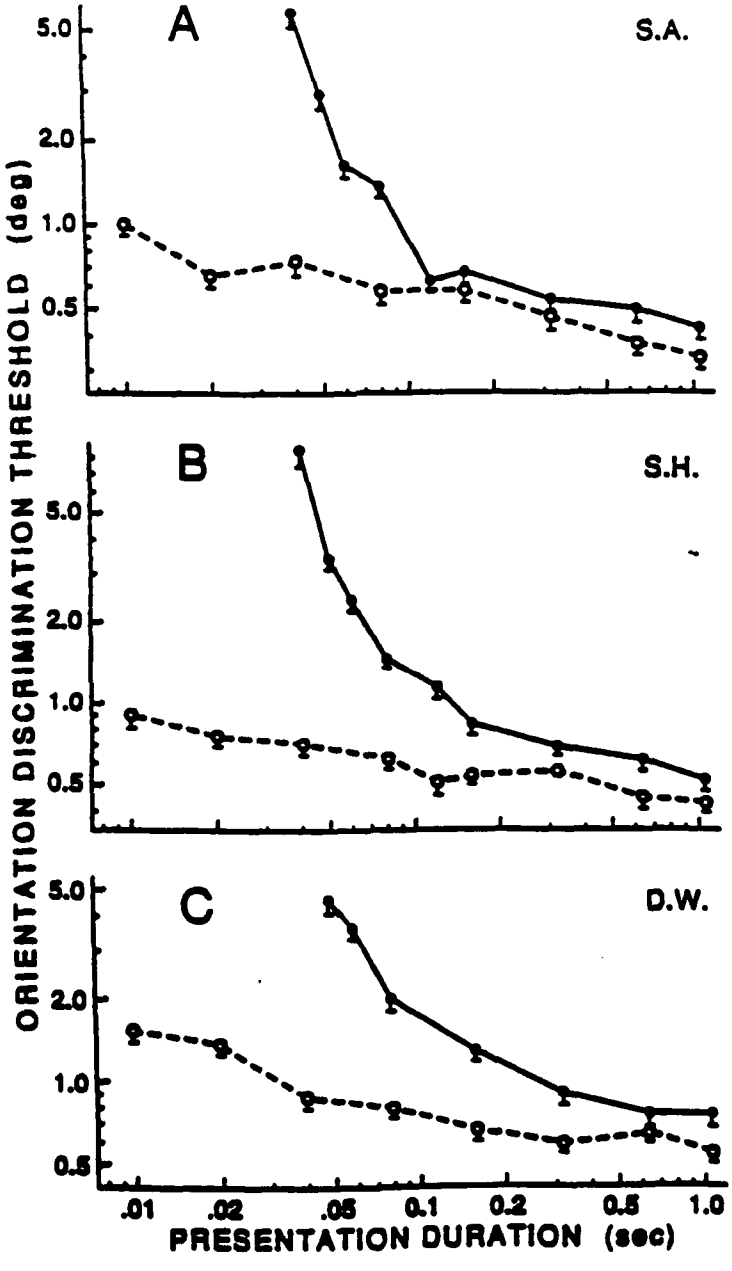

Figure 2. Orientation discrimination threshold (ordinates) versus presentation duration (abscissae) for a dotted bar defined by relative motion (●) and for the same dotted bar defined by luminance contrast (○). The vertical bars mark one standard error. Dot lifetime was equal to presentation duration. Dot speed was 0.68 deg/sec, so the relative dot speed was 1.4 deg/sec. A, subject 1. B, subject 2. C, subject 3.

Department of Psychology
UNIVERSITÉ YORK UNIVERSITY
FACULTY OF ARTS
4700 KEELE STREET • NORTH YORK • ONTARIO • CANADA • M3J 1P3

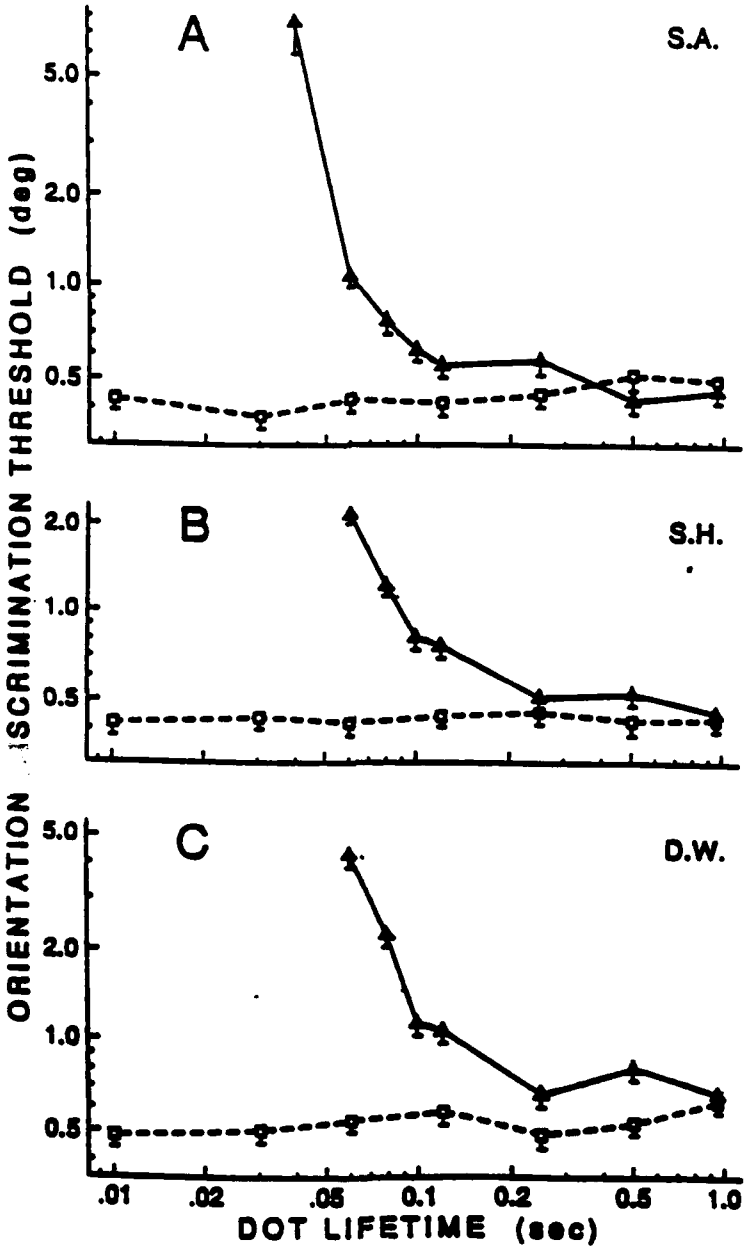

Figure 3. Orientation discrimination threshold (ordinates) versus dot lifetime (abscissae) for a dotted bar defined by relative motion (▲) and for the same dotted bar defined by luminance contrast (□). The vertical bars mark one standard error. Presentation duration was 1.0 sec throughout. Dot speed was 0.68 deg/sec, so the relative dot speed was 1.4 deg/sec. A, subject 1. B, subject 2. C, subject 3,

Department of Psychology

UNIVERSITÉ
YORK
UNIVERSITY

FACULTY OF ARTS

4700 KEELE STREET • NORTH YORK • ONTARIO • CANADA • M3J 1P3

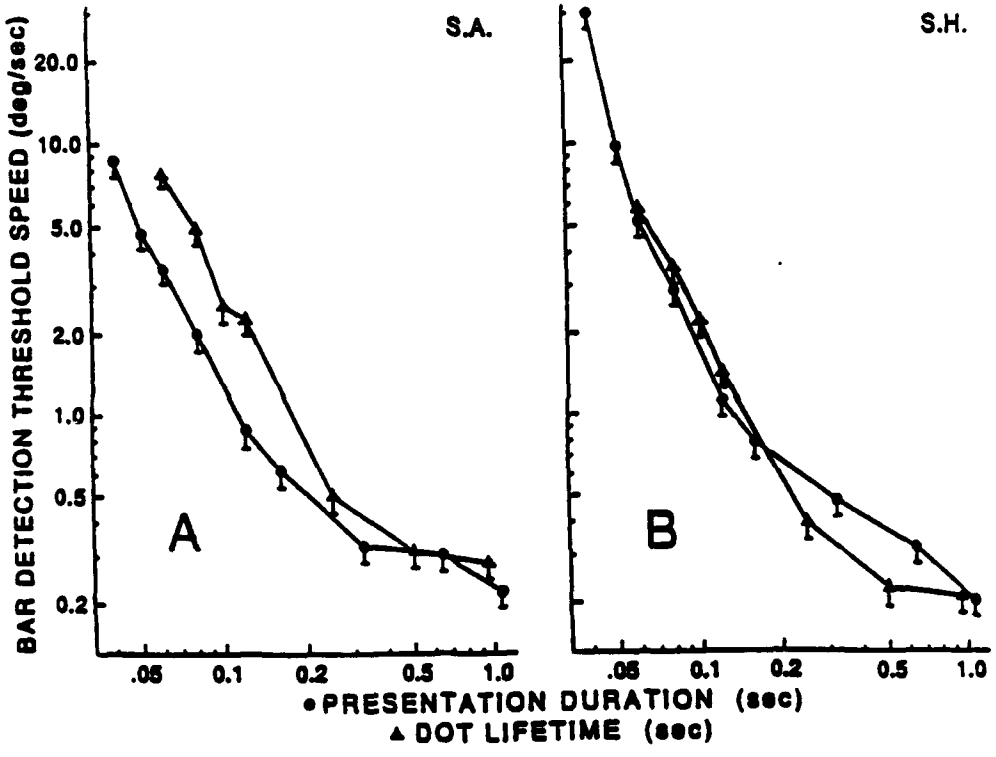

Figure 4. Bar detection threshold speed (ordinates) versus presentation duration (abscissae, ●) and versus dot lifetime (abscissae, ▲) for a dotted bar defined by relative motion. For presentation duration data, dot lifetime was equal to presentation duration. For dot lifetime data, presentation duration was constant at 1.0 sec. The vertical bars mark one standard error. Dot speed was 0.68 deg/sec, so the relative dot speed was 1.4 deg/sec. A, subject 1. B, subject 2.

Department of Psychology

UNIVERSITÉ YORK UNIVERSITY

FACULTY OF ARTS

4700 KEELE STREET • NORTH YORK • ONTARIO • CANADA • M3J 1P3

in which both presentation duration and dot lifetime were 1.0 sec, and increased progressively, reaching 0.13 deg/sec (i.e. relative speed 0.26 deg/sec) or more when either presentation duration or dot lifetime had decreased to 0.06 sec.

Solid circles in Fig. 5A, B plot bar detection contrast thresholds for LD bars versus presentation duration, with dot lifetime always equal to presentation duration. Threshold rose as duration was reduced, much as detection threshold for MD bars in Fig. 4 (solid circles). Solid triangles in Fig. 5A, B plot threshold contrast for LD bars versus dot lifetime, dot duration being constant at 1.0 sec. Dot lifetime has no effect on threshold. [Contrast this with the different behavior of detection threshold for MD bars shown in Fig. 4 (solid triangles).]

Orientation discrimination versus dot speed for MD bars of different presentation durations and dot lifetimes

Figure 6A and B shows that plots of orientation discrimination versus dot speed for MD bars were displaced progressively rightwards as presentation duration was decreased from 1.0 sec to 0.04 sec, dot lifetime being equal to presentation duration in every case. Similarly, Fig. 7A and B shows that plots of orientation discrimination versus dot speed for MD bars were displaced progressively rightwards as dot lifetime was decreased from 1.0 to 0.06 sec, presentation duration being held constant at 1.0 sec. In addition, there was an increase in slope at lifetimes less than 0.5 sec. Because of the shape of the curves, the progressive rightward shift had the result that the effect of presentation duration upon orientation discrimination for MD bars was considerably larger at high dot speed than at low dot speeds (Fig. 6). In Fig. 7 the progressive rightward shift combined with slope increase caused the effect of dot lifetime upon orientation discrimination to be considerably larger at low dot speeds than at high dot speeds. (This result can be verified by comparing the vertical spread of points at different speeds in Figs. 6 and 7.)

The data of Figs. 6 and 7 can also be used to compare the effects on orientation discrimina-

Department of Psychology

UNIVERSITÉ YORK UNIVERSITY

FACULTY OF ARTS

4700 KEELE STREET • NORTH YORK • ONTARIO • CANADA • M3J 1P3

tions of (1) reducing presentation duration from 1.0 sec (rightmost large solid square, Fig. 6) to 0.06 sec (rightmost solid square, Fig. 6) with (2) reducing dot lifetime from 1.0 sec (rightmost large solid square, Fig. 7) to 0.06 sec (rightmost small solid square, Fig. 7) with presentation duration held constant at 1.0 sec. The effect of presentation duration was about twice as large as the effect of dot lifetime for both subjects.

Orientation discrimination versus dot contrast for LD bars of different presentation durations and dot lifetimes

Figure 8A and B shows that plots of orientation discrimination versus dot contrast for LD bars were displaced progressively rightwards as presentation duration was decreased from 1.0 sec to 0.02 sec, dot lifetime being equal to presentation duration in every case. Because of the shape of the curves, this progressive shift had the result that the effect of presentation duration upon orientation discrimination for LD bars was considerably larger at high contrasts than at low contrasts – along the lines of the data for MD bars just discussed. In Fig. 9A and B, however, dot lifetime had no significant effect on orientation discrimination over the entire 40:1 range of dot contrasts tested.

Finally, a comparison of Figs. 6, 7, 8 and 9 confirms the previous finding (Ref 182) that orientation discrimination for MD and LD bars is closely similar at long durations and dot lifetimes, provided that dot speed and dot contrast are high.

Our conclusions are as follows:

Orientation discrimination in the everyday visual situation

The data of Fig. 2 relate to the situation described by Helmholtz where a camouflaged object is rendered visible through motion parallax created by self-motion. In particular these data relate to the question how, in the everyday visual situation, spatial discriminations are affected by the length of time for which such an MD object is viewed. In the specific case of orientation discrimination for constant dot speed and constant contrast, Fig. 2 shows that orientation discrimination

Department of Psychology

UNIVERSITÉ
YORK
UNIVERSITY

FACULTY OF ARTS

4700 KEELE STREET • NORTH YORK • ONTARIO • CANADA • M3J 1P3

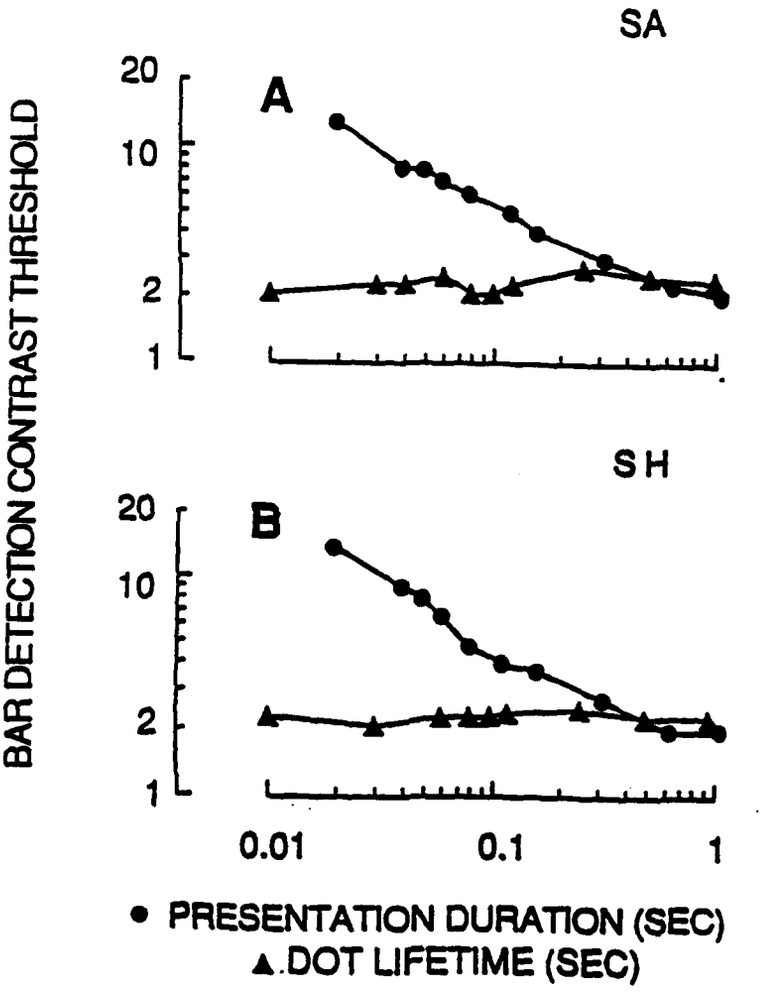

Figure 5. Bar detection threshold contrast (ordinates) versus presentation duration (abscissae, ●) and versus dot lifetime (abscissae, ▲) for a dotted bar defined by luminance contrast. For presentation duration data, dot lifetime was equal to presentation duration. For dot lifetime data, presentation duration was constant at 1.0 sec. Dot speed was 0.68 deg/sec, so the relative dot speed was 1.4 deg/sec. Contrast is in the same arbitrary units as in Figs. 8 and 9. A, subject 1. B, subject 2.

Department of Psychology

UNIVERSITÉ YORK UNIVERSITY

FACULTY OF ARTS

4700 KEELE STREET • NORTH YORK • ONTARIO • CANADA • M3J 1P3

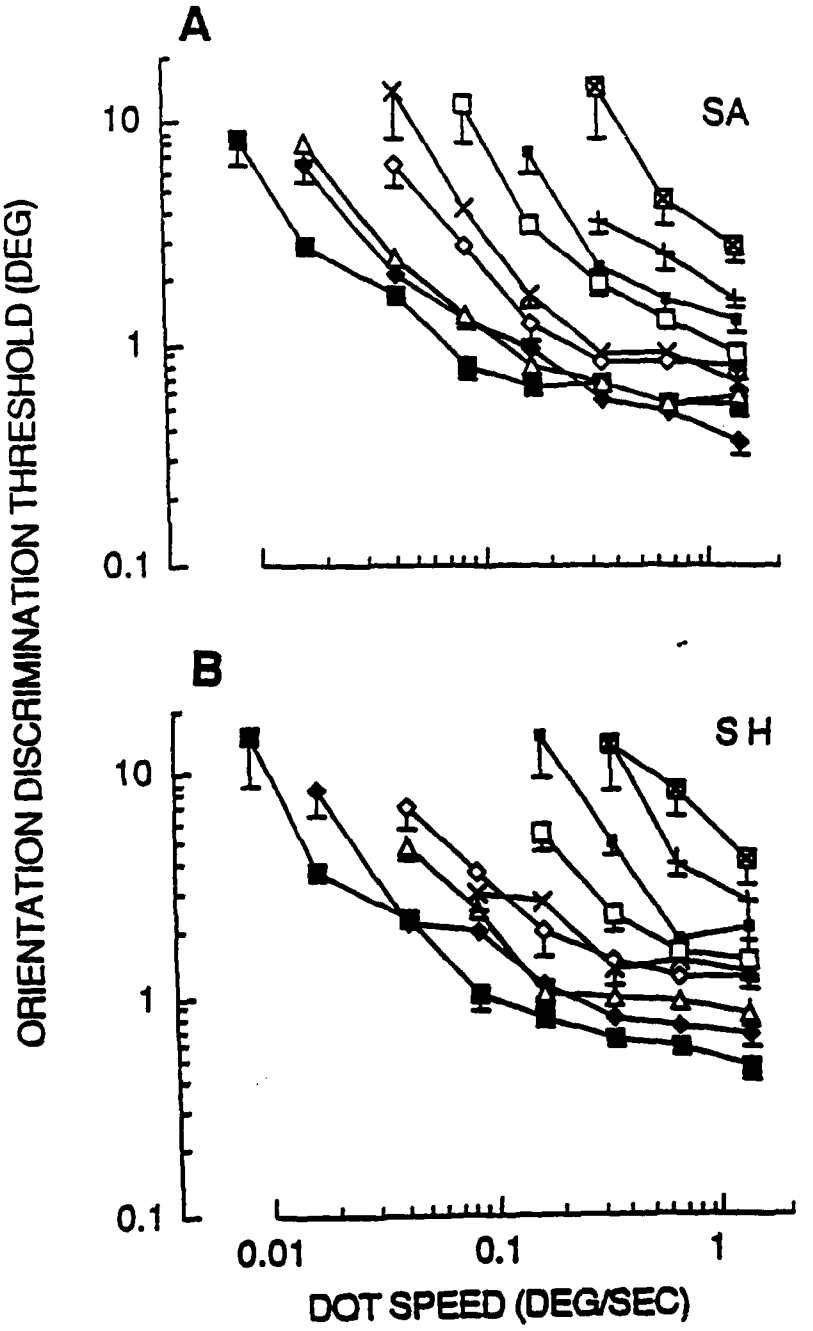

Figure 6. Orientation discrimination threshold (ordinates) versus dot speed for a dotted bar defined by relative motion for 9 presentation durations. Key: ■ – 1.0 sec; ◆ – 0.64 sec; Δ – 0.32 sec; ◊ – 0.16 sec; × – 0.12 sec; ❑ – 0.08 sec; ■ – 0.06 sec; + – 0.05 sec; × – 0.04 sec. The vertical bars mark one standard error. A, subject 1. B, subject 2.

Department of Psychology
UNIVERSITÉ YORK UNIVERSITY
FACULTY OF ARTS
4700 KEELE STREET • NORTH YORK • ONTARIO • CANADA • M3J 1P3

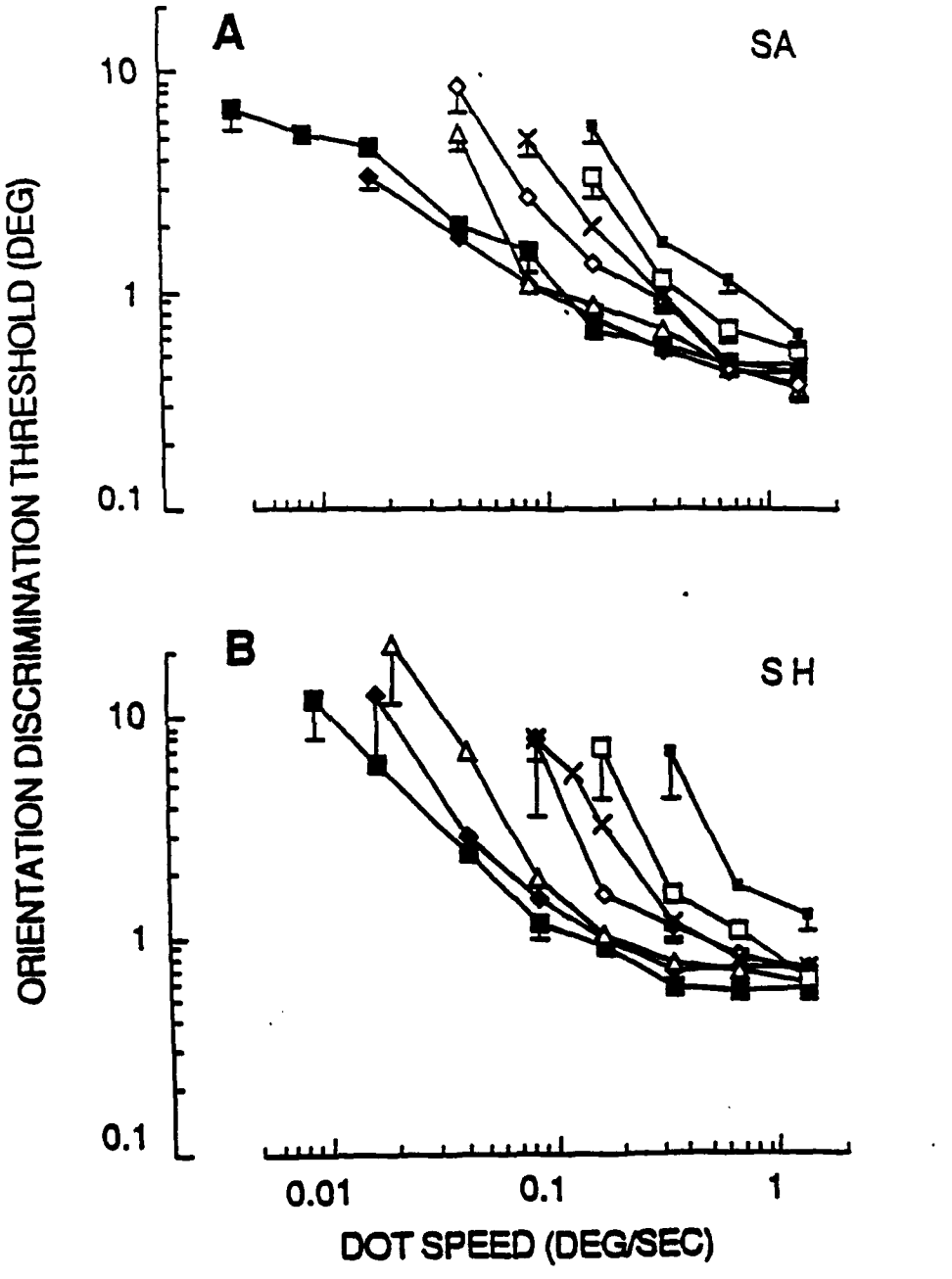

Figure 7. Orientation discrimination threshold (ordinates) versus dot speed for a dotted bar defined by relative motion for 7 dot lifetimes. Key: ■ – 1.0 sec; ◆ – 0.50 sec; Δ – 0.25 sec; ◊ – 0.12 sec; × – 0.10 sec; ❑ – 0.08 sec; ■ – 0.06 sec. Presentation duration was 1.0 sec throughout. The vertical bars mark one standard error. A, subject 1. B, subject 2.

Department of Psychology
UNIVERSITÉ YORK UNIVERSITY
FACULTY OF ARTS
4700 KEELE STREET • NORTH YORK • ONTARIO • CANADA • M3J 1P3

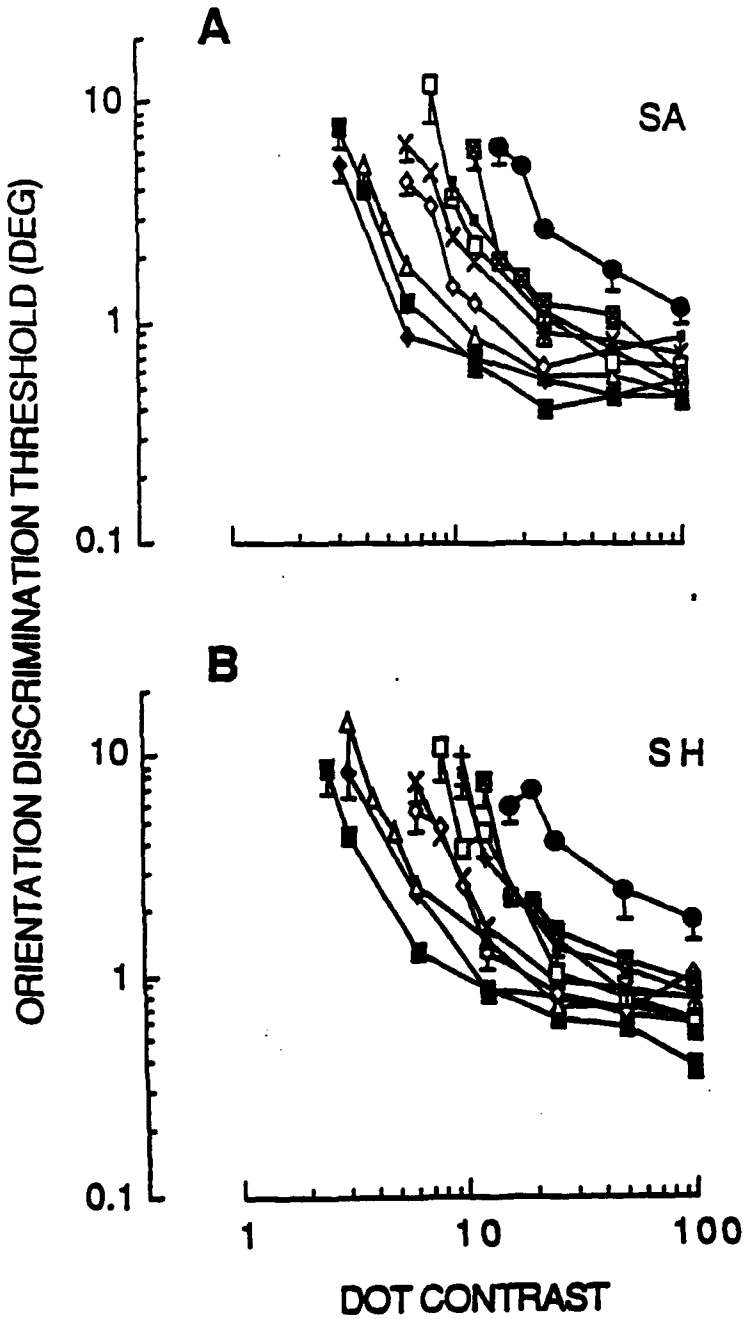

Figure 8. Orientation discrimination threshold (ordinates) versus dot contrast for a luminance-defined dotted bar for 10 presentation durations. Key: ■ – 1.0 sec; ◆ – 0.64 sec; Δ – 0.32 sec; ◊ – 0.16 sec; × – 0.12 sec; ❑ – 0.08 sec; ■ – 0.06 sec; + – 0.05 sec; × – 0.04 sec; ● – 0.02 sec. Contrast is in the same arbitrary units as in Fig. 5. The vertical bars mark one standard error. A, subject 1. B, subject 2.

Department of Psychology
UNIVERSITÉ YORK UNIVERSITY
FACULTY OF ARTS
4700 KEELE STREET • NORTH YORK • ONTARIO • CANADA • M3J 1P3

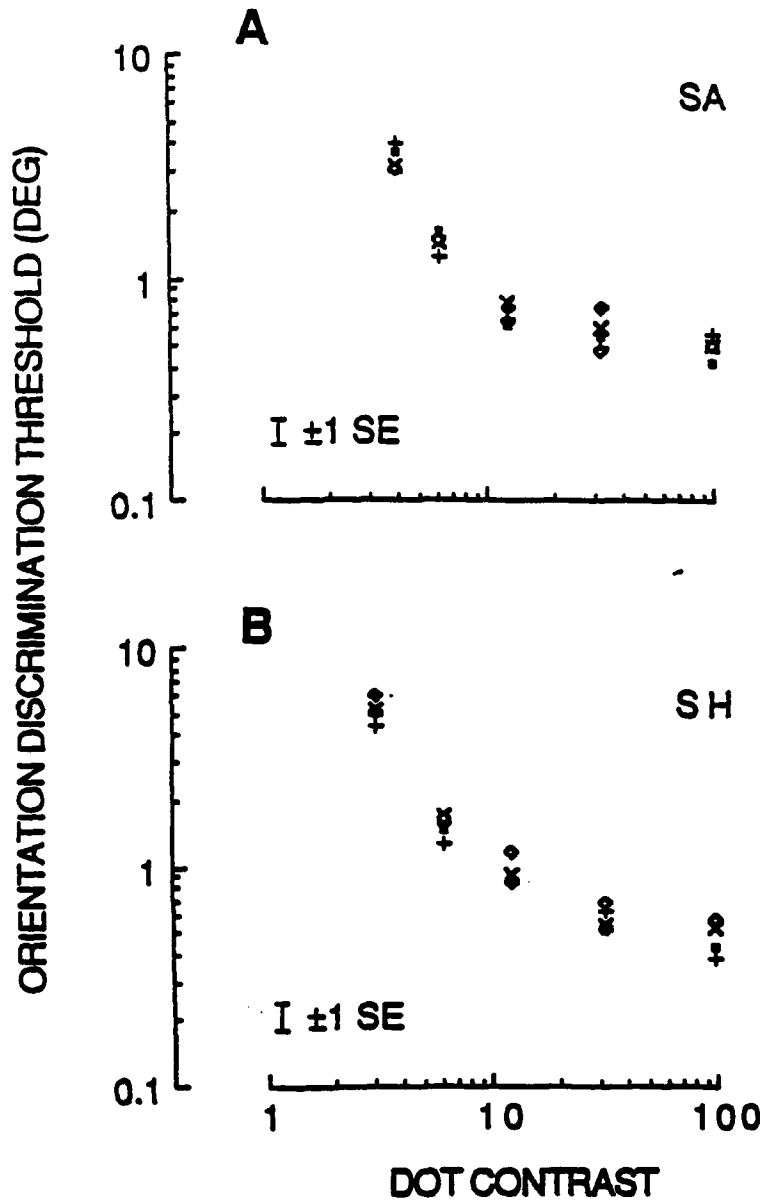

Figure 9. Orientation discrimination threshold (ordinates) versus dot contrast (arbitrary units) for a dotted bar defined by luminance contrast for five dot lifetimes. Key: + – 1.0 sec; ◆ – 0.25 sec; × – 0.10 sec; ◊ – 0.03 sec; ■ – 0.01 sec. Contrast is in the same arbitrary units as in Fig. 5. A, subject 1. B, subject 2.

Department of Psychology

UNIVERSITÉ YORK UNIVERSITY

FACULTY OF ARTS

4700 KEELE STREET • NORTH YORK • ONTARIO • CANADA • M3J 1P3

threshold fell approximately tenfold as presentation duration was increased from 0.05 to 1.0 sec. Figure 2 also shows discrimination threshold improved rapidly as inspection duration was increased from about 0.05 to 0.15 sec, then more slowly as duration increased beyond about 0.15 sec. For subjects 1 and 2 discrimination was still slowly improving at the longest duration of 1.0 sec (Fig. 2A, B). Inspection duration had a much weaker effect on orientation discrimination for LD bar than for an MD bar. Similar findings have been reported for shape discrimination.[34] If we can extrapolate these laboratory findings to the everyday visual situation, they imply that orientation discrimination for objects rendered visible by motion parallax rapidly worsens relative to orientation discrimination for contrast-defined objects as inspection duration is reduced below about 0.15 sec.

At first sight the findings just described might suggest that the neural mechanism(s) underlying orientation discrimination operate less effectively at low presentation durations and low dot lifetimes, and that this falloff of performance is more severe for MD form than for LD form. However, short presentation duration *per se* is not the only possible reason for these elevations of orientation discrimination threshold: a second possible cause is that bar visibility is reduced at short presentation durations and short dot lifetimes, and that the visibility to MD bars falls off more rapidly than the visibility of LD bars. In Helmholtz's everyday world motion parallax and also in the laboratory situation of Fig. 2 the effects of presentation duration on spatial discrimination are confounded with the effects of presentation duration on the visibility of the MD form. The next section concludes that the effect of presentation duration shown in Fig. 2 is almost entirely due to changes in bar visibility.

Orientation discrimination for bars normalized with respect to bar detection threshold

Noting that the visibility of MD bars was created by the difference in dot velocity inside and outside the bar, while the visibility of LD bars was created by the difference in dot luminance

Department of Psychology

UNIVERSITÉ YORK UNIVERSITY

FACULTY OF ARTS

4700 KEELE STREET • NORTH YORK • ONTARIO • CANADA • M3J 1P3

between dots inside and outside the bar we used the detection threshold speed data for MD bars shown in Fig. 4 to normalize the orientation discrimination data for MD bars shown in Figs. 6 and 7, and we used the detection threshold luminance contrast data for LD bars shown in Fig. 5 to normalize the orientation discrimination data for LD bars shown in Figs. 8 and 9. Figure 10 shows the effect of presentation duration on orientation discrimination for MD bars whose dot speeds were some fixed multiple (N_S) of the relevant bar detection speed threshold. Curves are shown for 7 values of N_S (2, 4, 8, 10, 15, 20 and 25). Similarly, Fig. 11 shows the effect of dot lifetime on orientation discrimination for MD bars whose dot speeds gave the same 7 fixed multiples of the relevant bar detection speed thresholds. Figure 12 shows the effect of presentation duration on orientation discrimination for LD bars whose luminance contrasts were some fixed multiple (N_L) of the relevant bar detection luminance contrast threshold. Curves are shown for 7 values of N_L (2, 4, 8, 10, 15, 20 and 25). Similarly, Fig. 13 shows the effect of dot lifetime on orientation discrimination for LD bars whose luminance contrasts were adjusted to give the same 7 fixed multiples of the relevant bar detection luminance contrast thresholds. This way of presenting our data leads to the following conclusions: (1) the accelerating rise of orientation discrimination threshold for MD bars at low presentation durations evident in Fig. 2 (solid circles) was completely abolished when MD bar visibility was normalized relative to bar detection threshold (Fig. 10); (2) the accelerating rise of orientation discrimination threshold for MD bars at low dot lifetimes evident in Fig. 3 (solid circles) was abolished and even reversed when MD bar visibility was normalized relative to bar detection threshold (Fig. 11); (3) the rise of orientation discrimination threshold for LD bars at low presentation durations evident in Fig. 2 (open circles) was completely abolished when LD bar visibility was normalized relative to bar detection threshold (Fig. 12).

These findings are consistent with the following hypotheses: (A) visibility for MD bars of different presentation durations is the same if dot speed for all the bars is the same multiple (N_S) of

Department of Psychology
UNIVERSITÉ YORK UNIVERSITY
FACULTY OF ARTS
4700 KEELE STREET • NORTH YORK • ONTARIO • CANADA • M3J 1P3

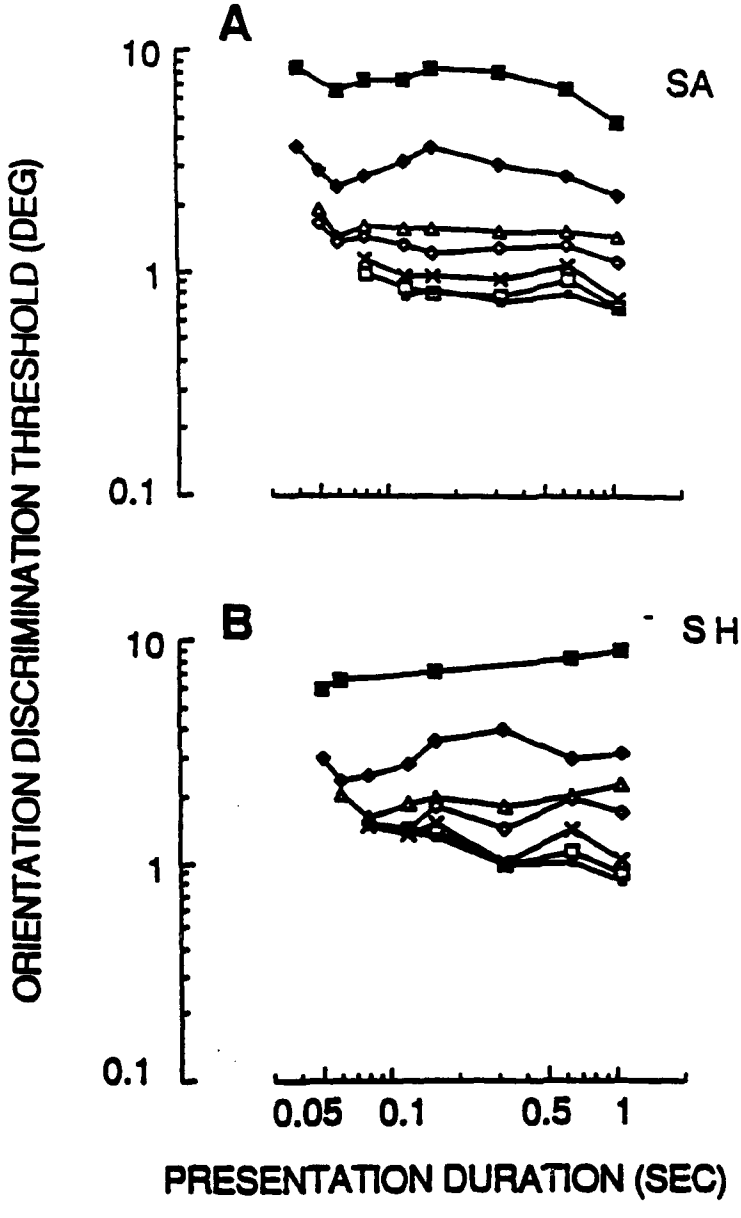

Figure 10. Orientation discrimination threshold (ordinates) versus presentation duration (abscissae) for a dotted bar defined by relative motion. Along any given curve, every point was recorded at a dot speed that was the same fixed multiple (N) of the relevant bar detection threshold. Thus, along any given curve, every point was recorded at a different dot speed. Key: ■, N=2; ◆, N=4; Δ, N=8; ◊, N=10; ×, N=15; □, N=20; ■, N=25. Dot lifetime was equal to presentation duration. A, subject 1. B, subject 2.

Department of Psychology

UNIVERSITÉ YORK UNIVERSITY

FACULTY OF ARTS

4700 KEELE STREET • NORTH YORK • ONTARIO • CANADA • M3J 1P3

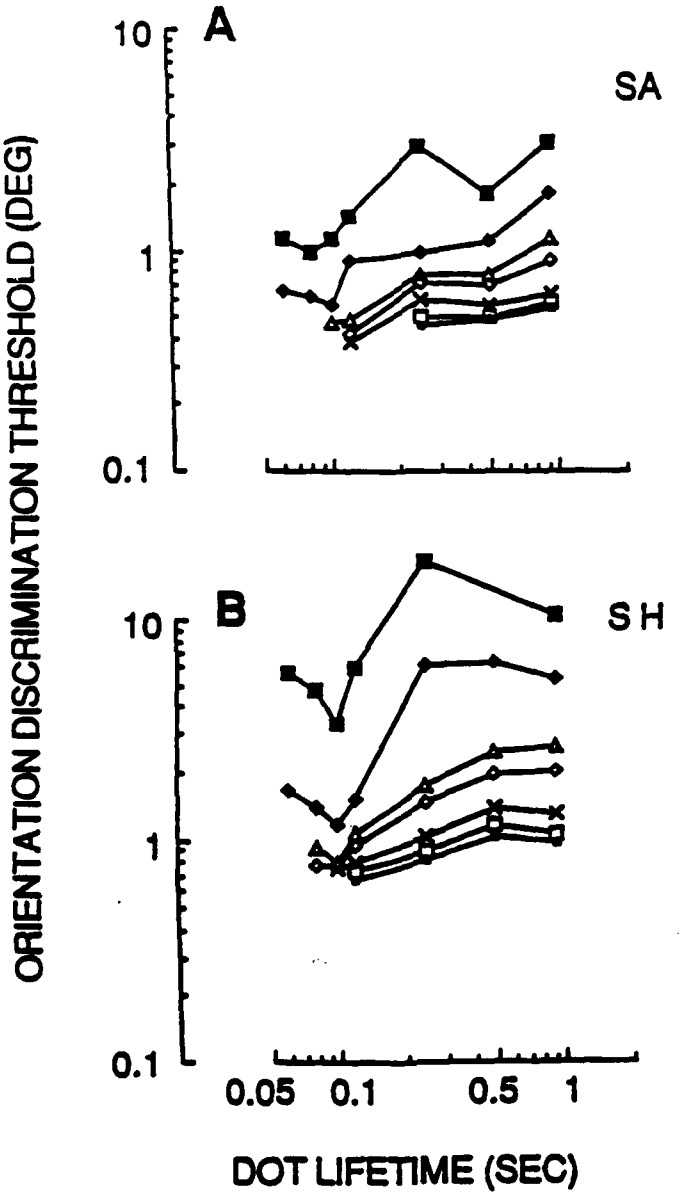

Figure 11. Orientation discrimination threshold (ordinates) versus dot lifetime (abscissae) for a dotted bar defined by relative motion. Along any given curve, every point was recorded at a dot speed that was the same fixed multiple (N) of the relevant bar detection threshold. Thus, along any given curve, every point was recorded at a different dot speed. Key to symbols as in Fig. 10. A, subject 1. B, subject 2.

Department of Psychology

UNIVERSITÉ YORK UNIVERSITY

FACULTY OF ARTS

4700 KEELE STREET • NORTH YORK • ONTARIO • CANADA • M3J 1P3

the relevant bar detection speed threshold; (B) bar visibility for LD bars of different presentation durations and dot lifetimes is the same if dot contrast for all the bars are the same multiple (N_L) of the relevant bar detection luminance contrast threshold; (C) the visibility of an MD bar of any given presentation duration is equal to the visibility of an LD bar of any given presentation duration or dot lifetime provided that $N_S = N_L$.

Out of the four conditions tested in Fig. 10–13, only one does not follow the rule that orientation discrimination is the same for any given value of N_S or N_L. This exception is the effect of dot lifetime on orientation discrimination for MD bars where discrimination was better at short dot lifetimes when N_S was held constant (Fig. 11). This effect was in the opposite direction to the effect of dot lifetime when dot speed rather than N_S was held constant (Fig. 3).

The data of Figs. 10 and 12 provide a means of addressing the question whether the absolute value of orientation discrimination threshold is approximately the same for MD and LD bars of matched visibilities over a range of visibilities and presentation durations. To a first approximation, discrimination thresholds were the same for MD and LD bars (no more than 50% difference) at high levels of visibility ($N_S = N_C = 10$ or more) though, in all cases, thresholds for MD bars were higher than for LD bars. At low levels of visibility ($N_S = N_C = 4$ or less) discrimination threshold remained higher for MD than for LD bars at all presentation durations, and for subject 1 (Figs. 10A and 12A) the difference was substantial (about 4:1).

Theoretical implications: hierarchical stages of processing for MD and LD form

We have previously suggested (Ref 182) that orientation discrimination for MD bars can be described in terms of the following sequence of processing stages: (Stage 1M) *Orientation-tuned filters* sensitive to MD (i.e. kinetic) edges that achieve figure-ground segregation and mediate detection for motion-defined form. We suppose that the orientation tuning bandwidths are considerably broader than 0.6 deg, and that all orientations are represented. (Stage 2M) *An opponent-*

Department of Psychology
UNIVERSITE YORK UNIVERSITY
FACULTY OF ARTS
4700 KEELE STREET • NORTH YORK • ONTARIO • CANADA • M3J 1P3

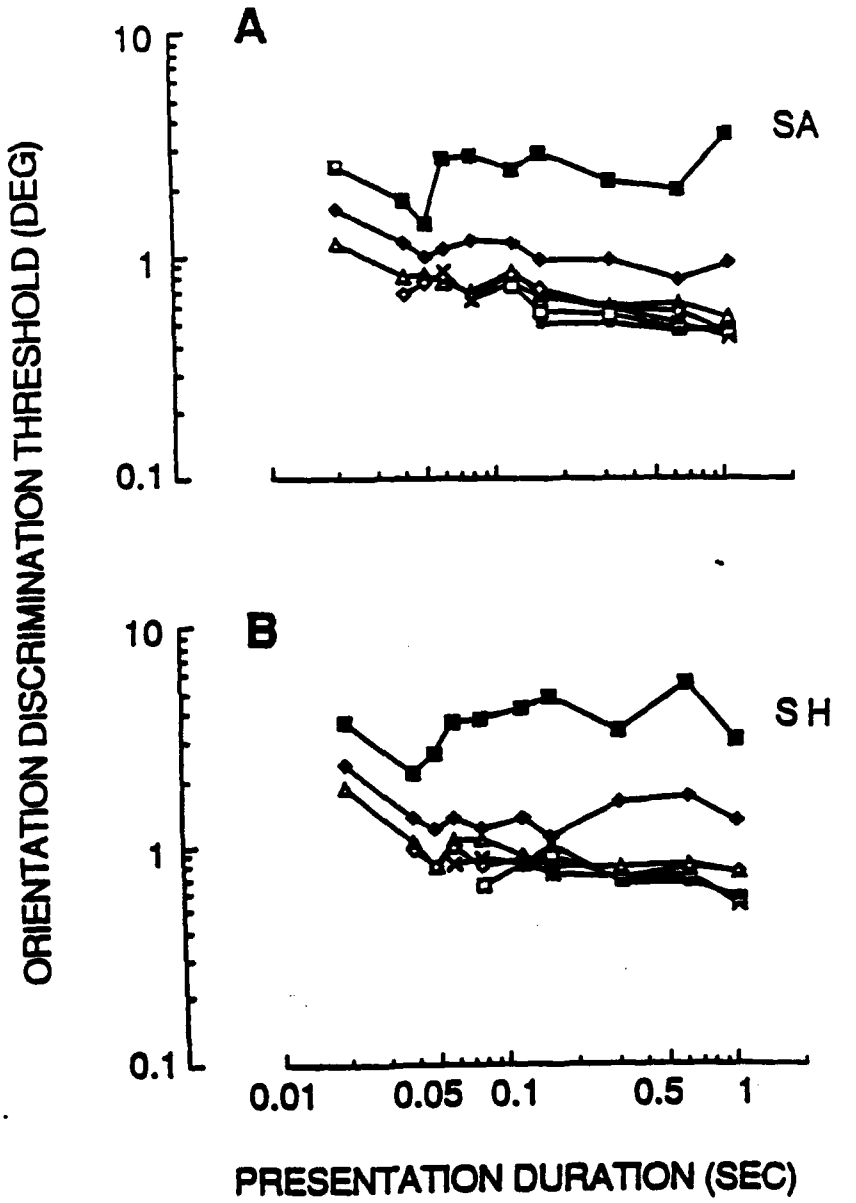

Figure 12. Orientation discrimination threshold (ordinates) versus presentation duration (abscissae) for a dotted bar defined by luminance contrast. Along any given curve, every point was recorded at a dot contrast that was the same fixed multiple (N) of the relevant bar detection threshold. Thus, along any given curve, every point was recorded at a different dot contrast. Key to symbols as in Fig. 10. Dot lifetime was equal to presentation duration. A, subject 1. B, subject 2.

Department of Psychology
UNIVERSITÉ YORK UNIVERSITY
FACULTY OF ARTS
4700 KEELE STREET • NORTH YORK • ONTARIO • CANADA • M3J 1P3

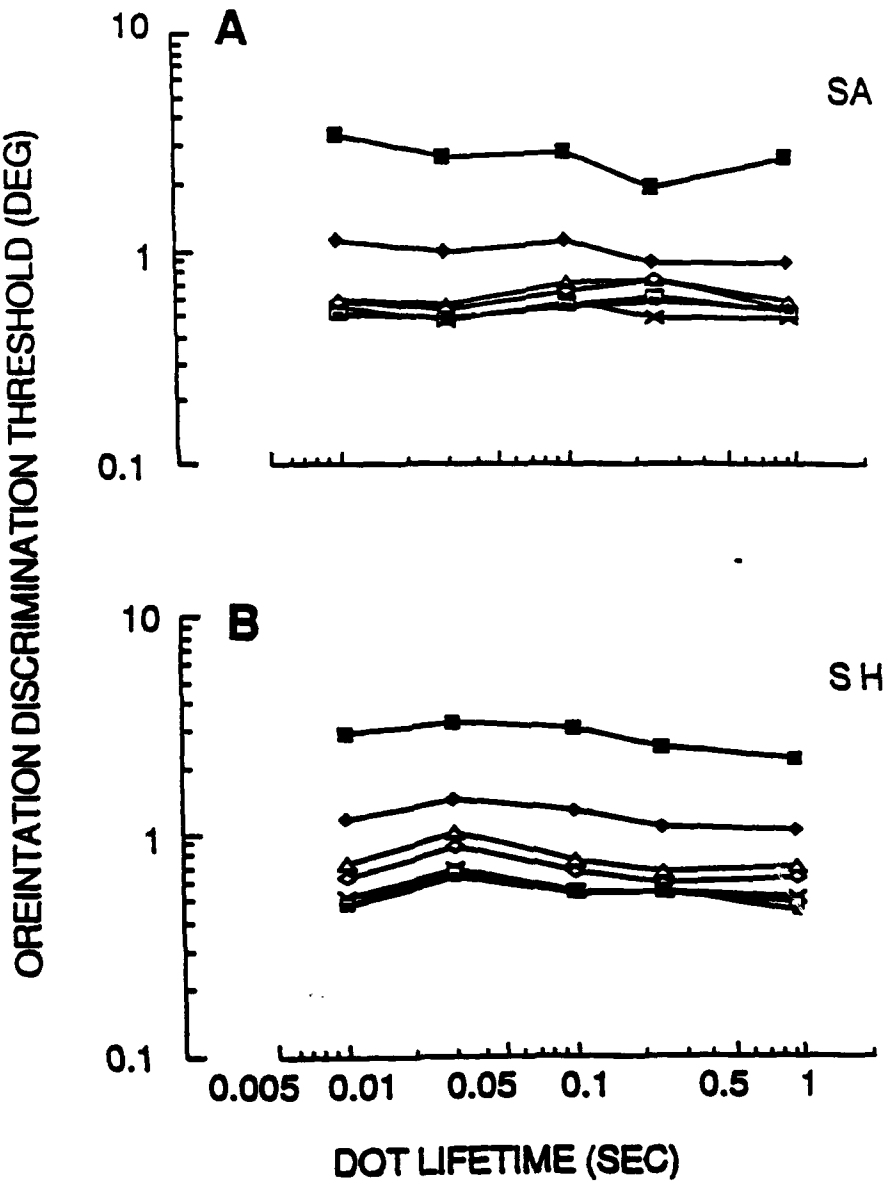

Figure 13. Orientation discrimination threshold (ordinates) versus dot lifetime (abscissae) for a dotted bar defined by luminance contrast. Along any given curve, every point was recorded at a dot contrast that was the same fixed multiple (N) of the relevant bar detection threshold. In general, therefore, along any given curve, every point was recorded at a different dot contrast. Key to symbols as in Fig. 10. Presentation duration was 1.0 sec. A, subject 1. B, subject 2.

Department of Psychology

UNIVERSITÉ YORK UNIVERSITY

FACULTY OF ARTS

4700 KEELE STREET • NORTH YORK • ONTARIO • CANADA • M3J 1P3

orientation stage that receives input from stage 1M and that determines orientation discrimination. In order to account for the finding that the best values of orientation discrimination for MD form are 0.3–0.6 deg (Ref 182) we suppose that discrimination is determined by the pattern of activity within the set of orientation-tuned filters.

A proposed hierarchical model of orientation discrimination for LD bars and gratings is as follows. Retinal image information passes first through orientation-tuned filters that achieve figure-ground segregation by responding to bars or gratings defined by luminance contrast (stage 1L), and this first stage feeds a second, opponent-orientation, stage that determines orientation discrimination (stage 2L) (Refs 145, 155). The model is intended to explain the discrepancy between the 0.3–0.6 deg best values of orientation discrimination and the 10–20 deg orientation tuning bandwidths of psychophysical channels in human or of striate cortical neurons in monkey.[7-11] An alternative model has been expressed in line-element rather than opponent-process format.[12-14] In principle, the two kinds of model are equivalent when both are linear. However, they are not necessarily equivalent when they are nonlinear.[15] But in the present context a more important difference is that opponent-process models assert that there exists in the brain a physical mechanism that carries out the opponent computation, whereas this physical mechanism is not explicit in line element models.[15]

Here we suggest that MD bars whose dot speeds are N times above detection threshold provide the same input to the discrimination stage (stage 2M above). This hypothesis is supported empirically in the case that presentation duration is the independent variable (Fig. 10). According to this line of thought, the discrimination stage 2M for MD bars is not directly affected by presentation duration. Similarly, for LD bars, the data of Fig. 12 lead us to conclude that the discrimination stage 2L above for LD bars is not directly affected by presentation duration.

For large values of N_S the effect of dot lifetime on orientation discrimination for MD bars is

Department of Psychology

UNIVERSITÉ YORK UNIVERSITY

FACULTY OF ARTS

4700 KEELE STREET • NORTH YORK • ONTARIO • CANADA • M3J 1P3

approximately the same as the effects of presentation duration (Figs. 10 & 11). However, for low values of N_S there are differences between the effects of dot lifetime and presentation duration upon orientation discrimination. In particular, discrimination is better for short than for long dot lifetimes in Fig. 11 rather than being worse as in Fig. 3. The most likely explanation for this reversal was that our bar detection data (Fig. 4) were incorrect so that we had overcompensated for reduced bar visibility at short durations. We therefore repeated the measurements of bar detection threshold versus dot lifetime for MD bars using a quite different procedure (see above). Detection thresholds, however, were essentially unchanged. We conclude that either the output of stage 1M is not constant for MD bars whose visibility is normalized relative to bar detection speed threshold, or the operation of the discrimination stage 2M is more effective at shorter than at longer dot lifetimes.

Is orientation discrimination for MD and LD bars determined by different neural mechanisms?

In comparing orientation discrimination for MD and LD form we proposed the following two alternative hypotheses: (a) the same neural mechanism determines orientation discrimination for MD and LD form; (b) different and independent neural mechanisms determine orientation discrimination for MD and LD form (Ref 182). The above hypotheses on orientation discrimination focus on one aspect of the broader question whether spatial discrimination in general are determined by different neural mechanisms for MD and LD form. In this more general context, data on normally-sighted subjects that are not consistent with the strongest form of hypothesis (a) include the effects of dot density on visual acuity for MD and LD letters (Ref 190) and on vernier acuity for MD and LD bars.[16] In both cases, spatial discrimination is similar for MD and LD form at low dot densities, but is superior for LD form at high dot densities. Below we report that data on patients are definitely inconsistent with hypothesis (a) above, but are consistent with hypothesis (b).

Department of Psychology

UNIVERSITÉ YORK UNIVERSITY

FACULTY OF ARTS

4700 KEELE STREET • NORTH YORK • ONTARIO • CANADA • M3J 1P3

3.2 Long Term Aim 1.1.1 and Specific Aim 1.2.1

Four papers have been published (Refs 197, 213, 214, 215), and two have been submitted (Refs 230, 234).

The broad question addressed here is whether spatial discriminations for motion-defined (MD) form and for luminance-defined (LD) form share a common neural mechanism. This question was brought to a head by our findings that the best values of orientation discrimination (Ref 182), shape discrimination (Ref 196) and vernier acuity (Ref 157) are approximately the same for MD and LD form.

We have addressed the question by measuring detection and discrimination for MD and LD form in patients. Our rationale is that a *selective* loss of a given visual capability provides evidence that the capability is mediated by a separate neural mechanism (Ref 115). We have used this argument before to explain our finding that some patients with multiple sclerosis experience selective contrast sensitivity loss for low and/or intermediate spatial frequencies (Refs 64, 89) and that about 20% of the normal population has visual field defects for stereomotion (Refs 159, 181).

As stimuli, we used a dot pattern displayed on a PC (Ref 190). The dot pattern could contain a perfectly camouflaged MD letter (Fig. 14A). The letter could be made visible to the normally-sighted eye by moving dots inside the letter at equal and opposite speed to dots outside the letter (Fig 14B). By switching dots off outside the letter we created a dotted LD letter of variable contrast (Fig. 14C). Figures 14E-G show why we moved dots inside and outside the letter at equal speeds in opposite directions. If the speeds (Fig. 14F) or directions of motion (Fig. 14G) differ, the letter can be seen by *texture contrast* so that the stimulus confounds the processing of motion contrast and the processing of texture contrast. Only for the equal-speed case (Fig. 14B) is the texture contrast cue absent.

In the first study we examined 50 control subjects and 25 patients with multiple sclerosis

Department of Psychology

UNIVERSITÉ YORK UNIVERSITY

FACULTY OF ARTS

4700 KEELE STREET • NORTH YORK • ONTARIO • CANADA • M3J 1P3

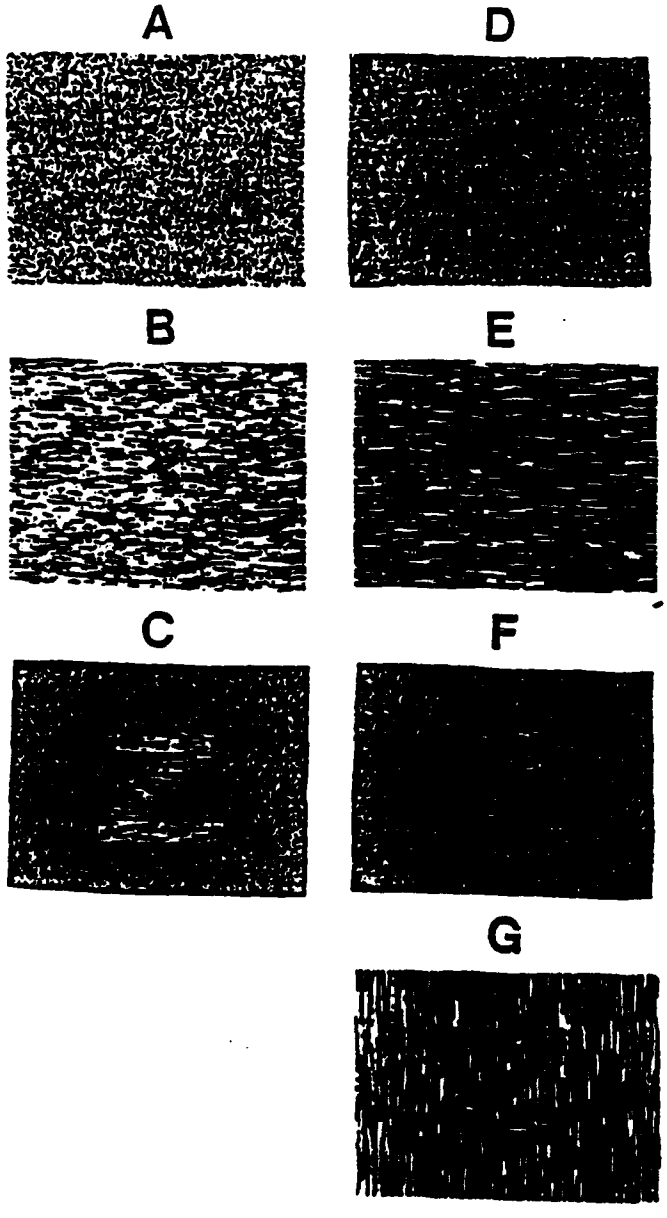

Figure 14. A, a letter was perfectly camouflaged within this pattern of dots. Dot density was 25%. B, dots within the letter moved rightwards at speed V while dots outside the letter moved leftwards at the same speed V. This motion rendered the letter visible to the eye but, as illustrated here, the letter was almost invisible to the camera because the edges of the letter were defined only by an abrupt change in the direction of motion. C, a contrast-defined letter was created by switching off all the dots outside the letter. D, as for A, but dot density was 2%. E, as for B, but dot density was 2%. F, as for E except that all dots outside the letter were stationary. G, as for E except that dots outside the letter moved vertically while dots inside the letter moved horizontally.

Department of Psychology

UNIVERSITE YORK UNIVERSITY

FACULTY OF ARTS

4700 KEELE STREET • NORTH YORK • ONTARIO • CANADA • M3J 1P3

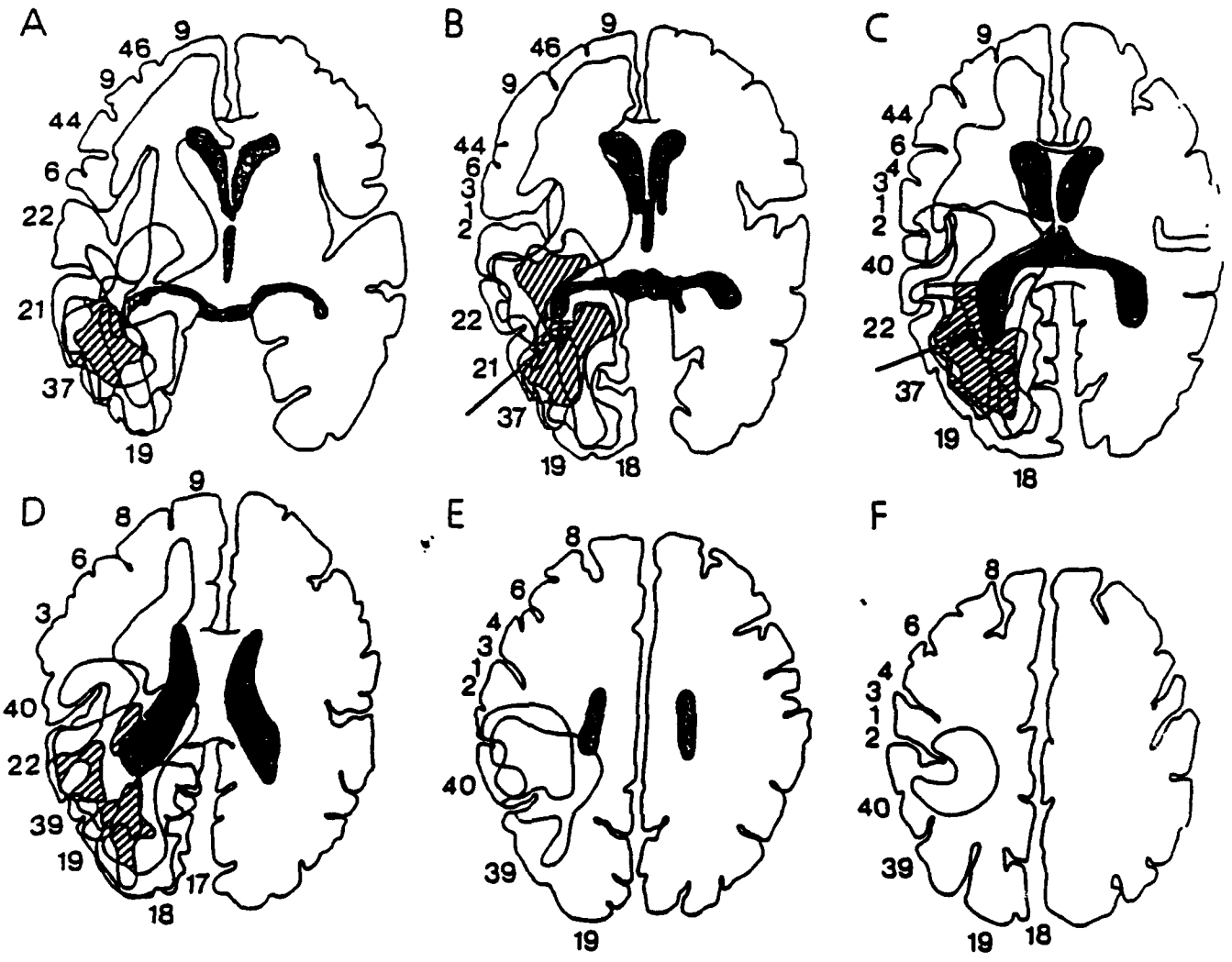

Figure 15. The outlines mark the lesion boundaries delineated by CT in 7 patients with unilateral cerebral hemisphere damage who had abnormal speed thresholds for recognizing motion-defined letters. Lesions are plotted onto 6 templates of axial brain anatomy. The templates represent slices approximately 8 mm apart, oriented 15 deg above the orbitomeatal line. Ventricles are marked in solid black. Brodmann numbers of adjacent cortical areas are marked. For explanatory purposes, all lesions are plotted only the right hemisphere. Hatching shows regions of overlap of 3 or more lesions. The black areas indicated by arrows in B and C indicate overlap between the lesions in 5 patients.

Department of Psychology

UNIVERSITÉ YORK UNIVERSITY

FACULTY OF ARTS

4700 KEELE STREET • NORTH YORK • ONTARIO • CANADA • M3J 1P3

(Ref 197) and in the second study we examined 25 control subjects and 10 patients with multiple sclerosis (Ref 216).

In the first study we found that elevated speed threshold for recognizing MD letters is common (34/50 eyes). In 10 eyes, recognition for MD letters was abnormal while contrast sensitivity for the same letters was normal, and visual (Snellen) acuity was normal for solid letters of 100% and 11% contrast. In the second study, 6 of 10 patients showed impaired *recognition* for MD letters although *detection* of the same letters was normal, as was visual acuity for letters of 100% and 11% contrast, speed threshold for detecting motion, and speed threshold for discriminating leftwards from rightward motion.

We conclude that: (1) spatial discrimination for MD and LD shapes are not entirely mediated by the same mechanism and intersubject differences in the ability to process MD shape is not predicted by the ability to process LD shape; (2) motion is processed in a hierarchical manner; (3) discrimination and detection can be dissociated for MD form.

A limitation of these two studies is that we did not know the sites of the neural damage that caused the visual loss. Therefore, we carried out a similar study on 20 control subjects and 13 patients who had experienced neurosurgery to remove unilateral hemispheric lesions (Ref 213). Seven patients lost ability to recognize MD letters while visual acuity for letters of 100% and 11% contrast was spared, as was speed thresholds for detecting motion and for discriminating leftward from rightward motion. Figure 15 shows tracings of axial CAT scans for these patients. The lesions are demarcated by lines. The arrow shows the area of overlap in white matter underlying striate cortex. We concluded that damage to the overlap area shown in Fig. 15 produces a specific loss of the ability to process MD form. We suggest that homologs of the so-called motion and color/form pathways (i.e. areas V1/MT/MST/7a and areas V1/V4/IT) are interconnected to form a distributed system that is important for recognizing MD form. We attribute the pattern of visual

Department of Psychology

UNIVERSITÉ YORK UNIVERSITY

FACULTY OF ARTS

4700 KEELE STREET • NORTH YORK • ONTARIO • CANADA • M3J 1P3

loss to damage to this system including damage to the interconnections between the cortical pathways just mentioned and possibly also the disruptions of connections between visual cortical areas and subcortical nuclei.

3.3 Experiment 2 and Specific Aim 1.2.1

This experiment has been completed. Part of the results have just been published (Ref 196, *Perception*, 1991, 20, 315-336) and part has been submitted (Ref 232).

We generated a camouflaged rectangular shape that was visible by motion alone. The rectangular area was rendered visible by moving the dots inside the rectangle obliquely downwards to the left at a constant speed that was equal and opposite to the speed of the dots in the remainder of the pattern. The reason for choosing oblique motion was to ensure that the rectangle's vertical and horizontal edges were all defined by the same mix of shearing and compressive motion. Although the rectangle was visible to the eye, a photographic time exposure did not reveal it (Fig. 16B). Contrast-defined rectangles were created by switching off all dots outside the rectangle (Fig. 16C). The ratio between the lengths of vertical and horizontal sides had 10 possible values, and these were presented randomly. The subject's task was to press one of two buttons depending on whether the longer sides were vertical or horizontal. To ensure that both dimensions must be compared in order to perform the task correctly, different areas of rectangle were interleaved randomly as illustrated in Fig. 17. To ensure that the distance of any edge from the boundary of the display provides no cue to shape, the rectangle's location was jittered randomly. Shape discrimination threshold was measured by two-alternative forced choice and Probit analysis.

We measured shape discrimination as a function of dot speed and dot contrast for camouflaged dotted rectangles and for uncamouflaged dotted rectangles. Figure 18 shows that, when dot speed and contrast were both high, aspect ratio discrimination threshold was as acute for a motion-

Department of Psychology
UNIVERSITÉ YORK UNIVERSITY
FACULTY OF ARTS
4700 KEELE STREET • NORTH YORK • ONTARIO • CANADA • M3J 1P3

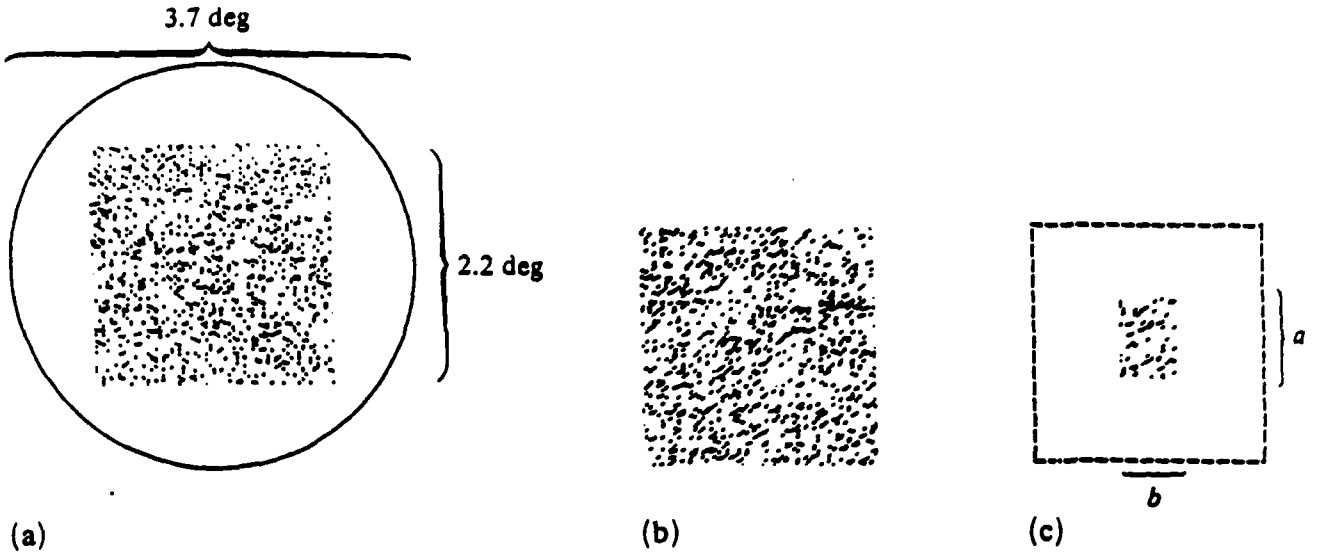

Figure 16. A – Photograph of a typical random dot pattern. The test rectangle was perfectly camouflaged. The outer circle marks the edge of the superimposed adapting field. B – Dots within the rectangle and outside the rectangle were moved at equal and opposite speeds. Although the rectangle was evident to the eye, it was not evident to the camera. C – All dots outside the rectangle were switched off to create an uncamouflaged rectangle. Aspect ratio was defined as a/b.

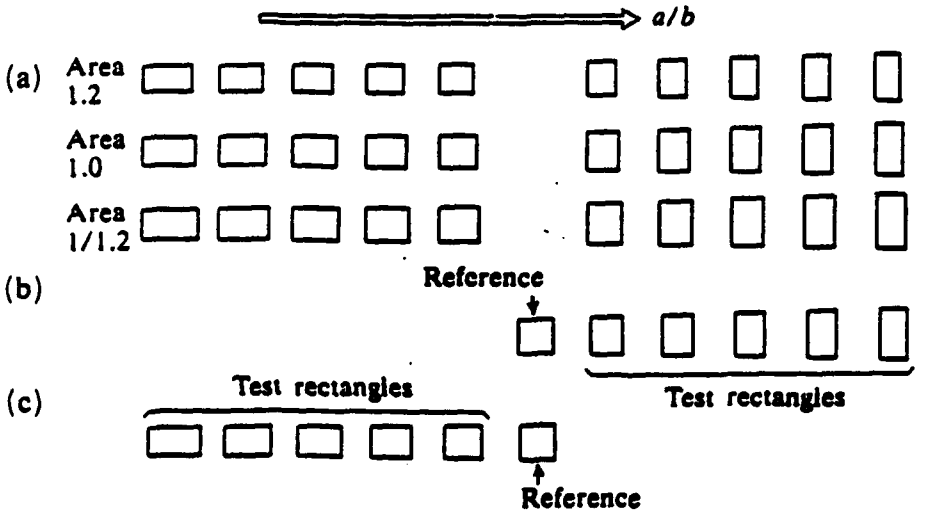

Figure 17. Dissociation of aspect ratio a/b from area and from any given linear dimension.

Department of Psychology
UNIVERSITÉ YORK UNIVERSITY
FACULTY OF ARTS
4700 KEELE STREET • NORTH YORK • ONTARIO • CANADA • M3J 1P3

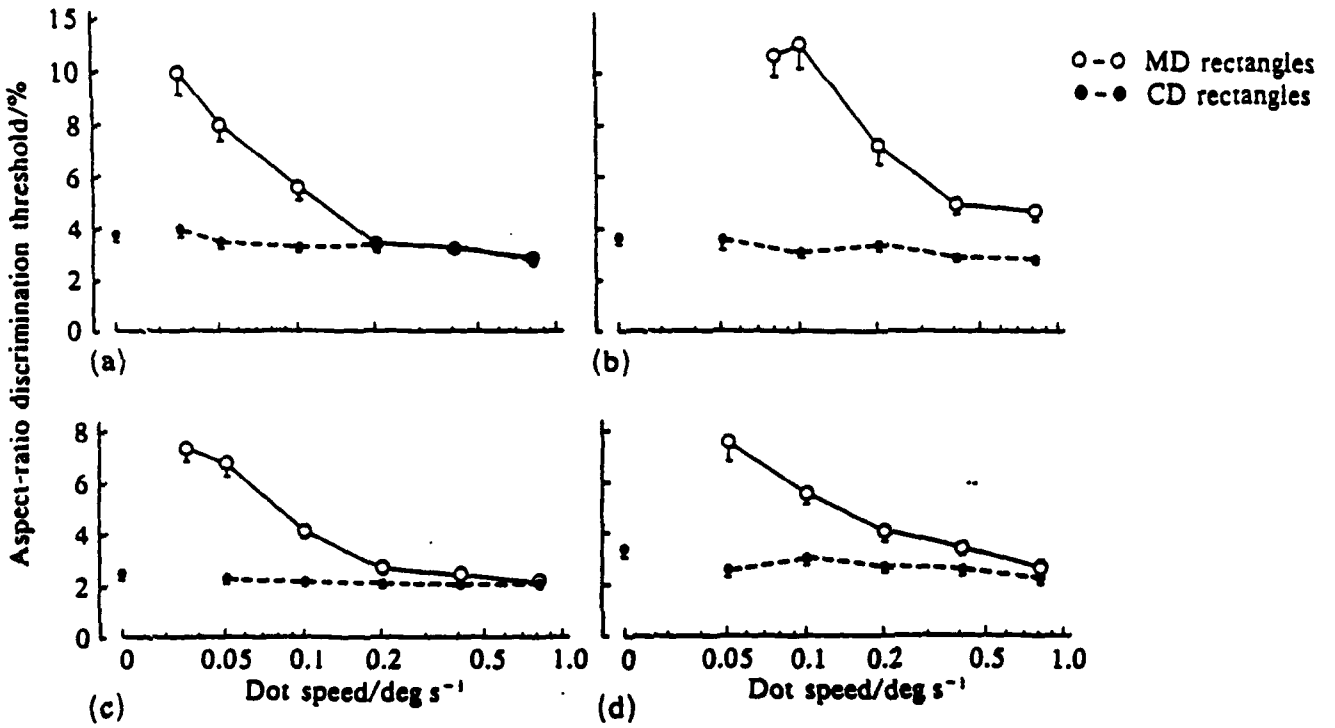

Figure 18. Ordinates plot shape discrimination thresholds D (a/b) expressed as a percentage, where D (a/b) is the smallest discriminable change in the ratio D (a/b). Abscissae plot dot speed (relative speed is twice dot speed). Open circles are for motion-defined rectangles and filled circles are for uncamouflaged rectangles. Dot contrast in B and D was 0.6 log units less than in A and C. The leftmost filled circle in each panel is for zero speed. A,B – subject 1. C,D – subject 2. Viewing was monocular.

Department of Psychology

UNIVERSITÉ YORK UNIVERSITY

FACULTY OF ARTS

4700 KEELE STREET • NORTH YORK • ONTARIO • CANADA • M3J 1P3

defined rectangle as for a contrast-defined rectangle and, at 2-3%, corresponded to a change of side length of about 24 arc sec. This is a remarkable visual performance, given that the mean dot separation was about 360 arc sec. Discrimination collapsed at low dot speeds and could not be measured at speeds less than about 0.1–0.2 deg/sec for motion-defined rectangles, but was almost unaffected by dot speed for contrast-defined rectangles. To explain how the visual system can dissociate changes of shape from changes of area we invoked a previous suggestion that the visual system contains a mechanism that compares the separation of pairs of contours along perpendicular azimuths. To explain the coincidence of shape discrimination thresholds for motion-defined and contrast-defined rectangles we suggest that in early visual development the underlying neural mechanisms are driven by the same environmental and behavioral pressures towards a common endpoint. In other words, "spatial vision is spatial vision" and the performance required for eye-hand coordination that is dictated by the outside environment independently of how the eye segregates figure from ground. This idea could also explain why orientation discrimination asymptotes towards the same value for motion-defined and contrast-defined bars.

3.4 Experiment 5

We have constructed a faster version of our dot generator (Ref 130) suitable for binocular stereoscopic stimulation. The new dot generator drives two electrostatic (Tektronix type 608) monitors that have been mounted in a rigid Wheatstone mirror stereoscope. Left and right eyes see independent 100 frames/sec displays. The equipment has been calibrated for the two protocols of Experiment 5, and preliminary measurements are underway.

3.5 Experiment 6

This experiment is completed. One paper is in press in *Vision Research* (Ref 212 below) and a report was presented at ARVO 1992. A second paper is in preparation (Ref 236 below).

Department of Psychology

UNIVERSITÉ YORK UNIVERSITY

FACULTY OF ARTS

4700 KEELE STREET • NORTH YORK • ONTARIO • CANADA • M3J 1P3

It was pointed out by Hoyle[31] in an astronomical context that, if an object is moving at constant speed along the line of sight towards the eye, then at time t = 0

$$T_0 = \frac{\theta_0}{\dot{\theta}_0} \quad \ldots\ldots (1)$$

where T_0 is the time to contact at time t = 0, θ_0 is the object's angular subtense (i.e. the angle subtended at the eye by the object) at time t = 0, and $\dot{\theta}_0$ is the object's rate of increase of angular subtense at time t = 0. (We assume that θ_0 is small.) In previous AFOSR-funded research we suggested that this geometrical fact is used by pilots (Refs 81, 86, 93, 104, 115, 119, 126) following a previous suggestion by Lee that the equation is used in driving[17] (see also [18-22] and Refs 163, 200). There is evidence that the visual pathways of humans and animals contain neural mechanisms sensitive to the angular size (θ) of a stimulus.[23-26] Also, we and others have reported evidence for neural mechanisms sensitive to the rate of expansion, $\dot{\theta}$ (Refs 72, 83-85, 90) and [27-29]. However evidence that the visual pathway is separately sensitive to θ and to $\dot{\theta}$ does not necessarily imply either (A) that the visual pathway contains a mechanism sensitive to the unitary higher-order variable ($\theta/\dot{\theta}$), nor (B) that such a mechanism is important in judging time to contact.

We have carried out an experiment designed to find whether subjects are sensitive to the unitary higher-order variable ($\theta/\dot{\theta}$) by requiring subjects to make discriminations based exclusively on differences in ($\theta/\dot{\theta}$). We have also measured discrimination thresholds for rate of expansion ($\dot{\theta}$) with changes in time to contact removed as a reliable cue.

First we must derive the relationship between time t and the angular subtense (θ_t) of an object that is moving towards the eye at constant speed along the line of sight. Figure 19 illustrates the case that a rigid spherical object of diameter 2S is moving along the z axis at constant linear speed v_z towards the eye. For our present purpose we define the z axis as the line passing through the eye's two nodal points. The situation depicted in Fig. 19 is at time t, when the object's angular

Department of Psychology

UNIVERSITÉ YORK UNIVERSITY

FACULTY OF ARTS

4700 KEELE STREET • NORTH YORK • ONTARIO • CANADA • M3J 1P3

subtense is $2\theta_t$ and the time to contact is T_t. (More exactly, T_t is the time that would be taken for the center of the sphere to reach the first nodal point N_1.) From Fig. 19 we have

$$\tan\theta_t = \frac{S}{D_t} \quad \text{.....(2)}$$

and

$$D_t = D_0 - v_z t \quad \text{.....(3)}$$

where D_0 and D_t are, respectively, the distance from the center of the sphere to point N_1 at time $t = 0$ and at time t.

From equations (2) and (3)

$$\tan\theta_t = \frac{S/D_0}{1-(v_z/D_0)t} \quad \text{.....(4)}$$

Since

$$v_z T_0 = D_0 \quad \text{.....(5)}$$

where T_0 is the time to contact at time $t = 0$, we have from Equation 4 the exact solution

$$\tan\theta_t = \frac{\tan\theta_0}{1-t/T_0} \quad \text{.....(6)}$$

where θ_0 is the object's angular subtense at time $t = 0$.

Figure 20 is a graph of Equation 6. As t approaches T_0, the value of θ_t increases at an accelerating rate, and reaches 90 deg at $t = T_0$. For practical reasons it was necessary to limit the percentage variation of angular size in our experiments, so we restricted ourselves to the part of the Fig. 20 curve between $t = 0$ and $t = 0.66T_0$.

A bright solid sharp-edged constant-luminance square was generated on a monitor (a Tektronix model 608 with P31 phosphor) by a special-purpose hardware square generator of our own design and construction. The frame rate was 104 Hz and there were 240 lines. The luminance of the square was 86 cd/m^2. Because the square generator was of analogue electronic design rather than being a pixel-based system, square size could be altered by indefinitely small amounts and indefinitely slowly while sampling remained at 104 Hz.

Department of Psychology
UNIVERSITÉ YORK UNIVERSITY
FACULTY OF ARTS
4700 KEELE STREET • NORTH YORK • ONTARIO • CANADA • M3J 1P3

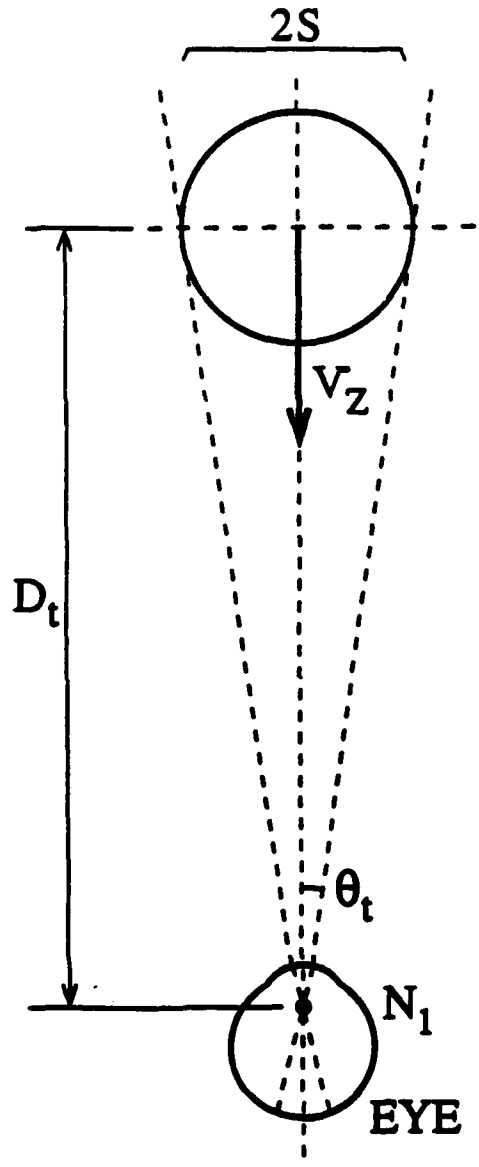

Figure 19. A rigid sphere of diameter 2S is shown moving at constant speed v_z along a line passing through the first nodal point of the eye (N_1). At time t the distance from N_1 to the center of the sphere is D_t, and the angular subtense of the ball at the eye is $2\theta_t$.

Department of Psychology

UNIVERSITÉ
YORK
UNIVERSITY

FACULTY OF ARTS

4700 KEELE STREET • NORTH YORK • ONTARIO • CANADA • M3J 1P3

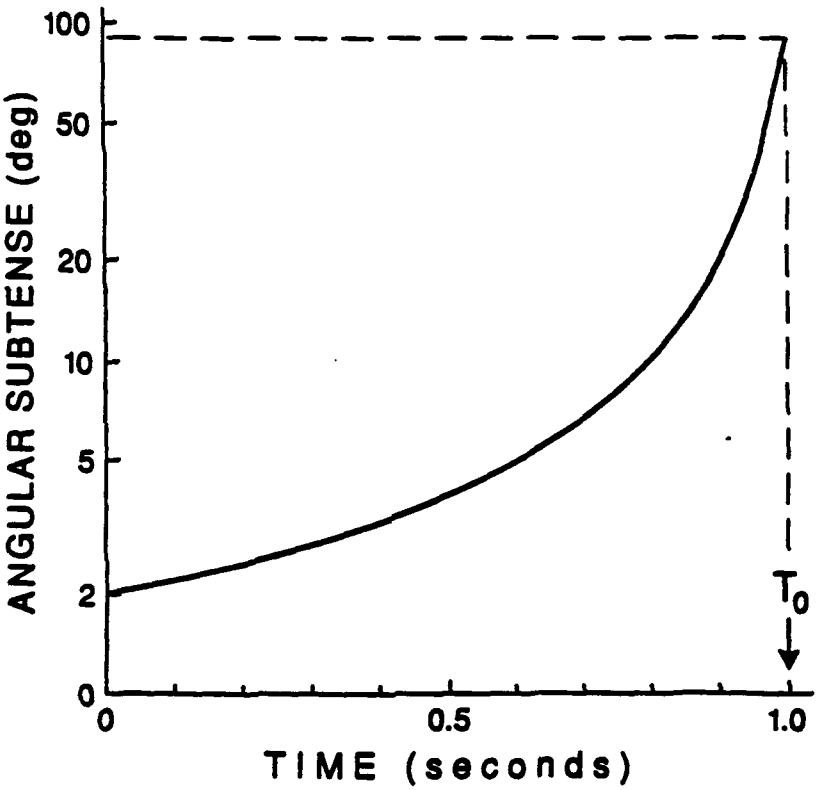

Figure 20. Ordinates plot the angular radius of the sphere shown in Fig. 1 as it approaches the eye at constant speed along the line of sight. Abscissae plot time as a fraction of T_0. In the case illustrated, angular radius is 2.0 deg at t = 0. Key: θ_t, the sphere's angular radius at time t; T_0, time to contact at time t = 0.

Department of Psychology

UNIVERSITÉ YORK UNIVERSITY

FACULTY OF ARTS

4700 KEELE STREET • NORTH YORK • ONTARIO • CANADA • M3J 1P3

Our major problem was to demonstrate experimentally that subjects really did use the cue they were told to use when carrying out the task. We did this by implementing the psychophysical matrix procedure described in the original grant proposal. This can be understood by refering to Fig. 21 which shows a matrix of 8 x 8 stimuli where variable r was $\theta/\dot{\theta}$ (i.e. time to contact) and variable s was rate of expansion ($\dot{\theta}$). The matrix is set out so that $\theta/\dot{\theta}$ increased from left to right, while $\dot{\theta}$ increased vertically. The 8 values of r and s followed the same geometrical progression as $n^{-1.0}$, $n^{-0.75}$, $n^{-0.5}$, $n^{-0.25}$, $n^{0.25}$, $n^{0.5}$, $n^{0.75}$ and $n^{1.0}$ where n was a fixed number that set the difficulty of the task. The computer delivered the 64 stimuli in random order. In the first experiment, the subject's task was to judge whether the stimulus would arrive sooner or later than the mean of the stimulus set (of 64). Three sessions were carried out, giving 9 trials for each of the 64 stimuli. The response matrix was then analyzed two ways. First, the response in each vertical column were summed, giving 72 responses for each value of $\dot{\theta}$, and a psychometric function plotted (Fig. 22A). Second, the data was re-analysed by summary responses in each horizontal row, giving 72 responses for each value of $\dot{\theta}$, and a psychometric function plotted (Fig. 22B). Clearly, threshold in Fig. 22A was far lower (95 times) than threshold for the same response set obtained from Fig. 22B. This shows that the subject performed the task entirely on the basis of trial-to-trial variations of $\theta/\dot{\theta}$.

We conclude that the human visual pathway contains a mechanism that encodes the ratio $\theta/\dot{\theta}$ rather independently of the absolute values of θ and $\dot{\theta}$, and suggest that this mechanism is the basis for estimating differences in the time to contact with an approaching object.

In a second experiment we used exactly the same 8 x 8 stimulus matrix as above. The only difference was that the subject was instructed to judge whether the stimulus was expanding faster or slower than the mean of the stimulus set. Although responses were analysed in the same way, the psychometric functions were mirror images (compare Figs. 23 and 22). In Fig. 23A threshold was

Department of Psychology

UNIVERSITÉ
YORK
UNIVERSITY

FACULTY OF ARTS

4700 KEELE STREET • NORTH YORK • ONTARIO • CANADA • M3J 1P3

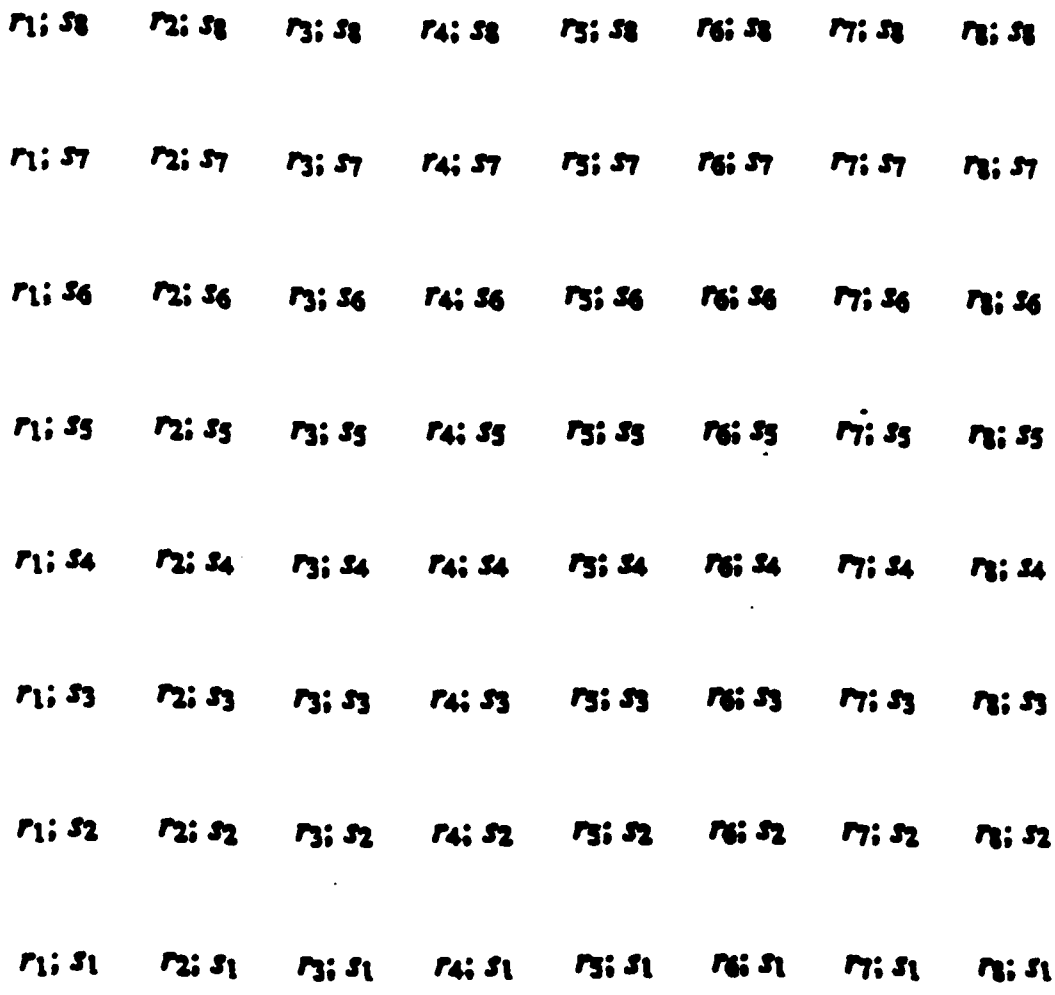

Figure 21. 8 x 8 stimulus set. Variable r is the ratio $\theta/\dot{\theta}$. Variable s is rate of expansion ($\dot{\theta}$).

Department of Psychology

UNIVERSITÉ
YORK
UNIVERSITY

FACULTY OF ARTS

4700 KEELE STREET • NORTH YORK • ONTARIO • CANADA • M3J 1P3

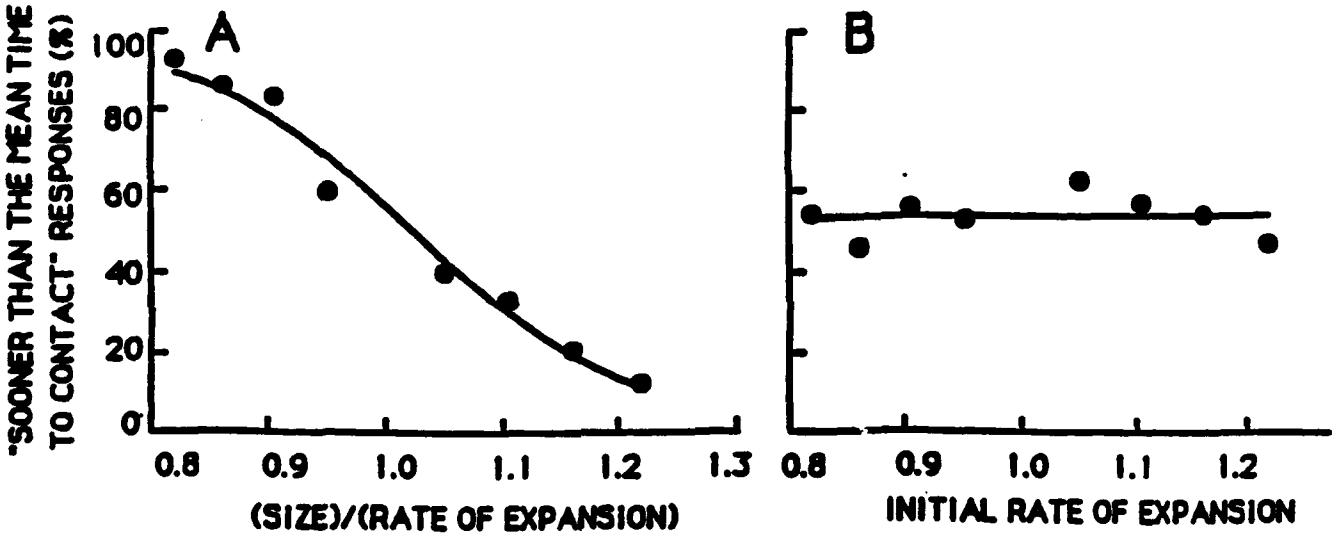

Figure 22. Two Psychometric functions for the same task. For each stimulus, the subject was instructed to judge whether the square would arrive sooner or later than the mean of the 64—stimulus set. The stimulus set was organized as illustrated in Fig. 21.

Department of Psychology

UNIVERSITÉ
YORK
UNIVERSITY

FACULTY OF ARTS

4700 KEELE STREET • NORTH YORK • ONTARIO • CANADA • M3J 1P3

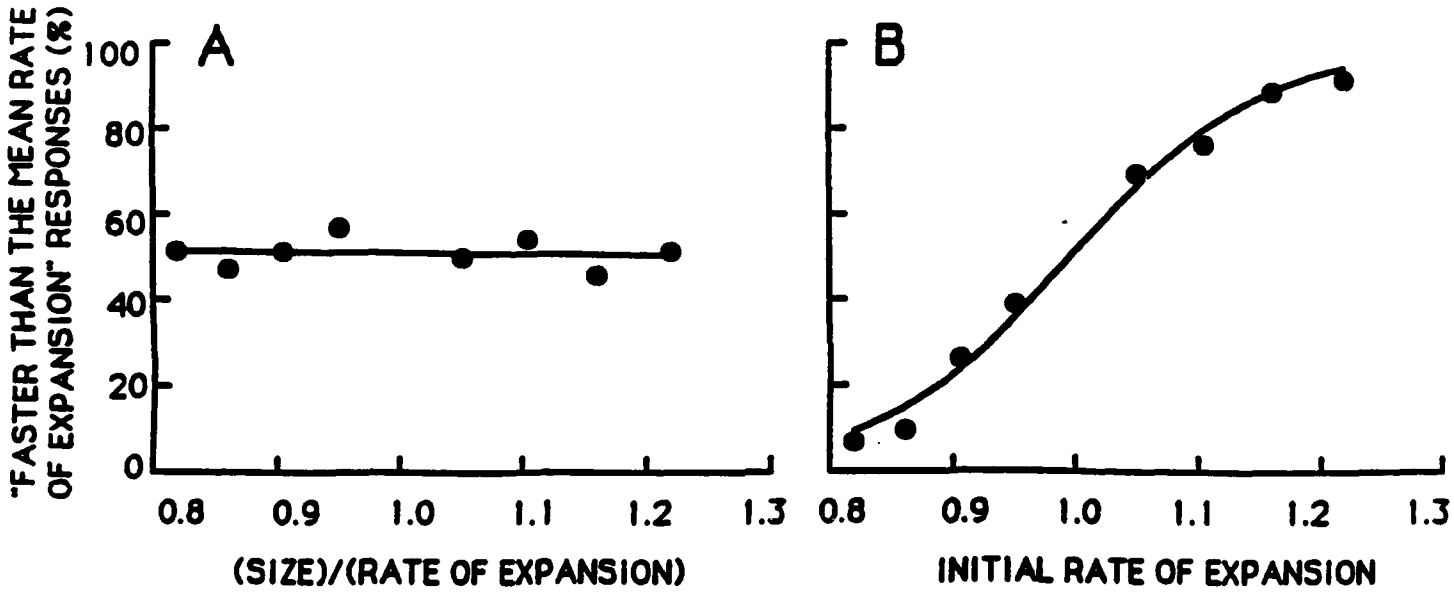

Figure 23. Two psychometric functions for the same task. For each stimulus, the subject was instructed to judge whether the rate of angular expansion was faster or slower than the mean of the 64—stimulus set. The stimulus was set exactly the same as in Fig. 22.

Department of Psychology

UNIVERSITÉ YORK UNIVERSITY

FACULTY OF ARTS

4700 KEELE STREET • NORTH YORK • ONTARIO • CANADA • M3J 1P3

far higher (107 times) than in Fig. 23B. This shows that the subject performed the task entirely on the basis of trial-to-trial variations of $\dot{\theta}$.

We conclude that the human visual pathway contains a mechanism that encodes rate of expansion ($\dot{\theta}$) rather independently of time to contact.

In a further experiment we removed rate of expansion as a reliable cue, leaving time to contact as the only reliable cue for the subject's task. The manipulation can be understood by referring to Fig. 20. As in Experiments 1 and 2, before each presentation the computer selected one of a set of 10 Fig. 20 curves, each with the same scaling factor for the ordinate, but a different value of time to contact (T_0). This set of 10 curves confounded differences in time to contact with differences in rate of expansion. In Experiment 3, however, the ordinate in Fig. 20 was then multiplied by one of 256 randomly-selected scaling factors between limits (1+*r*) and (1-*r*). Figure 24B shows the effect of applying three different scaling factors to the ordinate of Fig. 20. Curves a, b and c all have the same value of T_0 but, at any given time along the abscissa, the value of $\dot{\theta}$ (i.e. the slope of the curve) is different. For example, the dashed lines show how $\dot{\theta}_0$ differs for a, b and c. The magnitude of *r* was set by the experimenter so that the lowest possible rate of expansion at the shortest of the 10 times to contact was lower than the highest possible rate of expansion at the longest of the 10 times to contact. This overlap effectively removed variations in $\dot{\theta}_0$ as a reliable cue to the subject's task. We then confirmed by calibration that the random variation of presentation duration was still sufficiently large to ensure that variations in $\Delta\theta$ were not a reliable cue to the subject's task.

Filled circles in Fig. 25A,B show that, for values of T_0 of 1.0, 2.0 and 4.0 sec, discrimination threshold ranged from 7.0% to 9.4% for subject 1 and from 12.2% to 12.9% for subject 2. Thus, for the mean T_0 of 1.0 sec, the best discrimination thresholds were 0.07 sec, and 0.12 sec for subjects 1 and 2 respectively.

Department of Psychology

UNIVERSITÉ YORK UNIVERSITY

FACULTY OF ARTS

4700 KEELE STREET • NORTH YORK • ONTARIO • CANADA • M3J 1P3

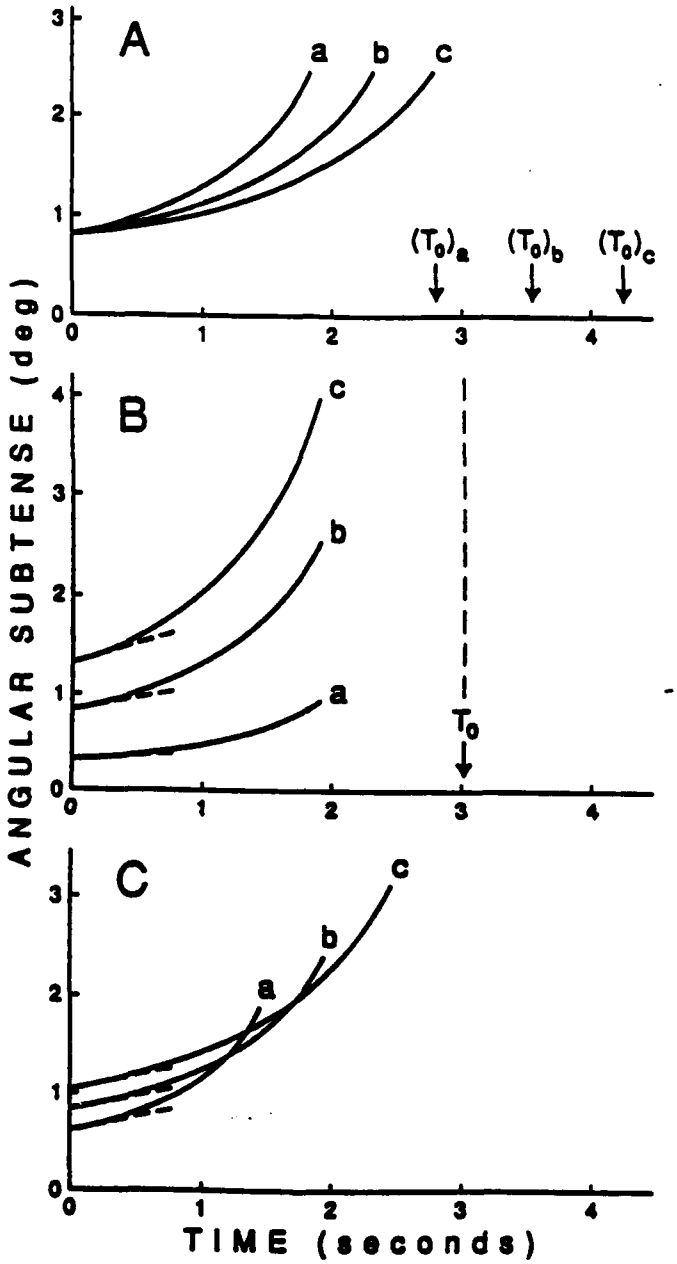

Figure 24. The angular subtense of the stimulus square (2θ) was plotted along the y-axis. Time was plotted along the x-axis. These are experimentally-measured calibration curves. A – three different scaling factors were applied to the x-axis, leaving the y-axis unchanged. This gave three values of time to contact (T_0). The vertical arrows show $(T_0)_a$, $(T_0)_b$ and $(T_0)_c$ for curves a, b and c respectively. B – three different scaling factors were applied to the y-axis, leaving the x-axis unchanged. This produced a yoked variation of the values of θ and $\dot{\theta}$ at any given time (t), while T_0 remained constant. C – the x- and y-axes were scaled simultaneously by the same factor. This produced a yoked variation of θ_0 and T_0 such that $\dot{\theta}_0$ remained constant. Curves a, b and c are for three different scaling factors

Department of Psychology
UNIVERSITÉ YORK UNIVERSITY
FACULTY OF ARTS
4700 KEELE STREET • NORTH YORK • ONTARIO • CANADA • M3J 1P3

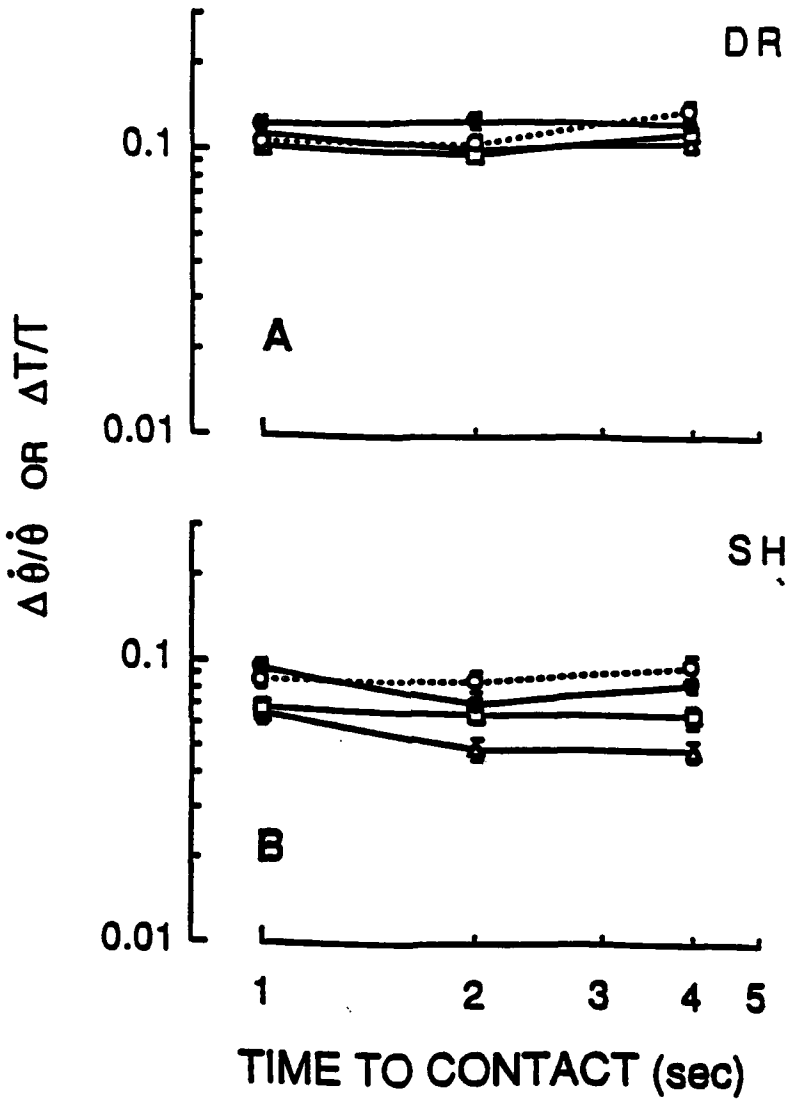

Figure 25. Ordinates plot discrimination threshold for time to contact as a Weber fraction (ΔT/T, filled circles) and discrimination threshold for rate of angular expansion as a Weber fraction ($\Delta \dot{\theta} / \dot{\theta}$, open circles). Abscissae plot mean time to contact. Key: ΔT is discrimination threshold for time to contact with variations in rate of expansion removed as a cue, and $\Delta \dot{\theta}$ is discrimination threshold for rate of isotropic expansion with variations in time to contact removed as a cue. Open squares – both rate of expansion and time to contact were available as cues. Open triangles – rate of expansion, time to contact and Δθ were available as cues, where Δθ was the change in size during the trial. Results are shown for two subjects.

Department of Psychology

UNIVERSITÉ YORK UNIVERSITY

FACULTY OF ARTS

4700 KEELE STREET • NORTH YORK • ONTARIO • CANADA • M3J 1P3

In the next experiment we removed trial-to-trial variations in time to contact as a reliable cue, leaving changes in rate of expansion as the only reliable cue to the subject's task. The manipulation can be understood by referring to Fig. 20. As in Experiment 1 and 2, before each presentation the computer selected one from a set of 10 Fig. 20 curves, each with the same scaling factor for the ordinate, but a different time to contact (T_0) on the abscissa, and this set of 10 curves confounded differences in time to contact with differences in rate of expansion. In Experiment 4, ordinate and abscissa in Fig. 20 were then simultaneously multiplied by the same scaling factor so that the magnification of the Fig. 20 graph was varied isotropically. It follows that $\dot{\theta}_0$ remained invariant. This scaling factor was one of 256 randomly-selected numbers between $(1+s)$ and $(1-s)$. Figure 24C illustrates the effect of this manipulation for three values of s. The dashed lines show that the initial slope (i.e. $\dot{\theta}_0$) was the same for curves a, b and c. The experimenter selected the value of s so that the lowest possible value of T_0 for the lowest of the 10 values of $\dot{\theta}_0$ was higher than the highest possible value of T_0 for the highest of the 10 values of $\dot{\theta}_0$. This overlap removed variations of T_0 as a reliable cue to the subject's task, leaving variations of $\dot{\theta}_0$ as the only reliable cue. After introducing this random variation of T_0, we confirmed by calibration that the random variation of presentation duration were sufficiently large to ensure that $\Delta\theta$ was effectively removed as a cue to $\dot{\theta}_0$.

For our two subjects, discrimination threshold for the ratio $(\theta/\dot{\theta})$ remained at approximately the same percentage when mean time to contact was changed from 1.0 sec through 4.0 sec so that, just like discrimination threshold for rate of expansion, this discrimination obeyed a kind of Weber's law. These findings can be explained in terms of a model (Fig. 26) proposed over 10 years ago in a context quite different from that of time to contact data (Refs 72, 90, 92). Our rationale here is that the value of $(\theta/\dot{\theta})$ provides an unequivocal index of time to contact with an approaching object only if the value of $(\theta/\dot{\theta})$ in the object's retinal image does not vary with

Department of Psychology

UNIVERSITÉ
YORK
UNIVERSITY

FACULTY OF ARTS

4700 KEELE STREET • NORTH YORK • ONTARIO • CANADA • M3J 1P3

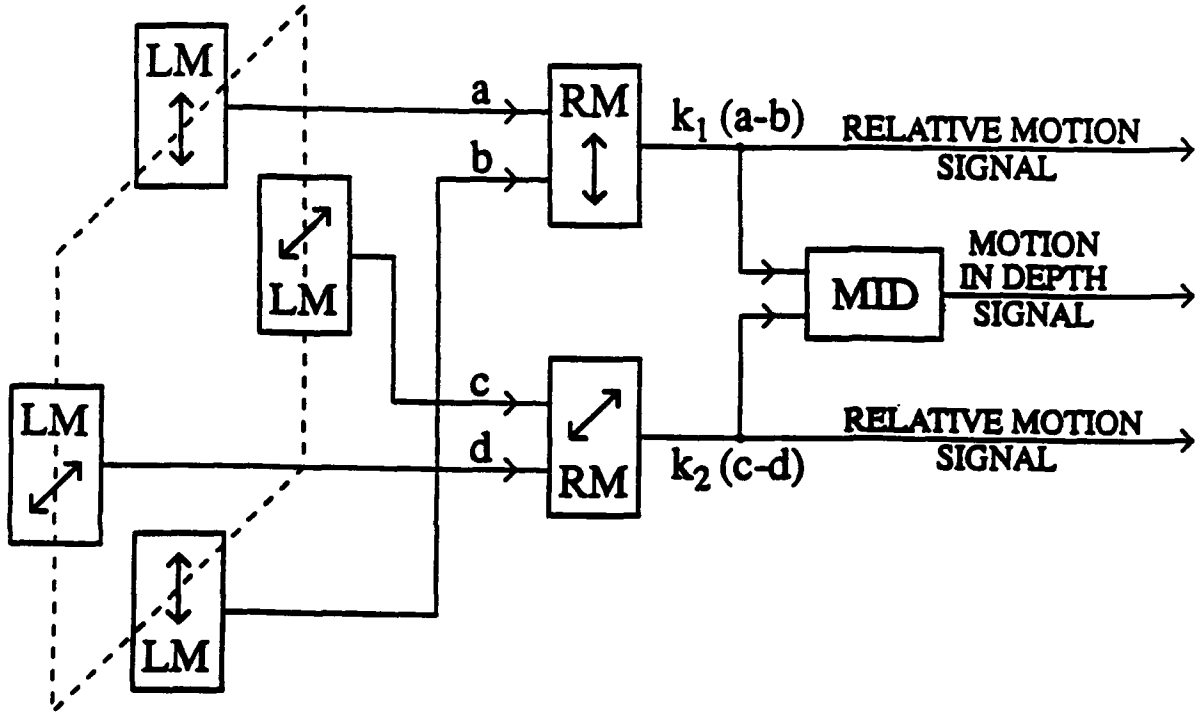

Figure 26. Model of the processing of changing size and encoding of time to contact. The boundaries of a solid untextured rectangular retinal image are shown dotted. Key: LM – filters that respond to local motion along the directions arrowed. Their outputs (a, b, c & d) assume an amplitude that is linearly proportional to local speed and a sign that signals the direction of motion. RM – one-dimensional relative motion filters whose outputs signal the speed and direction of relative motion along some given retinal azimuth. MID – two-dimensional relative motion filter that is strongly excited by isotropic expansion of the dotted retinal image, i.e. when k1(a–b) = k2(c–d). The amplitude of the output of filter MID is equal to any one of its inputs from RM filters and, therefore, is inversely proportional to time to contact. Modified from Fig. 1 in Ref 82 and Fig. 2 in Ref 154.

Department of Psychology

UNIVERSITÉ YORK UNIVERSITY

FACULTY OF ARTS

4700 KEELE STREET • NORTH YORK • ONTARIO • CANADA • M3J 1P3

azimuth. Such selectivity requires a filter that responds to isotropically-expanding retinal images, but rejects retinal images whose expansion is not isotropic. The MID filter in the previously-proposed model illustrated in Fig. 26 has just this property (see below) and, according to Equation 9, produces output z only when it receives identical inputs from relative motion filters for different azimuths. If, for our present purpose, we make the further assumption that in this situation the amplitude of z is equal to any one of the equal inputs, i.e.

$$z = A\left(\frac{\theta_V}{\dot{\theta}}\right) = A\left(\frac{\theta_H}{\dot{\theta}}\right) \quad , \text{ etc.} \qquad \text{.....(7)}$$

then

$$z = \frac{A}{T} \qquad \text{.....(8)}$$

where T is time to contact and A is a constant. In words: *the amplitude of the motion-in-depth output of the MID filter is inversely proportional to time to contact.*

Figure 26 illustrates a model of changing-size processing that was based on data obtained in several empirical studies on threshold elevations and aftereffects produced by adapting to changing-size stimuli (Refs 72, 75, 81-83, 85, 92, 125, 154). The dotted outline in Fig. 26 represents the outer boundary of a rectangular horizontal/vertical untextured retinal image whose size is changing. The speeds of the upper and lower edges are encoded by local motion filters (LM) that prefer vertical motion and whose outputs are labelled a and b. The magnitudes of a and b are linearly proportional to local retinal image speed and the polarities depend on whether motion is upwards or downwards. Similarly, the speed and direction (leftwards versus rightwards) of the rectangle's vertical edges are encoded by local motion filters that prefer horizontal motion. Outputs a and b feed a one-dimensional relative motion filter whose output, $k_1(a-b)$, is linearly proportional to the algebraic difference in the absolute vertical velocities of the retinal image's horizontal edges (Fig. 1, Ref 85). Similarly, outputs a and b feed a one-dimensional relative motion filter whose output, $k_2(c-d)$, is linearly proportional to the algebraic difference in the absolute horizontal

Department of Psychology

UNIVERSITÉ YORK UNIVERSITY

FACULTY OF ARTS

4700 KEELE STREET • NORTH YORK • ONTARIO • CANADA • M3J 1P3

velocities of the retinal image's vertical edges. Evidence for the existence of relative motion (RM) stages that are separate from local motion (LM) stages is as follows: (1) For rectangles less than about 1.5 deg wide, visual thresholds for detecting isotropic two-dimensional oscillations of size are much more elevated by adapting to isotropic two-dimensional oscillations of size than by adapting to oscillations of location (i.e. oscillatory motion). This is the case even when each edge of the adapting rectangle, viewed in isolation executes exactly similar oscillations (Ref 72). A similarly selective threshold elevation is observed for detecting one-dimensional oscillations of the rectangle's width (Refs 83, 92). With no further evidence one might conclude that this threshold elevation is selective to the phase difference between the oscillations of the rectangle's opposite edges (i.e. antiphase versus inphase oscillations). But (2) threshold elevation for detecting isotropic two-dimensional oscillations of size is unaffected by adding oscillatory translational motion to the adapting stimulus, i.e. the threshold elevation is selective, not to the phase difference *per se*, but rather to the velocity difference between opposite edges (Ref 90); (3) visual threshold for detecting oscillatory translational motion is comparatively unaffected by adapting to either isotropic two-dimensional oscillations of the rectangle's size or one-dimensional oscillations of the rectangle's width (Refs 72, 83, 85, 92); (4) adapting to oscillatory translational motion of the rectangle produces a comparatively small elevation of detection threshold, whether the test stimulus is oscillatory translational motion of isotropic two-dimensional oscillations of size (Ref 72). (Note that the above findings are all for oscillatory changes in the size and/or location of a solid, untextured rectangular stimulus.)

The selective threshold elevations just described cannot be understood entirely in terms of local motion detectors. Rather, they can be understood if, at least for untextured solid targets subtending less than 1.5 deg, changes in retinal image size are processed by adaptable one-dimensional filters (RM in Fig. 26) sensitive to the velocity difference between opposite edges.

Department of Psychology

UNIVERSITÉ YORK UNIVERSITY

FACULTY OF ARTS

4700 KEELE STREET • NORTH YORK • ONTARIO • CANADA • M3J 1P3

These one-dimensional filters can be regarded as filters for relative motion that reject translational motion information.

In Fig. 26, pairs of one-dimensional filters feed a two-dimensional filter (MID) that compares inputs $k_1(a-b)$ and $k_2(c-d)$. The activity of the MID filters suppress the perception of changing-size and leads to a perception of motion-in-depth when

$$\frac{\theta_V}{\dot{\theta}_V} = \frac{\theta_H}{\dot{\theta}_H} \quad \text{.....(9)}$$

This equation characterizes the retinal image of a rigid nonrotating object moving in depth along the line of sight and, therefore, the MID filter can be regarded as imposing a rigidity constraint (Refs 82, 92). One simple way of modelling sensitivity to this two-dimensional relation would be to assume that k_1 and k_2 are directly proportional to the instantaneous size of the stimulus rectangle so that, for example

$$k_1 = \frac{K}{\theta_H} \quad \text{.....(10)}$$

and

$$k_2 = \frac{K}{\theta_V} \quad \text{.....(11)}$$

where K is a constant. In addition to imposing a rigidity constraint, Equations 10 and 11 also account for the finding that the selective elevation of changing-size threshold produced by adapting to changing-size falls off rapidly as the mean size of the adapting rectangle is increased and cannot be measured for rectangles wider than about 1.5 deg (Ref 83). Experimental evidence for the existence of a separate two-dimensional motion filter with the properties just described include the following findings: (1) the initial aftereffect produced by adapting to a changing-size stimulus is a pure motion-in-depth aftereffect if

$$\frac{\theta_V}{\dot{\theta}_V} = \frac{\theta_H}{\dot{\theta}_H} \quad \text{.....(12)}$$

for the adapting stimulus and a pure changing-size aftereffect if

Department of Psychology

UNIVERSITÉ YORK UNIVERSITY

FACULTY OF ARTS

4700 KEELE STREET • NORTH YORK • ONTARIO • CANADA • M3J 1P3

$$\frac{\theta_V}{\dot{\theta}_V} = \frac{\theta_H}{\dot{\theta}_H} \quad \text{.....(13)}$$

(Ref 82); (2) The motion-in-depth aftereffect, but not the changing-size aftereffect, produced by adapting to changing-size can be cancelled by oscillating or ramping changes of binocular disparity (Ref 85); (3) there is a nonlinear interaction between adaptation to vertical and horizontal one-dimensional relative motion, and this interaction is maximum when

$$\frac{\theta_V}{\dot{\theta}_V} = \frac{\theta_H}{\dot{\theta}_H} \quad \text{.....(14)}$$

(Ref 92).

Implications for Aviation. Accurate and precise judgments of time to contact are crucial in flying fixed wing aircraft (landing, aircraft avoidance, terrain avoidance in low-level flight) and in flying rotary-wing aircraft, especially in low-level and nap-of-the-Earth flight (terrain avoidance). A geometrical cue is available for judging time to contact, namely the ratio ($\theta/\dot{\theta}$). We report here evidence that the human visual pathway contains a neural mechanism sensitive to the ratio ($\theta/\dot{\theta}$) rather independently of θ and $\dot{\theta}$. We also report a method for measuring intersubject differences in discriminating time to contact ($\theta/\dot{\theta}$) independently of other cues that may be present in the laboratory situation, but which are largely artifactual in the real flying environment.

3.6 Experiment 7

We have extended the work on nonlinear systems characterization by the two-sinewave method described in the Final Report for 1987-90, and have developed a mathematical approach for calculating the response of a sum of two sinewaves input for a sequence of n cascaded rectifiers, each of which is preceded and followed by a linear frequency-dependent filter. We are

Department of Psychology

UNIVERSITÉ YORK UNIVERSITY

FACULTY OF ARTS

4700 KEELE STREET • NORTH YORK • ONTARIO • CANADA • M3J 1P3

investigating the value of such rectifier/filter sequences as nonlinear multi-neuron models. We are now developing software that will allow the predicted responses of different cascaded sequences to be plotted graphically as graphs of amplitude and phase of cross-modulation terms versus the amplitudes of the two inputs. [The cross modulation terms in the output have discrete frequencies ($nF_1 \pm mF_2$), where F_1 and F_2 are the input frequencies and n and m are integers.]

3.7 Experiment 8

We have developed a mathematical procedure for calculating the amplitudes and phases of the discrete frequency terms in the output of a single rectifier whose input is the sum of two amplitude modulated (AM) sinusoids. The mathematical treatment covers the suppressed-carrier and unsuppressed-carrier cases for linear, compressive and accelerating rectifiers. We have also treated the case where the two AM signals have different carrier frequencies.

This mathematical research is directly applicable to psychophysical research on hearing and also to testing neural models of audition by recording magnetic and electrical responses of the brain. In particular, according to Hudspeth's empirical data, the transducer function of the hair cells of the inner ear approximates a compressive rectifier (Fig. 27). We have calculated the discrete frequency terms that would result from feeding the hair cell transducer function with the sum of two AM tones. This theoretical treatment successfully predicts the strikingly nonlinear phenomenon we found in the electrical and magnetic brain responses evoked in human by applying the sum of two AM tones to one ear (Refs 173, 177, 188). In particular, the theory predicts: (1) that one AM tone, $y_1 = A(\sin 2\pi Ft)(\sin 2\pi ft)$, will generate a response at frequency 2f (F is the carrier frequency and f the modulation frequency); (2) that two AM tones, $y_1 = A(\sin 2\pi Ft)(\sin 2\pi ft)$ and $y_2 = B(\sin 2\pi Ft)(\sin 2\pi gt)$, when added and fed to one ear will produce no power at frequencies 2f or 2g, but will produce a term of frequency (f+g); (3) that when the two AM tones

Department of Psychology

UNIVERSITÉ
YORK
UNIVERSITY

FACULTY OF ARTS

4700 KEELE STREET • NORTH YORK • ONTARIO • CANADA • M3J 1P3

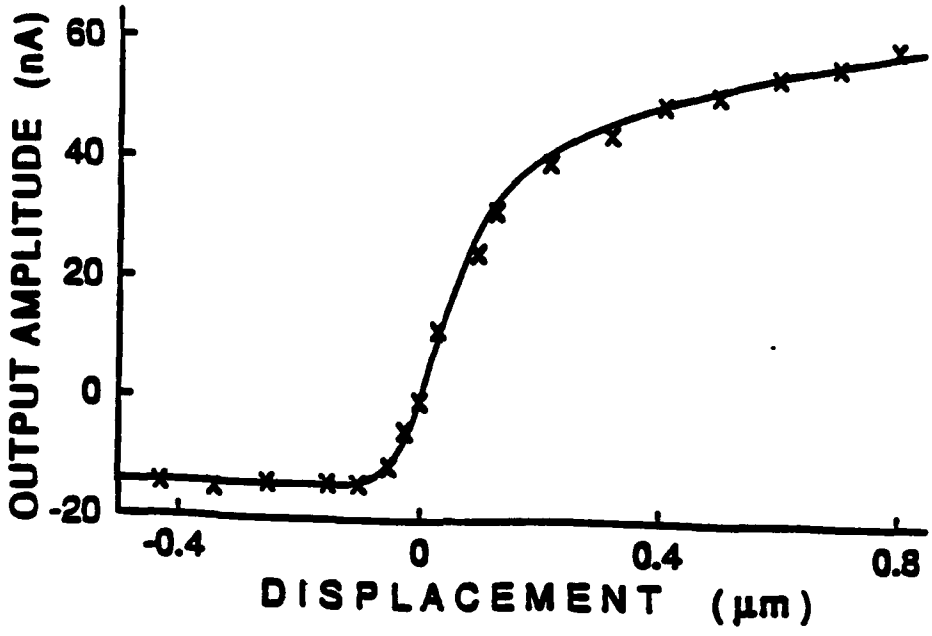

Figure 27. Hair cell transducer funtion. Form D. P. Corey and A. J. Hudspeth (1983) "Kinetics of the receptor current in bullfrog saccular hair cells," J. Neuroscience, 3, 962-976.

Department of Psychology

UNIVERSITÉ
YORK
UNIVERSITY

FACULTY OF ARTS

4700 KEELE STREET • NORTH YORK • ONTARIO • CANADA • M3J 1P3

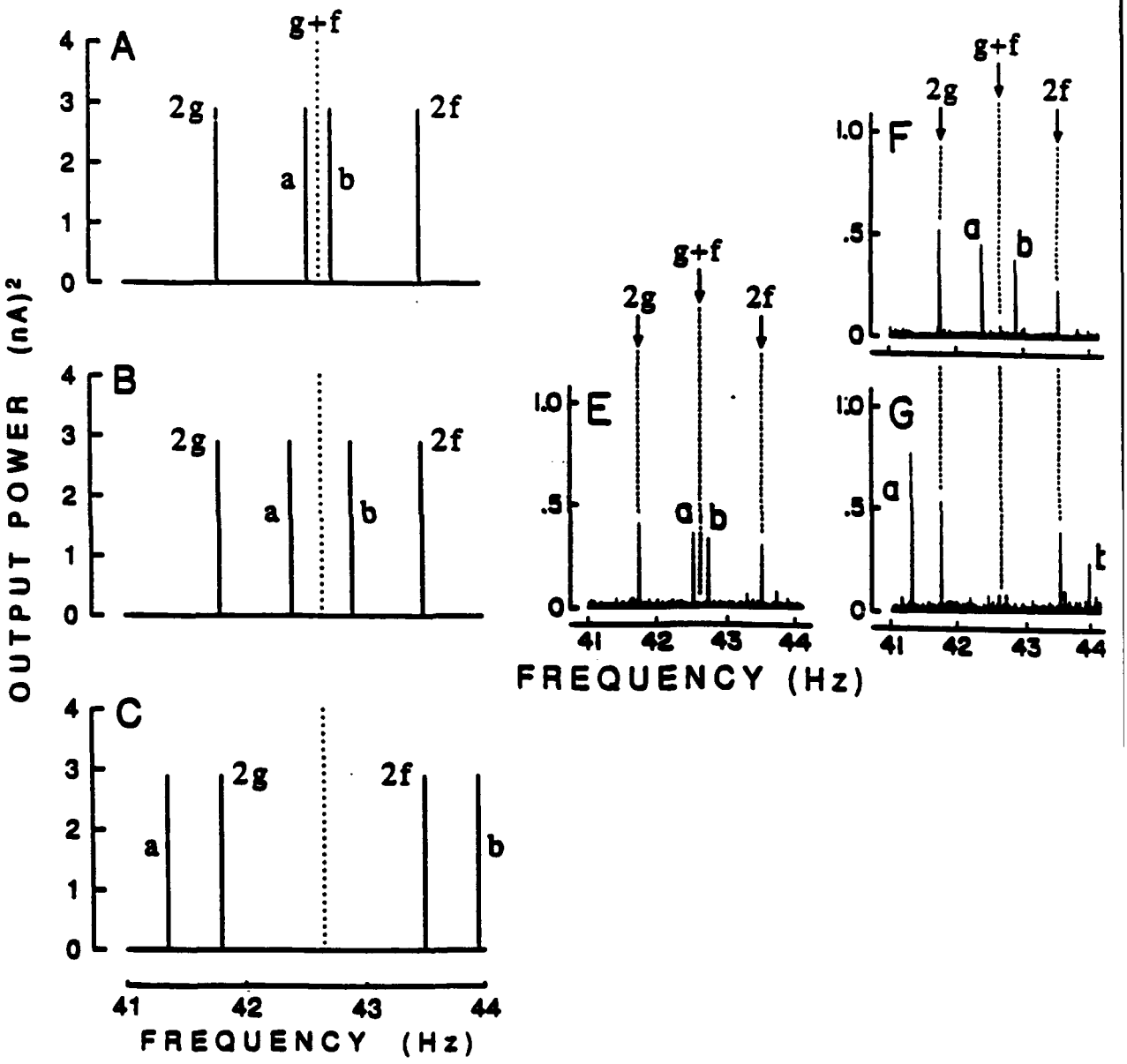

Figure 28. A-C: Theoretical prediction of the output of the hair cell transducer function. A: (F-G) =0.1 Hz. B: (F-G) =0.25 Hz. C: (F-G) =1.3 Hz. E-G: Experimental data corresponding to predictions A-B respectively.

Department of Psychology

UNIVERSITÉ YORK UNIVERSITY

FACULTY OF ARTS

4700 KEELE STREET • NORTH YORK • ONTARIO • CANADA • M3J 1P3

have different carrier frequencies so that a wave [A(sin 2πFt)(sin 2πft) + B(sin 2πGt)(sin 2πgt)] is applied to one ear, there will be no power at 2F, 2G or (f+g). Rather the (f+g) term will split into two parts, one of frequency [(f+g) – (F-G)] and the other of frequency [(f+g) + (F-G)]. Fig. 28 illustrates the close correspondence between this theoretical work and experimental data we have obtained from the human brain. Fig. 28A plots the output from the hair cell transducer function shown in Fig. 27 when the input to the hair cell transducer function is the sum of two AM tones, one of carrier frequency F= 1048.00 Hz modulated at f=20.9 Hz, the other of carrier frequency G=1048.10 Hz modulated at g=21.8 Hz. The figure clearly shows the split frequency components a and b, separated by 0.2 Hz (0.2 =2[1048.10 - 1048.00]). Fig. 28E shows corresponding experimental data recorded from the human brain. The fit with theory is clearly very close. Fig. 28B shows the theoretical prediction when the G=1048.10 Hz carrier frequency is changed to 1048.25, everything else remaining the same. Fig. 28B clearly shows the split frequency components a and b, separated now by 0.5 Hz (0.5=2[1048.25 - 1048.00]) rather than by 0.2 Hz. Fig. 28F shows corresponding experimental data recorded from the human brain. Again, the fit with theory is very close. Finally, Fig. 28C shows the theoretical prediction when carrier frequency G is changed to G=1049.30 Hz, everything else remaining the same. Fig. 28C clearly shows how the split frequncy components a and b are separated now by 2.6 Hz (2.6 =2[1049.30 - 1048.00]) so that a and b move to the far sides of the 2g and 2f components. Fig. 28G shows corresponding experimental data recorded from the human brain. Once again, the fit with theory is very close.

The significance of this line of research is in advancing our ability to calculate mathematically the response of the hair cells to auditory waveforms more complex than simple tones. This work has been submitted for publication (Ref 231).

Department of Psychology

UNIVERSITÉ YORK UNIVERSITY

FACULTY OF ARTS

4700 KEELE STREET • NORTH YORK • ONTARIO • CANADA • M3J 1P3

3.8 Experiment 10

We have recorded the topographical distributions of human magnetic brain responses to 40 Hz flicker and compared them with the distributions of responses to luminance-defined form and to coherent motion. These three responses have different sites of origin in striate and prestriate cortex. A report on this work is in preparation (Ref 241 and an abstract has been submitted for ARVO 1993).

3.9 Experiment 12

We have succeeded in recording magnetic brain responses to texture-defined form. We have characterized their waveform and compared their site of origin in the brain to the site of origin of responses to luminance-defined form.

When attempting to record brain responses to texture-defined form it is by no means sufficient to merely record responses evoked by stimulating the eye with texture-defined form, because such a stimulus confounds a change in local texture with a change in spatial form. We have developed a procedure for unconfounding these two variables. The principle is that texture-defined form is made to appear by abruptly changing the orientations of a subset of short line elements. Whether the texture appears or disappears is determined by the orientation of a subset of constant line elements. Thus, the appearance of form can be dissociated from the change in local texture that creates the form. We have used this procedure to map and estimate source locations for responses to texture-defined form and for the change in local texture that creates the form. Stimulation was to a single macular quadrant (lower left). Figure 29 shows averaged transient responses to the appearance and disappearance of texture-defined form recorded from 7 coils (BTi 7-channel magnetometer). Figure 30 shows a map of the appearance response. Using analogous reasoning we have recorded magnetic responses to luminance-defined form and to the local luminance changes that define the form. Figure 31 shows averaged transient responses to the appearance and

Department of Psychology

UNIVERSITÉ
YORK
UNIVERSITY

FACULTY OF ARTS

4700 KEELE STREET • NORTH YORK • ONTARIO • CANADA • M3J 1P3

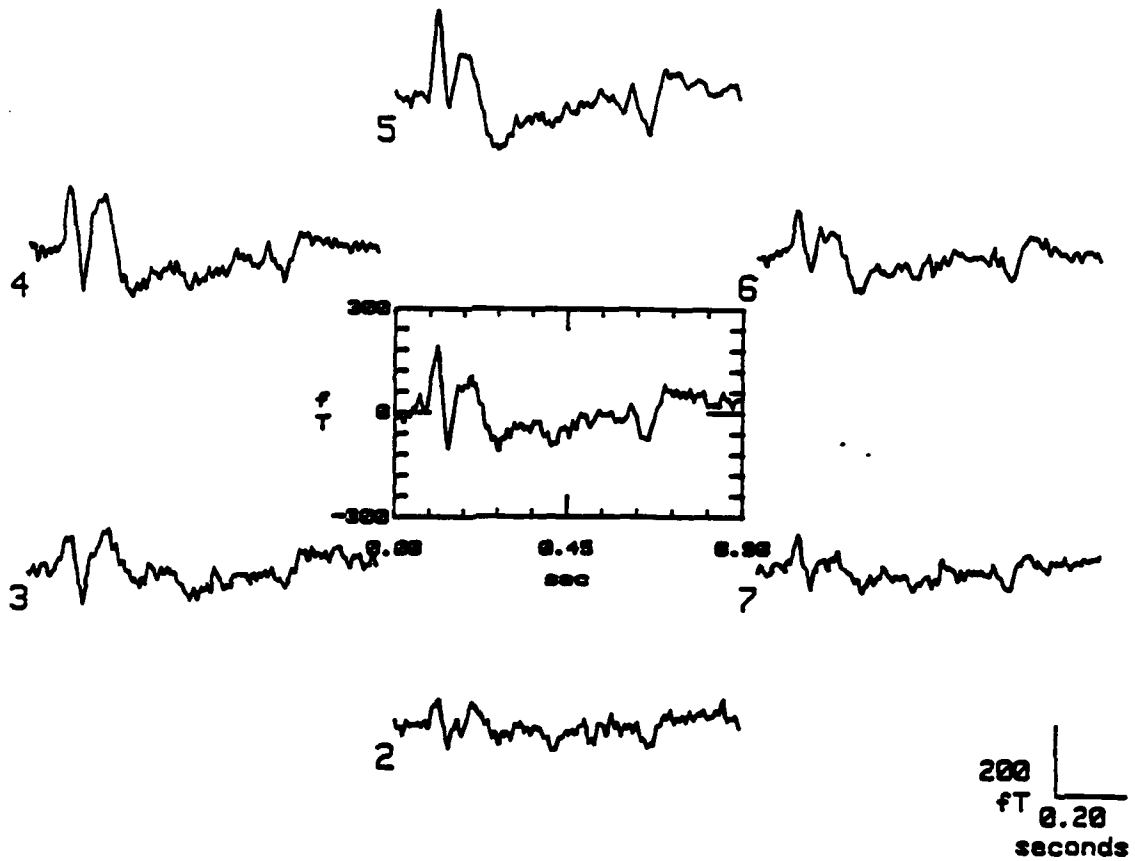

Figure 29. Magnetic responses of the brain to texture-defined form. The stimulus was the appearance and disappearance of a 4 x 4 deg pattern of checks. The 7 coils were centered 5 cm obliquely to the upper right of the inion.

Department of Psychology

UNIVERSITÉ
YORK
UNIVERSITY

FACULTY OF ARTS

4700 KEELE STREET • NORTH YORK • ONTARIO • CANADA • M3J 1P3

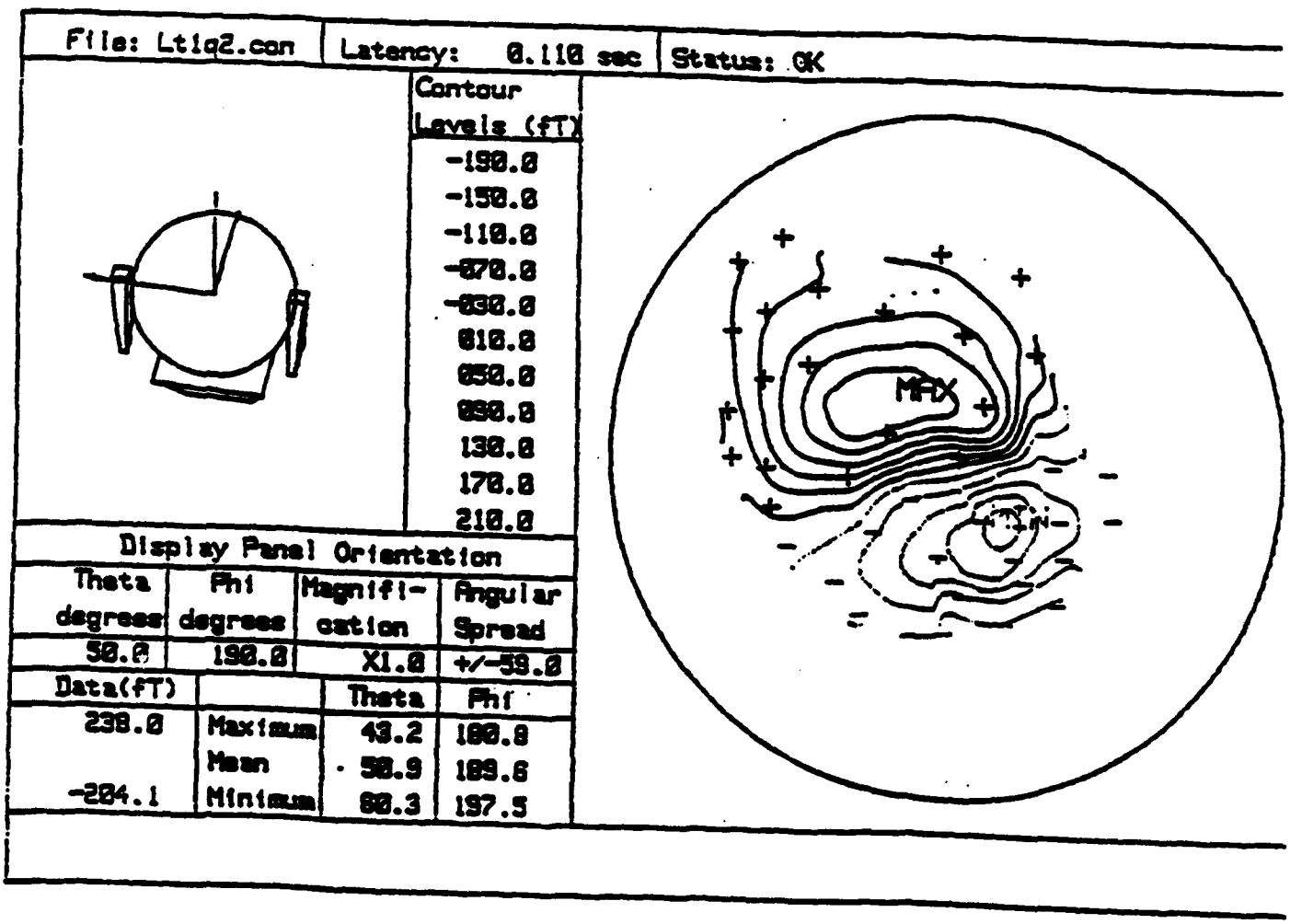

Figure 30. Magnetic responses of the brain to texture-defined form. A map of the magnetic field evoked by the appearance of texture-defined form. See Fig. 29 for the response waveforms. This map was derived from responses at 56 coil locations over the head.

Department of Psychology

UNIVERSITÉ
YORK
UNIVERSITY

FACULTY OF ARTS

4700 KEELE STREET • NORTH YORK • ONTARIO • CANADA • M3J 1P3

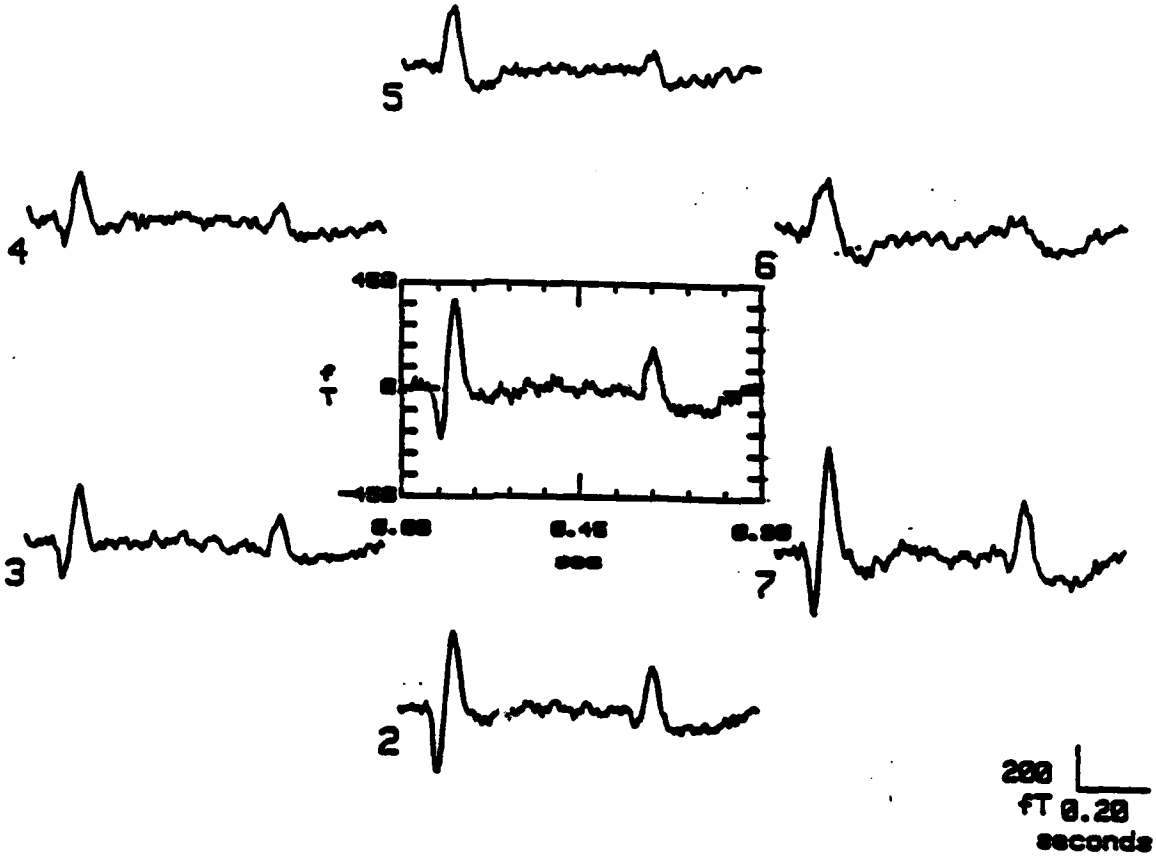

Figure 31. Magnetic responses of the brain to luminance-defined form. The stimulus was the appearance and disappearance of a 4 x 4 deg pattern of checks. The 7 coils were centered on the inion.

Department of Psychology

UNIVERSITÉ YORK UNIVERSITY

FACULTY OF ARTS

4700 KEELE STREET • NORTH YORK • ONTARIO • CANADA • M3J 1P3

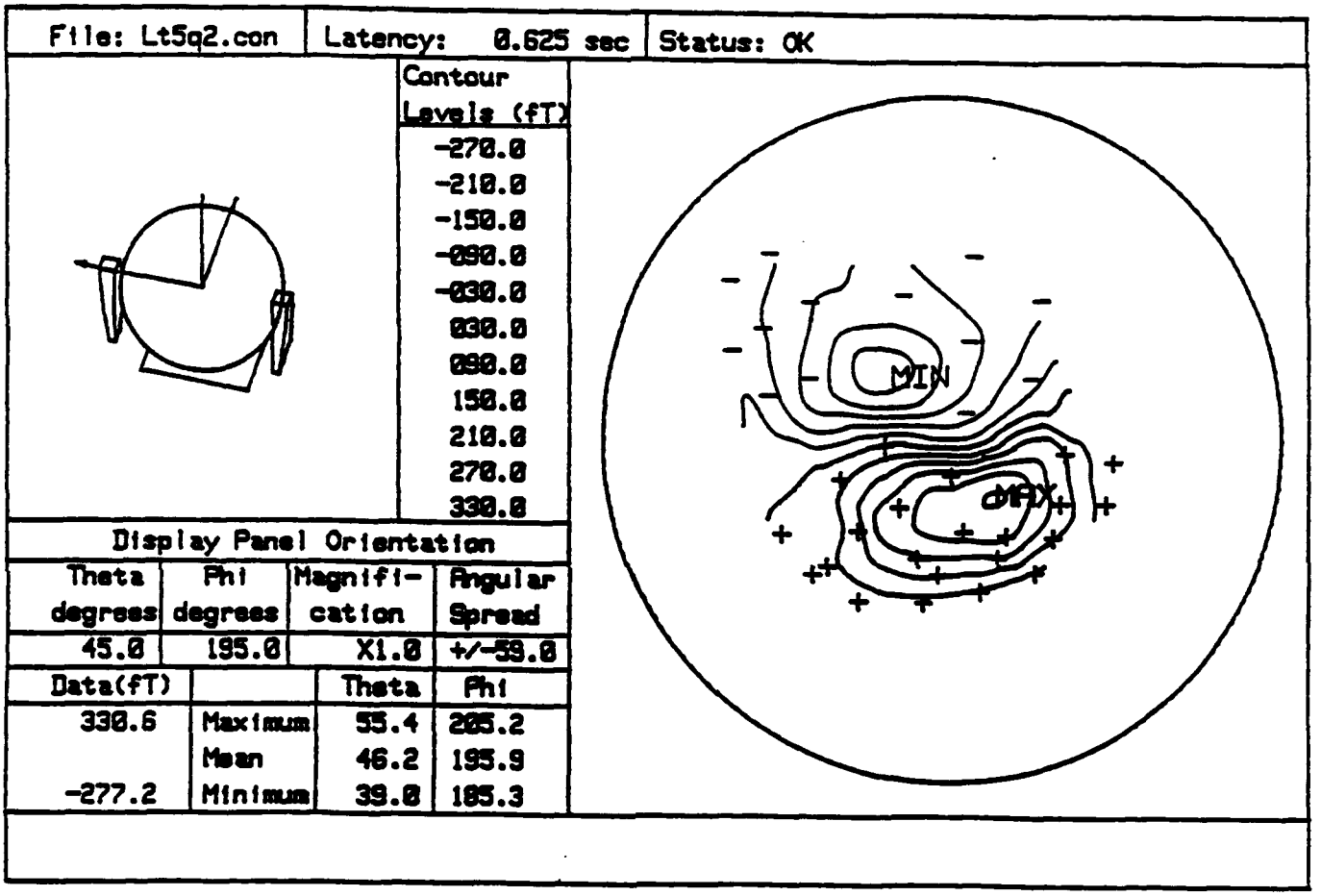

Figure 32. Magnetic responses of the brain to luminance-defined form. A map of the magnetic field evoked by the appearance of luminance defined form. See Fig. 31 for the response waveforms. This map was derived from responses at 58 coil locations over the head.

Department of Psychology

UNIVERSITÉ YORK UNIVERSITY

FACULTY OF ARTS

4700 KEELE STREET • NORTH YORK • ONTARIO • CANADA • M3J 1P3

disappearance of texture-defined form recorded from 7 coils. Figure 32 shows a map of the appearance response. The texture-defined form response contains components that are quite different in topography from the components of the luminance-defined response and with different sites of origin within the brain. When only one retinal quadrant was stimulated, and stimulation restricted to the macula, the distribution of the field approximated closely to a single-dipole field whose site of origin was different from that of responses to luminance-defined pattern. We conclude that different brain sites respond to spatial form defined by texture and by luminance even when the spatial form and retinal site of stimulation is identical in the two cases. This work was reported to for ARVO 1992, and a paper is in preparation (Ref 237).

3.10 Experiment 13

We have obtained objective evidence for an audio-visual convergence area in the human brain. Subjects were stimulated by a 1000 Hz tone that was amplitude-modulated at F_A Hz while they simultaneously viewed a light flickering at F_V Hz. The magnetic field of the brain was recorded and analyzed at ultra-high resolution (0.004 Hz) using our nondestructive zoom-FFT technique described in the Final Report for 1987–90 and Refs 183 and Book 2. Figure 33 shows a cross-modulation term of frequency $(3F_V - 2F_A)$ in the magnetic brain response. This response must have been generated after convergence of auditory and visual signals, because the visual pathway could only have generated harmonics of F_V, and the auditory pathway could only have generated harmonics of F_A. We are now mapping these audio-visual interaction terms over the head, and attempting to localize the source of the interaction within the brain.

3.11 Experiment 15

We have developed a circuit for converting single-unit responses into an analog voltage

Department of Psychology

UNIVERSITÉ
YORK
UNIVERSITY

FACULTY OF ARTS

4700 KEELE STREET • NORTH YORK • ONTARIO • CANADA • M3J 1P3

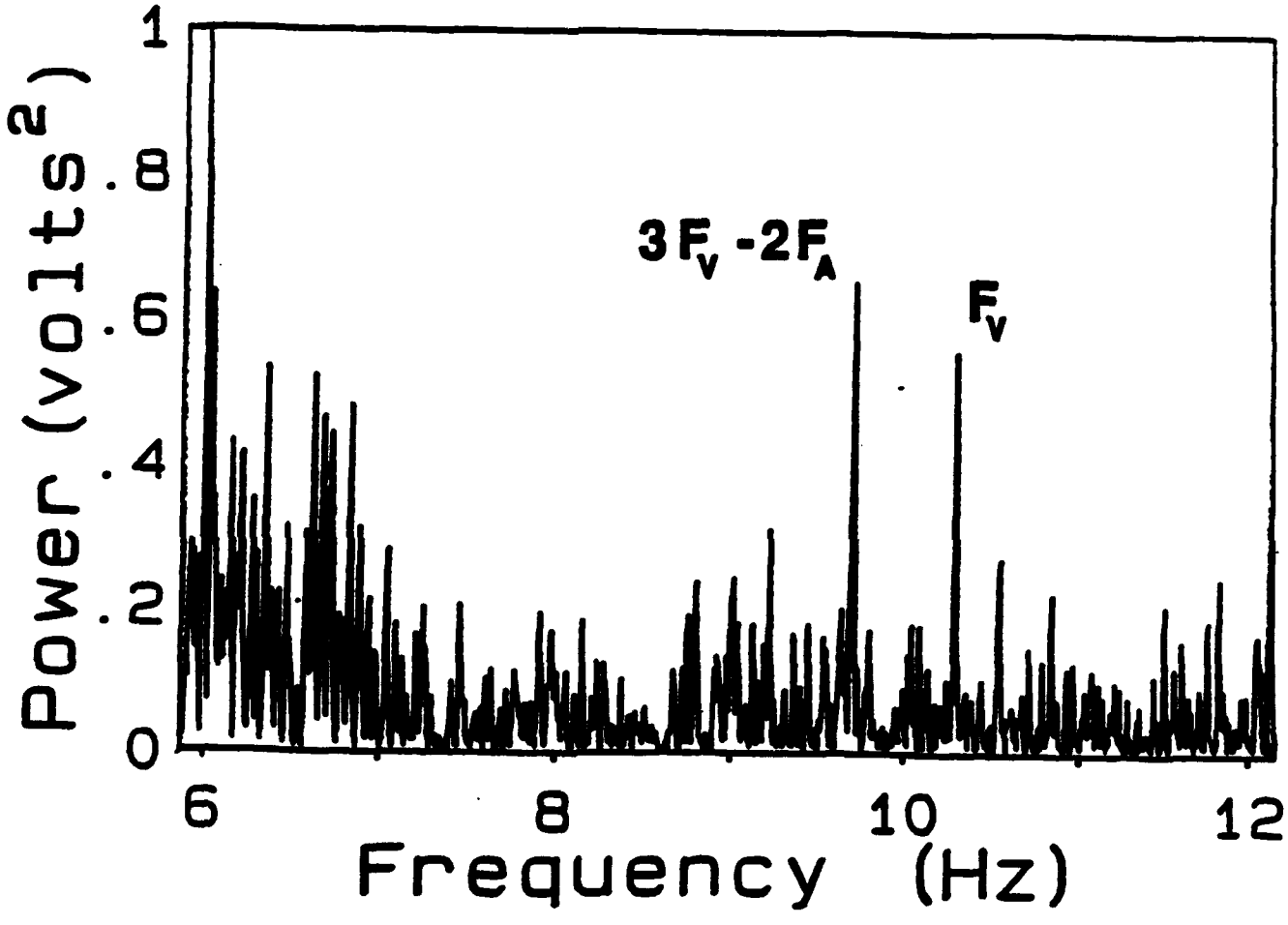

Figure 33. Magnetic brain response from audio-visual integration area.

Department of Psychology

UNIVERSITE YORK UNIVERSITY

FACULTY OF ARTS

4700 KEELE STREET • NORTH YORK • ONTARIO • CANADA • M3J 1P3

proportional to instantaneous firing rate that can be analyzed by our nondestructive zoom-FFT procedure described in the Final Report for 1987–90. We have made preliminary recordings of single unit responses to sinewave gratings from area 17 of cat, but found that spike rates were too low for analysis. On the other hand, local cortical slow wave responses to sum of two sinewave stimulation were successfully analyzed by zoom FFT in a way that looks suitable for our nonlinear systems characterization approach (Ref 179). We plan to record from area 18 where spike firing rates should be higher.

3.12 Experiment 16: Medical Tests

3.12.1 *Parkinson's Disease*

We measured psychophysical contrast threshold for: (1) a 3.5 c/deg sinewave grating when counterphase-modulated (8 Hz) and when temporally unmodulated, i.e. static; (2) speed threshold for 75% reading accuracy for our motion-defined letter test (Ref 190); (3) Snellen acuity. Measurements were carried out while the patient was on medication, then after discontinuing medication overnight, then 1 hour after taking medication orally. The "off medication" measurements showed a large sensitivity loss for the temporally-modulated grating that was not shown for a static grating of the same spatial frequency. Contrast sensitivity was restored to normal (>10 SD change) within 1.5 hours of re-starting medication. We conclude that the loss of contrast sensitivity was specific to temporally-modulated gratings and this loss was not caused by long-term damage to contrast-sensitive neurons but, rather, *directly by an absence of systemic dopamine*. The relevance of this finding is that we (Ref 166) and others[34] had independently found that many patients with Parkinson's disease have contrast sensitivity loss specifically for temporally-modulated gratings of low spatial frequency. A single-case report has been submitted for publication (Ref 230).

A problem for the ongoing US/Canadian DATATOP multi-center trial of the drug Deprenyl

Department of Psychology

UNIVERSITÉ YORK UNIVERSITY

FACULTY OF ARTS

4700 KEELE STREET • NORTH YORK • ONTARIO • CANADA • M3J 1P3

in the management of Parkinson's disease is the lack of an objective index of the progress of the disease. We are comparing motion-defined letter test results and contrast sensitivity results with other methods of assessment in a longitudinal study, now in its third year.

3.12.2 *Multiple Sclerosis (MS) and Brain Lesions*

Results of studies using our motion-defined letter test on patients with MS and following neurosurgery are reported under 3.3 above.

3.12.3 *Amblyopia*

We have found that our motion-defined letter test picks up visual damage in the "unaffected" eye of 90% of all patients tested. This work has been published in Invest. Ophthalmol. and Vis. Sci. (Ref 215) and reported to ARVO 1992.

We previously developed a new kind of visual test chart, the repeat-letter chart, illustrated in Fig. 34. This test can pick up errors of gaze control considerably smaller than can be picked up by the scleral coil method or by the double-Purkinje eye tracker. Furthermore, our test is simple, noninvasive and cheap.

The rationale is that if visual acuity on the repeat-letter test is significantly better than visual acuity on the Snellen line chart, then the reduced line chart acuity is due to poor gaze control rather than abnormal lateral interactions between adjacent contours. A gaze control error of only 2.5 min arc will reduce Snellen acuity from 6/3 to a lower value.

We have found that a combination of Snellen (line) acuity and results on our repeat-letter test sub-classifies children with amblyopia. We suggest that it identifies a sub-class whose Snellen acuity loss is due to defective selection/control of gaze rather than abnormal neural lateral interactions. If this is verified, there are important implications for the choice of therapy. A paper has been published (Ref 216).

Department of Psychology

UNIVERSITÉ
YORK
UNIVERSITY

FACULTY OF ARTS

4700 KEELE STREET • NORTH YORK • ONTARIO • CANADA • M3J 1P3

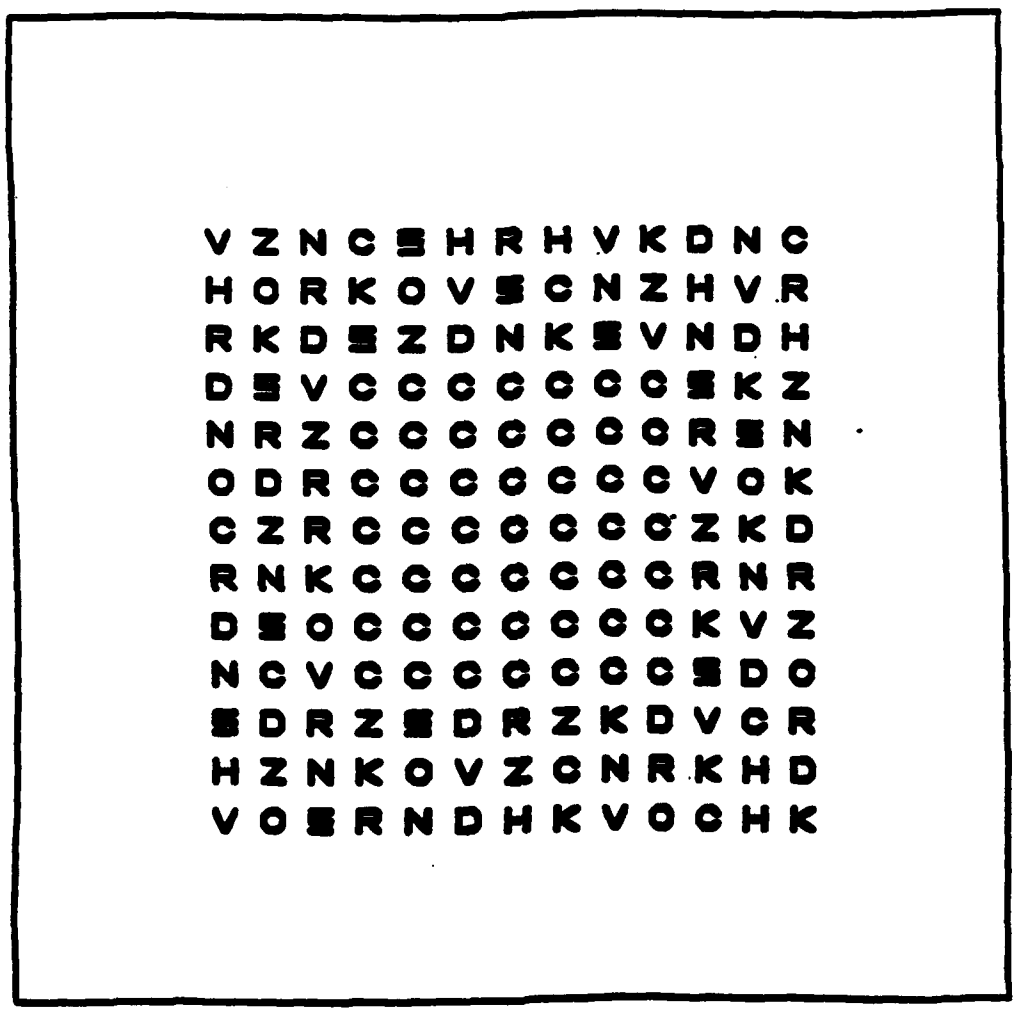

Figure 34. An example of a repeat-letter flash card. There is a separate flash card for each of 10 letters and for each of 8 letter sizes.

Department of Psychology

UNIVERSITÉ YORK UNIVERSITY

FACULTY OF ARTS

4700 KEELE STREET • NORTH YORK • ONTARIO • CANADA • M3J 1P3

3.12.4 *Ocular Hypertension (OHT) and Early Glaucoma*

We have submitted a paper for publication in Invest. Ophthalmol. and Vis. Sci. on preliminary evidence suggesting that our motion-defined letter test can identify patients with OHT who will go on to develop glaucoma (Ref 234).

3.12.5 *Glare Susceptibility in Cataract*

A group of elderly patients, some of whom have cataract in addition to the expected lens changes associated with aging, have been studied using our glare susceptibility test (see 3.13 below). Some elderly patients have glare susceptibilities that compare well with normally-sighted subjects 10 or even 20 years younger. Those with cataract evident to slit lamp examination have glare susceptibilities that do not seem to be simply correlated with the appearance of the cataract. Preliminary findings were reported at ARVO 1991, and a paper has been submitted for publication (Ref 225).

3.13 Glare susceptibility test

We have developed a glare susceptibility test. The rationale can be understood as follows. The effect of scattered-light glare is to reduce letter-reading acuity, the reduction increasing progressively as letter contrast is progressively reduced. In the everyday visual environment this translates as follows. A low level of scattered-light glare produces a selective invisibility of small, low-contrast objects in the environment. With increased glare, low-contrast objects of all sizes disappear and small objects of medium contrast disappear also. A further increase of glare renders invisible small objects of fairly high contrast unrecognizable or invisible as well as rendering invisible low- and medium-contrast objects of all sizes. A still higher level renders invisible or unrecognizable all objects except large objects of fairly high contrast and large and medium-sized objects of high contrast.

Department of Psychology

UNIVERSITÉ YORK UNIVERSITY

FACULTY OF ARTS

4700 KEELE STREET • NORTH YORK • ONTARIO • CANADA • M3J 1P3

The procedure is to measure visual acuity in minimal-glare conditions using the Regan Low Contrast Acuity Charts. Five charts are available, with letters of 100%, 50%, 25%, 11% and 4% contrasts (Fig. 35A,C). Then the measurements are repeated using a glare source (Fig. 35B,D). Acuities are defined as the letter size for 75% correct letter reading, and are obtained from the psychometric functions by Probit analysis.

We define the Glare Susceptibility Ratio as the ratio between visual acuities under minimal-glare and with-glare conditions. There is a separate glare susceptibility ratio for each of the five letter contrasts (Fig. 36). The ratios for 4% and 11% contrast are very sensitive measures. They reveal large intersubject differences in normally-sighted subjects in the 10–25 years age group.

The glare susceptibility ratio is an index of disability glare that might be of use in quantifying intersubject differences in glare disability in relation to night-time driving or driving in low-sun conditions. The index might also be of use in screening aircraft pilots who are required to fly in high-glare environments.

All entrants to Canadian Forces flying school are being screened with this test to find whether results predict which individuals will encounter problems in flying over snow-covered terrain, and especially in terrain avoidance.

The test is being used at about 100 test sites in the USA in a multi-center study on multi-focal cataract implant lenses under FDA auspices. The test has been described and its possible use in aviation pointed out, citing AFOSR sponsorship (Refs 195, 208). We supply the software gratis to research laboratories citing AFOSR sponsorship (see below).

3.13 Shape discrimination and the judgement of perfect symmetry: dissociation of shape from size. (Long term aims 1.1.1, an extension of Expt. 2)

This experiment on visual channeling reports psychophysical data on independent processing of shape and size. Results have been reported to ARVO 1991 and published in Vision

Department of Psychology

UNIVERSITÉ
YORK
UNIVERSITY

FACULTY OF ARTS

4700 KEELE STREET • NORTH YORK • ONTARIO • CANADA • M3J 1P3

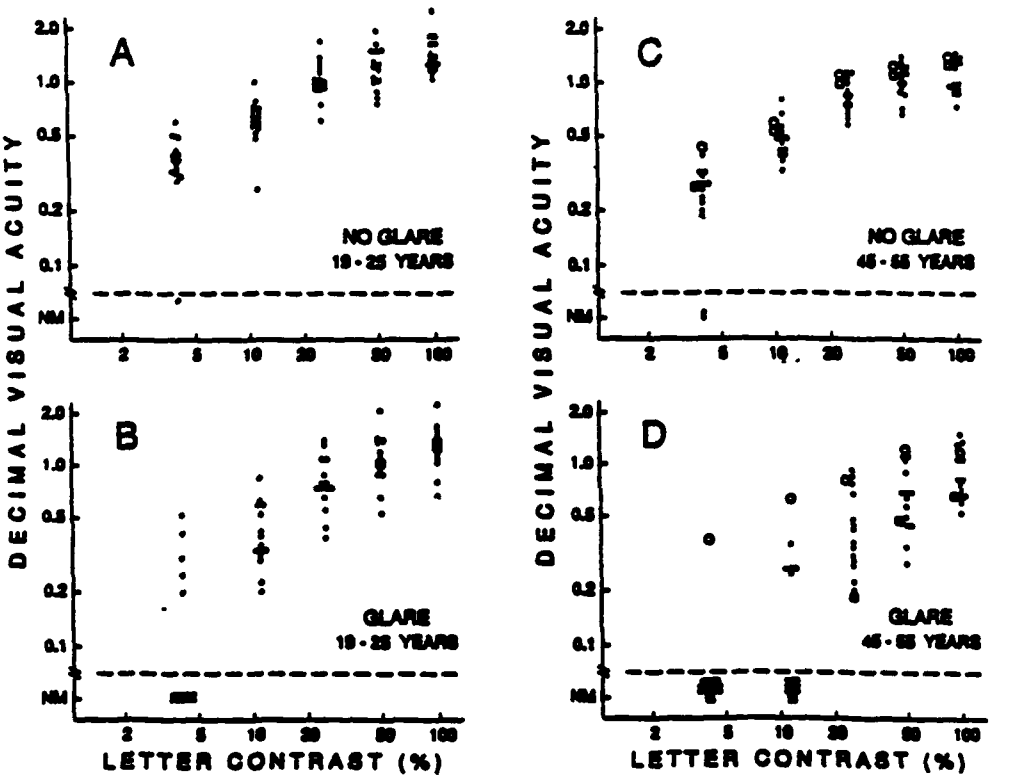

Figure 35. Decimal visual acuity (ordinate) versus letter contrast (abscissa) without glare and with glare for 15 subjects aged 19 to 25 years and for 15 subjects aged 45 to 55 years. Both axes are logarithmic. Viewing was monocular and one eye per subject was tested. Each symbol represents one eye. In the 45 to 55 years age group ○ = the eye shown in Fig. 36 to be least affected by glare, and □ = the eye most affected by glare. NM on the ordinate signifies "not measurable).

Department of Psychology

UNIVERSITÉ
YORK
UNIVERSITY

FACULTY OF ARTS

4700 KEELE STREET • NORTH YORK • ONTARIO • CANADA • M3J 1P3

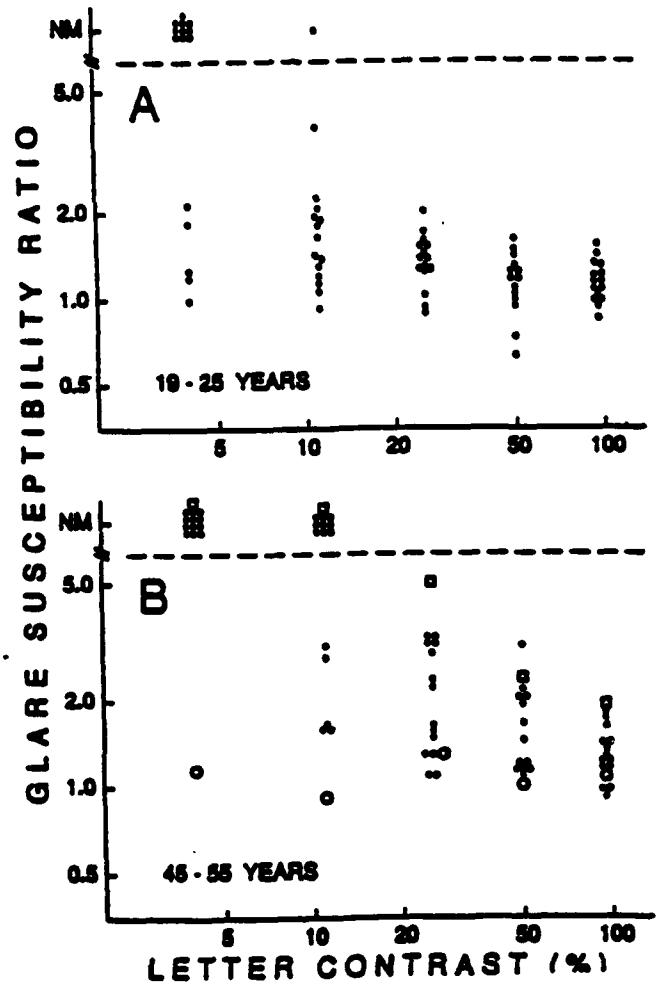

Figure 36. Glare susceptibility ratio (ordinates) versus letter contrast (abscissae) obtained from the Fig. 35 data. Both axes are logarithmic. Glare susceptibility ratio was defined as decimal visual acuity for the no-glare condition divided by decimal visual acuity measured in the glare condition. A – 15 subjects in the 19–25 year age group. B – 15 subjects in the 45–55 year age group. Viewing was monocular. Each symbol represents one eye. NM on the ordinate signifies that acuity under glare conditions was so low that the ratio was not measurable. ○ = the eye that was least affected by glare, and □ = the eye that was most affected by glare.

Department of Psychology

UNIVERSITÉ YORK UNIVERSITY

FACULTY OF ARTS

4700 KEELE STREET • NORTH YORK • ONTARIO • CANADA • M3J 1P3

Research (Ref 211).

In everyday life we receive a large amount of important information by recognizing the shapes of two-dimensional symbols such as traffic signs or numbers presented as outlines or as filled areas. Clearly, a requisite of shape recognition is the ability to discriminate between shapes.

Rather than attempting to investigate the grand problem of two-dimensional shape discrimination we restricted ourselves to a very simple case. We chose the special task of discriminating between rectangles (or ellipses) entirely on the basis of aspect ratio (a/b) where a and b were, respectively, the rectangle's (or ellipse's) height and width. In designing the present study, our aim was that subjects should distinguish between two shapes entirely on the basis of a difference in *relative* dimensions along different azimuths in the fronto-parallel plane. Therefore, we designed a shape discrimination task that could not be performed correctly on the basis of contour separation along any one direction. In addition, subjects were forced to disregard random changes in stimulus area, luminance and total light flux.

EXPERIMENT 1: TWO DIMENSIONAL SHAPE DISCRIMINATION FOR SOLID RECTANGLES

Methods

Stimulus Generation

Solid, bright, sharp-edged rectangles were generated on a monitor (Tektronix model 608 with green P31 phosphor) by means of hardware of our own design and construction. The frame rate was 125 Hz and the rectangle was drawn with 200 lines. Because the rectangle's dimensions were controlled by analogue hardware, they could be varied by indefinitely small steps. The screen was switched off by applying a voltage to the Z blank input at all times except during the 1.5-sec presentations.

Procedure

Department of Psychology

UNIVERSITÉ YORK UNIVERSITY

FACULTY OF ARTS

4700 KEELE STREET • NORTH YORK • ONTARIO • CANADA • M3J 1P3

Each trial consisted of a pair of 1.5 sec presentations. One presentation was of a reference rectangle with some fixed aspect ratio $(a/b)_{REF}$ where a and b were, respectively, the rectangle's height and width. In the other presentation a test rectangle was presented whose aspect ratio $(a/b)_{TEST}$ was selected by the computer from one of 10 preset values.

Three viewing distances were used: 63 cm, at which the mean area of the rectangle was 4.0 deg^2 (i.e., equivalent to a 2.0 x 2.0 deg square); 126 cm, at which the mean area was 1.0 deg^2 (i.e., equivalent to a 1.0 x 1.0 deg square); and 252 cm, at which the mean area was 0.25 deg^2 (i.e., equivalent to a 0.5 x 0.5 deg square).

Results

Fig. 37 shows the results of Experiment 1 for all four subjects. Filled data points indicate that all test stimuli were elongated horizontally, while open data points indicate that all test stimuli were elongated vertically. In each curve there were two data points for an aspect ratio of 1.0 (see *Methods*). In Fig. 37A the major finding was that the just-noticeable change of aspect ratio was smallest for $(a/b)_{REF} = 1.0$. Fig. 37A-C shows that this finding held over a range of mean areas from 0.25 deg^2 to 4.0 deg^2, i.e. a range of 16:1.

Fig. 37D-L confirms this main finding for the other three subjects. The steepness of the V-shaped curve, however, differed for the different subjects. The best values of aspect ratio discrimination were 1.6%, 2.1%, 2.9% and 2.7% for subjects 1, 2, 3 and 4 respectively.

EXPERIMENT 2: DISCRIMINATION OF THE ANGLE OF INTERSECTION OF TWO STRAIGHT LINES

Methods

Rationale

In principle it was possible in Experiment 1 for subjects to base judgements of aspect ratio

Department of Psychology

UNIVERSITÉ
YORK
UNIVERSITY

FACULTY OF ARTS

4700 KEELE STREET • NORTH YORK • ONTARIO • CANADA • M3J 1P3

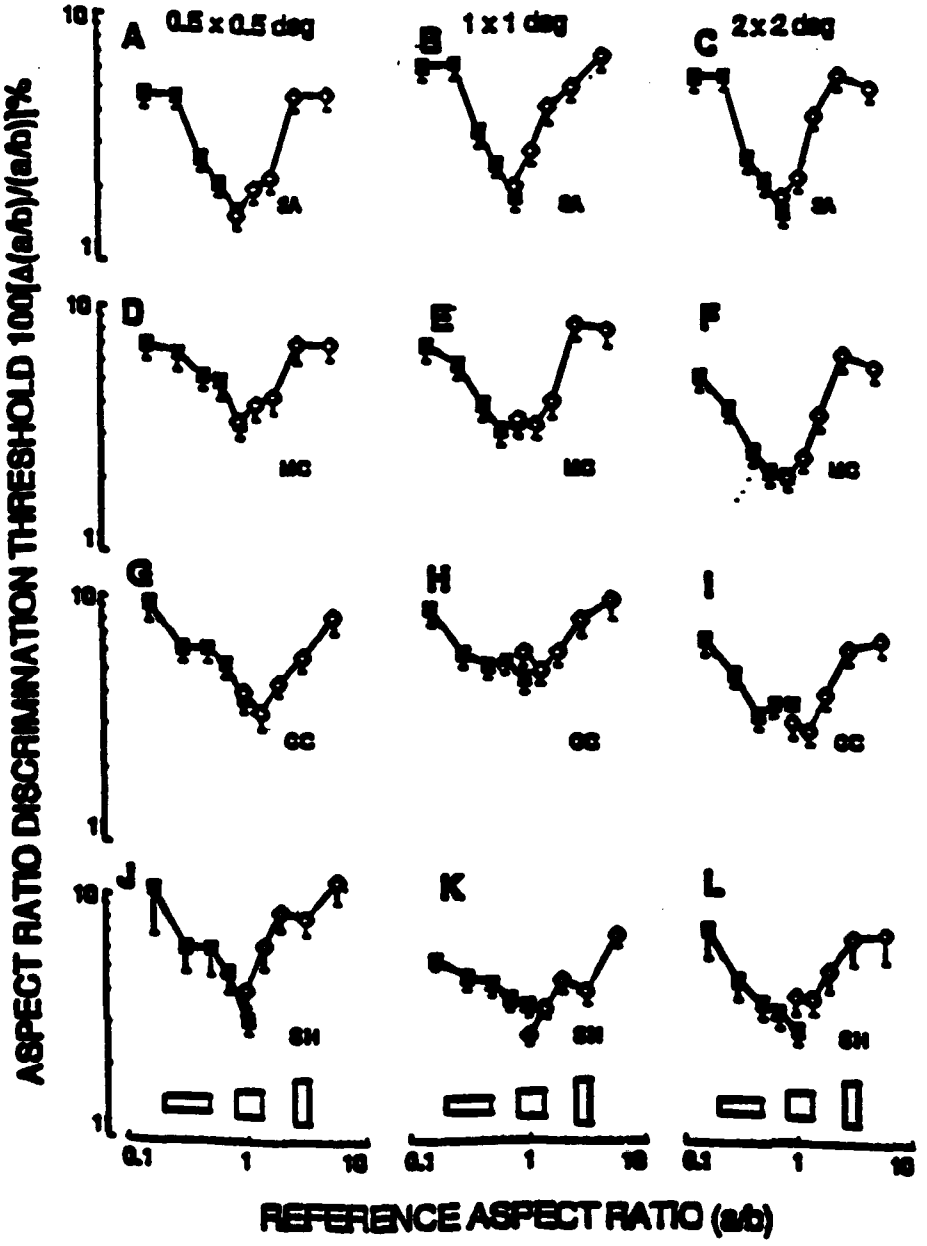

Figure 37. Results of Experiment 1. A-L: The just-detectable percentage change in aspect ratio (ordinate) for rectangles of different aspect ratios (abscissa). A-C: Data for subject 1 for rectangles of area 0.25 deg^2 (A), 1.0 deg^2 (B) and 4.0 deg^2 (C). D-F: Corresponding data for subject 3. C-I: Corresponding data for subject 3. J-L: Corresponding data for subject 4.

Department of Psychology

UNIVERSITÉ YORK UNIVERSITY

FACULTY OF ARTS

4700 KEELE STREET • NORTH YORK • ONTARIO • CANADA • M3J 1P3

on either the angle of intersection between imaginary lines joining obliquely-opposite corners of the rectangle (θ) or on the absolute orientation of one or other line rather than on the value of (a/b). The present experiment was designed to find whether discrimination threshold for relative or absolute orientation was sufficiently low to explain the data of Experiment 1. The reason for randomly jittering the length of each line on a trial-to-trial basis was to prevent subjects from basing judgements on the aspect ratio (a/b) of a rectangle formed by imaginary lines joining the ends of the oblique stimulus lines.

Procedure

Each trial consisted of a pair of 1.5 sec presentations. One presentation was of a reference angle θ_{REF}. In the other presentation the angle of intersection of the two lines, θ_{TEST}, was selected by computer from one of 5 preset values (Fig. 38). The order of presentation of the reference and trial stimuli was randomized within each trial, giving 10 pairs of trials, and the order of the 10 trial pairs was also randomized. The method of constant stimuli was used with temporal two-alternative forced choice. Subjects were provided with two buttons and instructed to press button number one if angle θ was greater in the first than in the second presentation of the pair, and button number two if angle θ was greater in the second presentation. All 5 values of θ_{TEST} were greater than θ_{REF} when θ_{REF} was larger than 90 deg, and all 5 values of θ_{TEST} were less than θ_{REF} was smaller than 90 deg. Two sets of data were collected for θ_{TEST} = 90 deg: one with all 5 values of θ_{TEST} greater than 90 deg, and one with all 5 values less than 90 deg.

Results

Angular discrimination thresholds ($\Delta\theta$) for two-line angle of intersection are plotted in Fig. 39 in terms of the equivalent percentage aspect ratio discrimination thresholds for rectangles. The best discrimination thresholds for subjects 1, 4 and 5 (plotted in A, B and C respectively) were 1.5%, 2.8% and 4.2%, respectively. For the two subjects tested, these thresholds were in close

Department of Psychology

UNIVERSITÉ
YORK
UNIVERSITY

FACULTY OF ARTS

4700 KEELE STREET • NORTH YORK • ONTARIO • CANADA • M3J 1P3

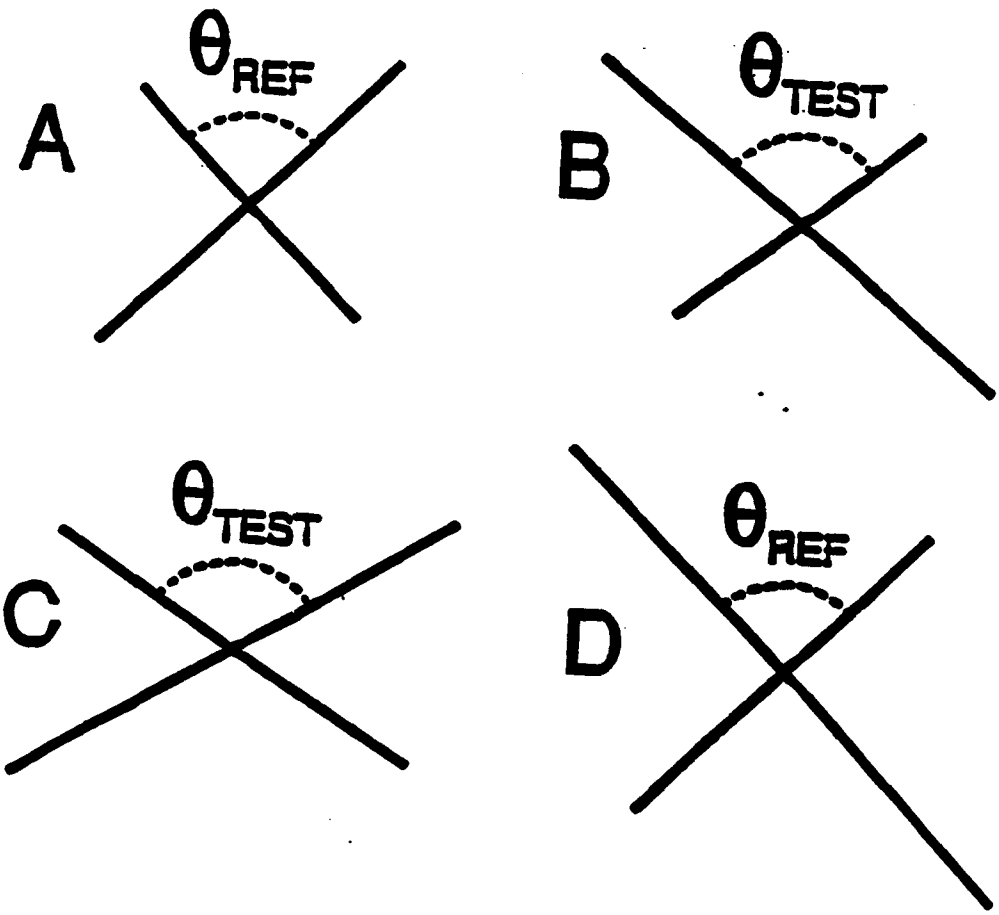

Figure 38. A and B show the reference angle and one of the 5 different test angles. C and D show the same reference angle and a second one of the 5 test angles. The length of each line was independently and randomly varied on each presentation. Note that the difference between θ_{REF} and θ_{TEST} were usually considerably smaller than shown here.

Department of Psychology

UNIVERSITÉ
YORK
UNIVERSITY

FACULTY OF ARTS

4700 KEELE STREET • NORTH YORK • ONTARIO • CANADA • M3J 1P3

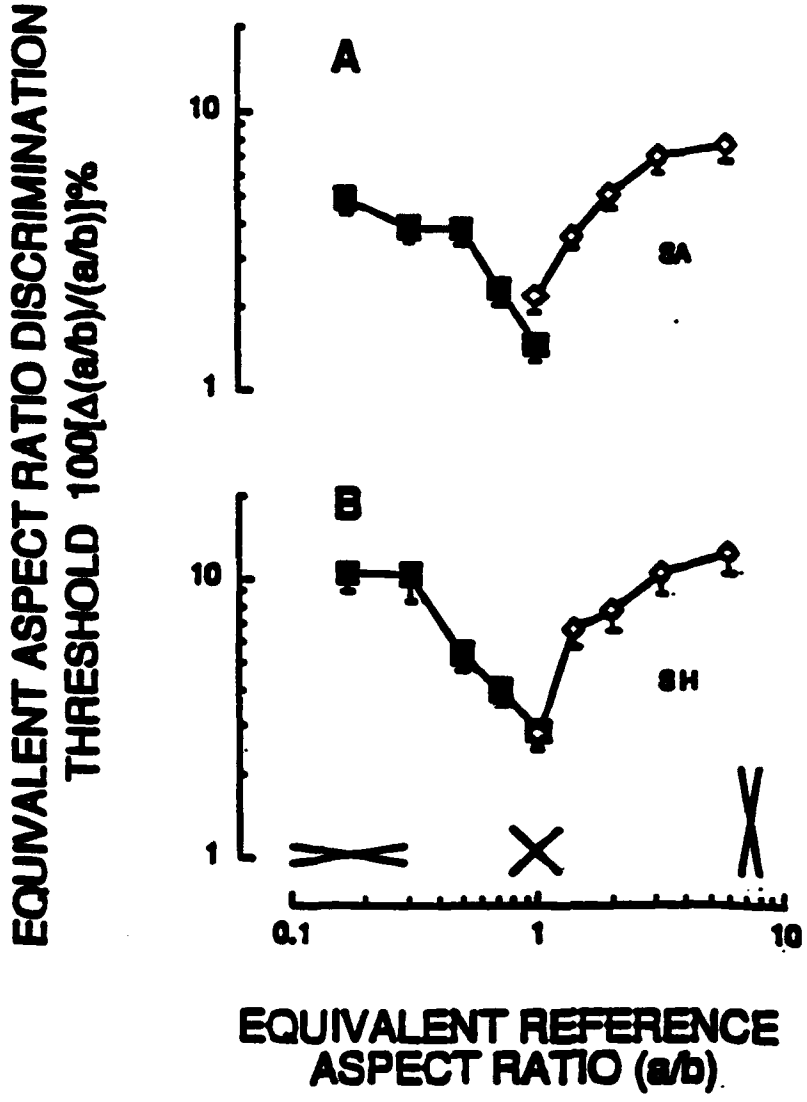

Figure 39. The just-detectable difference in angle subtended between two lines (ordinate) for different mean angles (abscissa). The abscissa is scaled in terms of the aspect ratio of a rectangle such that the angle between lines joining its corners is θ_{REF}.

Department of Psychology

UNIVERSITÉ YORK UNIVERSITY

FACULTY OF ARTS

4700 KEELE STREET • NORTH YORK • ONTARIO • CANADA • M3J 1P3

agreement with the best values of aspect ratio discrimination thresholds for a rectangle obtained in Experiment 1 (1.6% for subject 1 and 2.7% for subject 4). Furthermore, the corresponding curves had similar V-shapes (compare Fig. 39A with 37A-C and Fig. 39B with 37J-L). This correspondence between the data of Figs. 39 and 37 is consistent with the hypothesis that, in Experiment 1, subjects based their judgement of aspect ratios of solid rectangles on estimation of the angle of intersection of imaginary lines joining opposite corners of the rectangles.

EXPERIMENT 3: TWO-DIMENSIONAL SHAPE DISCRIMINATION FOR ELLIPSES.

Methods

Rationale

As mentioned above, in Experiment 1 it was possible, in principle, for subjects to base judgements of aspect ratio on the angle of intersection between imaginary lines joining the obliquely-opposite corners of the rectangle and/or the absolute orientation of one or other imaginary line. In Experiment 3 we further addressed this point by measuring aspect ratio discrimination for an ellipse rather than for a rectangle. Our rationale was that subjects could not draw imaginary lines between corners, because an ellipse has no corners. Furthermore the absolute orientations of major and minor axes were the same for every ellipse presented.

Stimulus Generation

Stimuli were generated on a monitor (Tektronix model 608 with green P31 phosphor) by means of analogue hardware of our own design and construction. The stimulus was the outline of an ellipse whose major and minor axes were vertical and horizontal. The line's width was about 0.3 mm, and the ellipse was redrawn 1000 times per sec. The aspect ratio and area of the ellipse could be varied by indefinitely small amounts. The viewing distance was 126 cm at which the diameter of the ellipse was 1.0 deg when its aspect ratio was equal to 1.0.

Results

Department of Psychology

UNIVERSITÉ
YORK
UNIVERSITY

FACULTY OF ARTS

4700 KEELE STREET • NORTH YORK • ONTARIO • CANADA • M3J 1P3

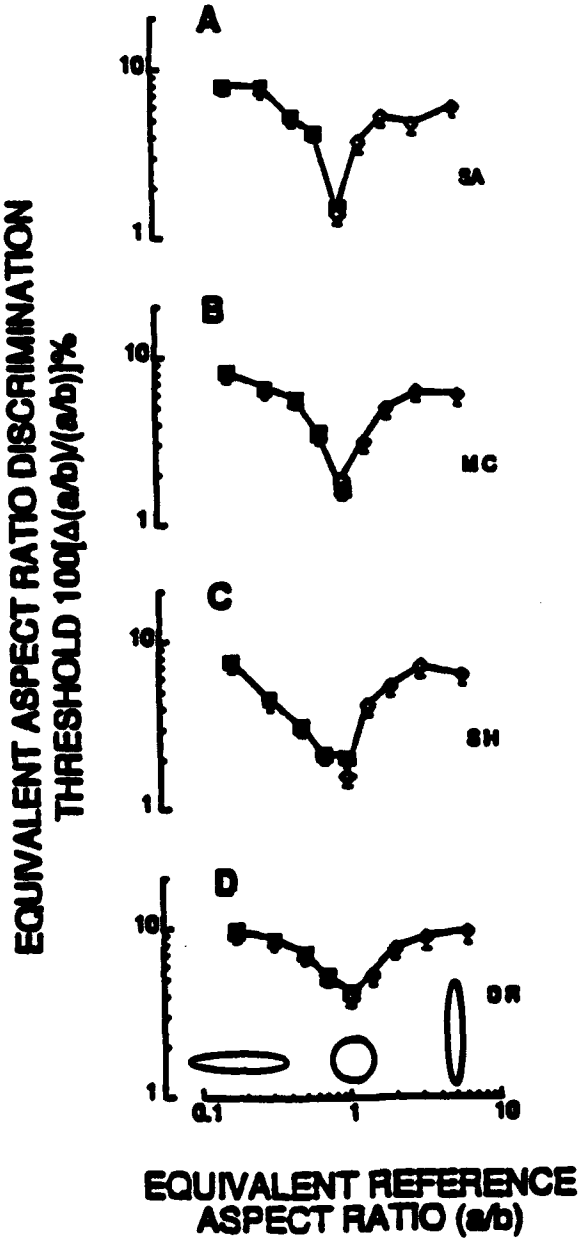

Figure 40. The just-detectable difference in aspect ratio (ordinate) for outlined ellipses of different aspect ratios (abscissa). Data are shown for four subjects.

Department of Psychology

UNIVERSITÉ YORK UNIVERSITY

FACULTY OF ARTS

4700 KEELE STREET • NORTH YORK • ONTARIO • CANADA • M3J 1P3

Figure 40(A-D) shows that the best values of aspect ratio discrimination threshold were 1.4%, 1.7%, 1.6% and 4.0% for subjects 1, 2, 4 and 5 respectively. For the three subjects who performed Experiment 1, these data are in close to fair agreement with aspect ratios for solid rectangles measured in Experiment 1 (1.6%, 2.1% and 2.7% for subjects 1, 2 and 4 respectively). As was the case for the solid rectangle (Fig. 37), discrimination threshold was lower for a 1.0 aspect ratio than for higher or lower aspect ratios.

EXPERIMENT 4: ASPECT RATIO ADAPTATION FOR A SOLID TEST RECTANGLE

Methods

Rationale

The design of Experiment 4 was dictated by the hypothesis that aspect ratio discrimination for a solid rectangle in Experiment 1 was determined by the relative activity of multiple mechanisms that responded to different ranges of aspect ratios. In Experiment 4 we explored whether a selective adaptation procedure could produce evidence for these multiple mechanisms.

Procedure

The experiment was controlled by a microcomputer that also recorded the subject's responses. Before recording quantitative data, subjects were instructed to fixate the centre of the adapting rectangle during an initial 10 min adaptation period, and to maintain this fixation throughout the entire experiment. The adapt rectangle was elongated either vertically (a/b = 1.5) or horizontally (a/b = 1/1.5) and had an area 1.0 deg^2. After the initial 10 min adaptation period the screen was blanked for 0.1 sec, a test rectangle was presented for 0.5 sec, the screen was blanked for 0.1 sec, then the adapting rectangle was presented for 7 sec to refresh the level of adaptation, the screen was blanked for 0.1 sec, another test rectangle was presented for 0.5 sec, the screen was blanked for 0.1 sec, the adapting rectangle was presented for 7 sec and so on. There were 10

Department of Psychology

UNIVERSITÉ
YORK
UNIVERSITY

FACULTY OF ARTS

4700 KEELE STREET • NORTH YORK • ONTARIO • CANADA • M3J 1P3

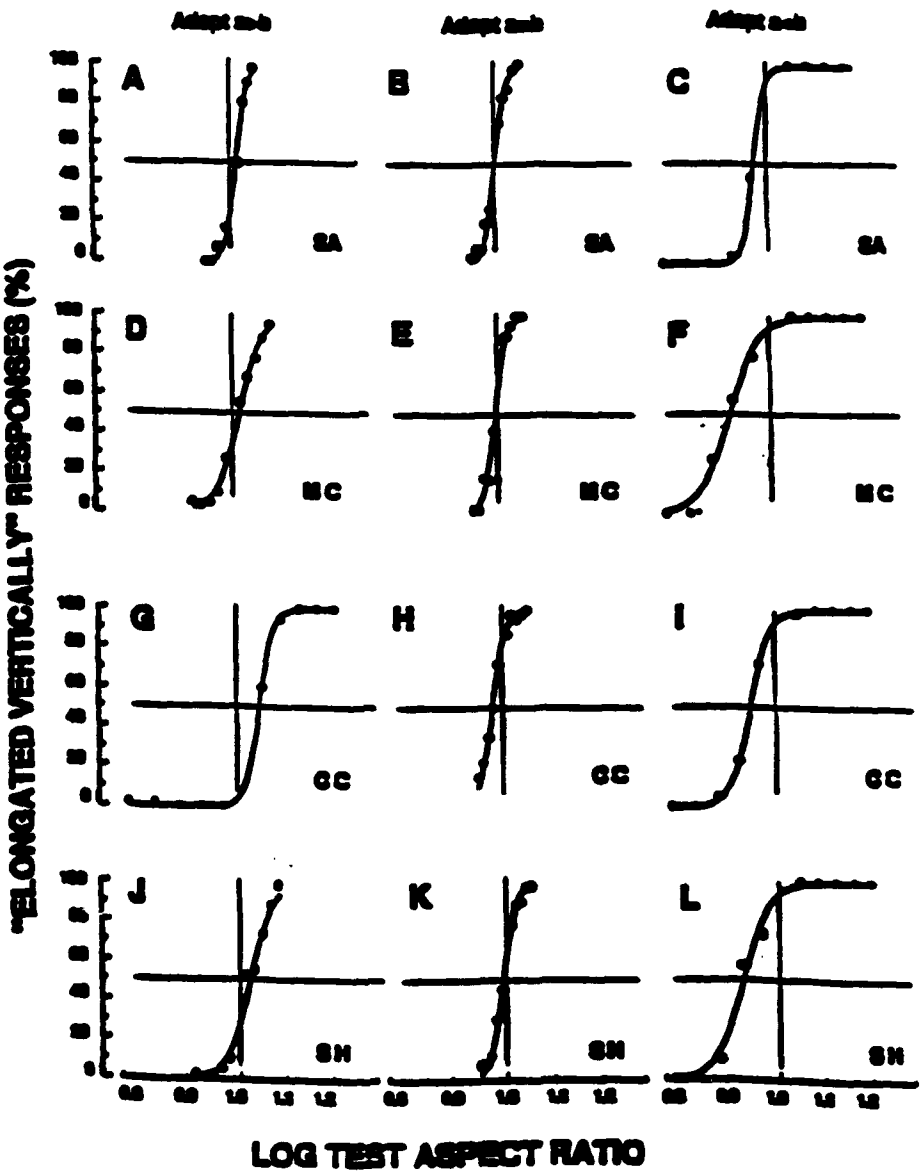

Figure 41. Results of Experiment 4. A-L: Aspect ratio aftereffect caused by adapting to a rectangle. Ordinates plot on a linear axis the percentage of times that subject judged that the test rectangle was elongated vertically. The aspect ratio of the test rectangle is plotted on a logarithmic axis along the abscissaa. A-C: Data for subject 1 after adapting to a vertically-elongated rectangle of aspect ratio (a/b) = 1/1.5 (c). D-F: Correspnding data for subject 2. G-I: Corresponding data for subject 3. J-L: Corresponding data for subject 4.

Department of Psychology

UNIVERSITÉ YORK UNIVERSITY

FACULTY OF ARTS

4700 KEELE STREET • NORTH YORK • ONTARIO • CANADA • M3J 1P3

different test rectangles with the values of $(a/b)_{TEST}$ spaced symmetrically on either side of (a/b) = 1.0. The different test rectangles were presented in randomized order until the predetermined number of repeats had been completed. In a typical 2 - 3 hour session we collected responses to 300 test presentations. The method of constant stimuli was used with two-alternative forced choice. Subjects were instructed to press one of two buttons depending on whether the test rectangle was elongated more in the horizontal than in the vertical direction or vice versa. The area of the adapt rectangle was always 1.0 deg^2. The area of the test rectangle on any given trial was selected randomly from one of 256 values between 0.2 deg^2 and 1.0 deg^2.

Fig. 41 A-L shows postadaptation psychometric functions for subjects 1-4 obtained with the adapt and test rectangles of equal area. The first column in Fig. 41 (Fig. 41A, D, G and J) is for a vertically-elongated adapt rectangle of aspect ratio 1.5, the second column (Fig. 41B, E, H and K) shows control data for a square adapt stimulus [i.e. $(a/b)_{ADAPT}$ = 1.0] and the third column (Fig. 41C, F, I and L) is for a horizontally-elongated adapt rectangle of aspect ratio 1/1.5.

EXPERIMENT 5: ASPECT RATIO AFTEREFFECT FOR AN ELLIPTICAL TEST STIMULUS OF VARIABLE AREA (CROSS-ADAPTATION).

Methods

Rationale

If the same mechanism determines aspect ratio discrimination threshold for rectangles and ellipses, then we would expect the aspect ratio aftereffect to show cross-adaptation between rectangles and ellipses.

Procedure and Analysis of Data

In the ADAPT condition, a solid bright rectangle whose aspect ratio was $(a/b)_{ADAPT}$ was presented at the centre of the screen. The sides of the rectangle were horizontal or vertical. In the TEST condition an outlined ellipse whose aspect ratio was $(a/b)_{TEST}$ was presented centred on the

Department of Psychology

UNIVERSITÉ YORK UNIVERSITY

FACULTY OF ARTS

4700 KEELE STREET • NORTH YORK • ONTARIO • CANADA • M3J 1P3

location previously occupied by the adapting rectangle. The major axis of the ellipse was horizontal or vertical. The area of the adapting rectangle was always 1.0 deg^2. The mean area of the test ellipse was 0.38 deg^2. On each trial, the area of the test ellipse was selected randomly from 256 values in a range of 0.15 deg^2 to 0.75 deg^2 (i.e., a range of 5:1).

Results

To a first approximation, adapting to a solid rectangle of fixed 1.0 deg^2 area produced similar aspect ratio aftereffects when the test stimulus was a variable-area outlined ellipse, and when the test stimulus was a variable-area solid rectangle.

SUMMARY AND CONCLUSIONS

We measured the *accuracy* with which subjects judged that a square or circle was perfectly symmetrical i.e., that aspect ratio (a/b) was exactly unity (where a and b were, respectively, the vertical and horizontal dimensions). Errors were remarkably small, ranging from 0.7% to 0.4% for the judgement of squareness and from 1.4% to < 0.1% for the judgement of circularity. *Precision* in judging aspect ratio was measured by requiring subjects to judge whether the aspect ratio $(a/b)_{TEST}$ of a test rectangle was greater or less than the aspect ratio $(a/b)_{REF}$ of a reference rectangle. Similar measurements were made for elliptical targets. To ensure that subjects based judgements on aspect ratio rather than a, b or $(a-b)$, the area of each successive presentation was varied randomly. The just-discriminable percentage change of aspect ratio was as low as 1.6% at $(a/b)_{REF} = 1.0$ (i.e. for a square or circular reference), and rose progressively as $(a/b)_{REF}$ was made progressively larger or smaller than 1.0. Aspect ratio discrimination threshold was independent of mean area over a sixteen-fold range of 0.25 to 4.0 deg^2. For both rectangles and ellipses, the best value of aspect ratio discrimination threshold corresponded to a precision of encoding a and b of 14 sec arc or better. In further experiments, the method of constant stimuli was used to measure an aspect ratio aftereffect produced by adapting separately to rectangles of $(a/b)_{ADAPT}$ equal to 1.5, 1.0

Department of Psychology

UNIVERSITÉ YORK UNIVERSITY

FACULTY OF ARTS

4700 KEELE STREET • NORTH YORK • ONTARIO • CANADA • M3J 1P3

and (1/1.5). Similar aftereffects were obtained whether the area of the test stimulus was fixed or varied randomly from trial to trial, and whether the test stimulus was rectangular or elliptical. The aftereffect could not be explained in terms of fatigue of neurons sensitive to linear dimension *a* or *b*. Nor could the aftereffect be explained in terms of the "contour repulsion" hypothesis, or in terms of orientation discrimination.

We conclude that our psychophysical data demonstrates the existence of a neural mechanism sensitive to two-dimensional shape independently of size. In particular (1) that the same neural mechanism determines aspect ratio discrimination threshold for rectangles and ellipses and (2) that this mechanism is sensitive to aspect ratio independently of linear dimensions. We propose that aspect ratio perception is determined by the balance of excitation of two pools of neurons that are selectively sensitive to different, but overlapping ranges of (a/b). One pool prefers aspect ratios > 1.0 and the other prefers aspect ratios < 1.0. We suppose that the two pools respond identically to changes in area ($a*b$). The aspect ratio aftereffect occurs when one pool is fatigued more than the other, thus altering the balance of excitation. This hypothesis can explain why aspect ratio discrimination is best at $(a/b)_{REF}$ = 1.0, why co-varying changes of area are not confounded with changes of (a/b), and why aspect ratio discrimination threshold is not affected by mean area.

3.14 Colour-defined form and luminance-defined form (long-term aims 1.1.2)

The aims of this experiment are (1) to distinguish between the processing of equiluminant colour-defined form and luminance-defined form by means of combined neuromagnetic and

Department of Psychology

UNIVERSITÉ
YORK
UNIVERSITY

FACULTY OF ARTS

4700 KEELE STREET • NORTH YORK • ONTARIO • CANADA • M3J 1P3

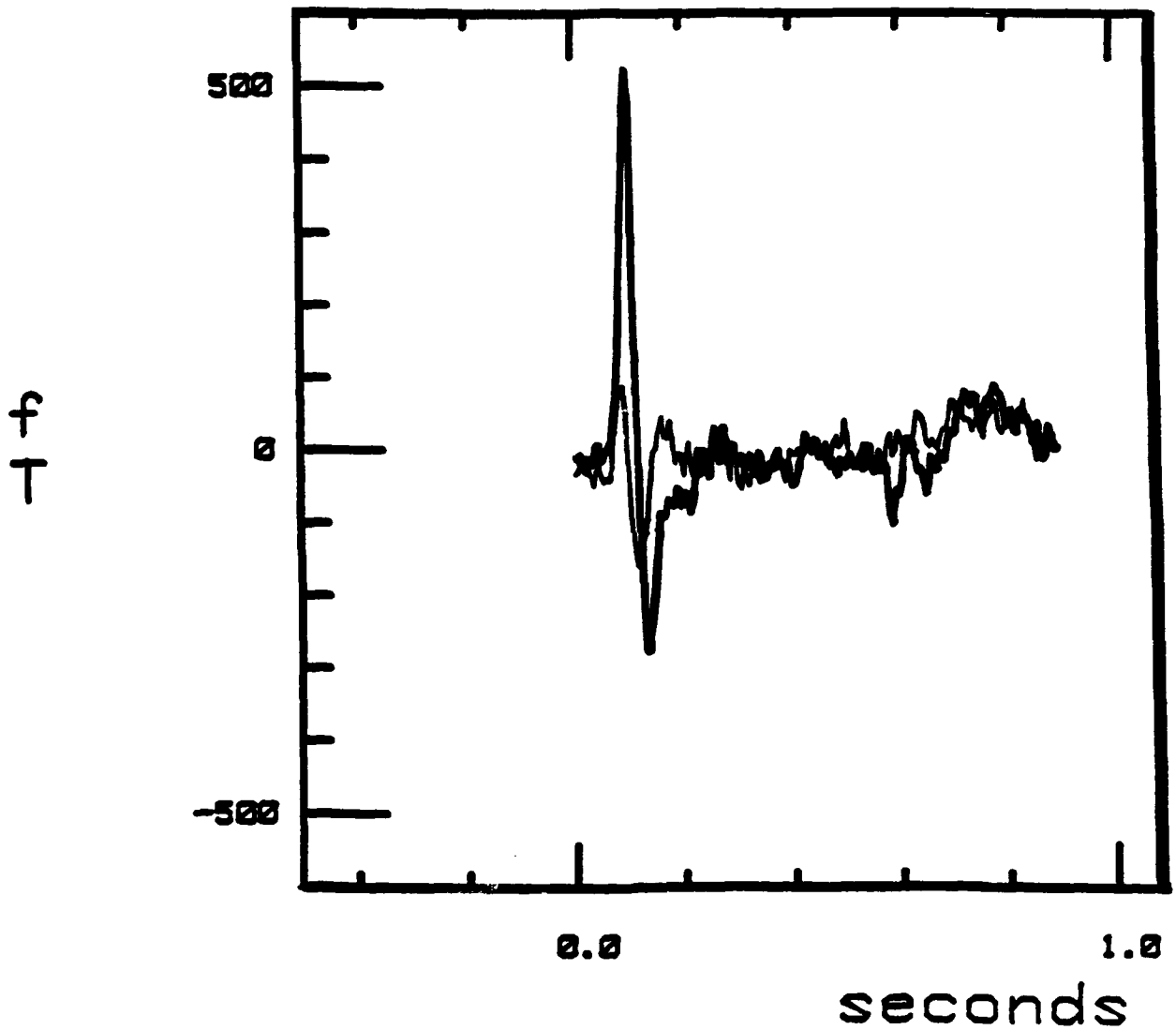

Figure 42. Neuromagnetic response to the onset of an equiluminant red-green chromatic grating (thick trace) and to the onset of a yellow luminance grating (thin trace). The chromatic and luminace gratings were made by superimposing equiluminant red and green gratings in, respectively, 180 deg and 0 deg spatial phase. Spatial frequency 2.0 c/deg.

Department of Psychology

UNIVERSITÉ YORK UNIVERSITY

FACULTY OF ARTS

4700 KEELE STREET • NORTH YORK • ONTARIO • CANADA • M3J 1P3

evoked potential recording, (2) to find whether responses to the two kinds of form are generated in different brain locations and, if so, (3) to compare the site of responses to colour-defined form with the supposed location of V4 in human.

Our red-green stimulus is a 4 x 4 deg sinewave grating produced by superimposing equiluminant red and green sinewaves in 180° spatial phase. The corresponding yellow luminance contrast stimulus is composed of the same red and green gratings in 0° spatial phase. Our blue-yellow chromatic and white luminance gratings are made similarly from blue and yellow components.

Figure 42 shows that, at some recording locations, the equiluminant red-green chromatic grating produces a much larger neuromagnetic response than the yellow luminance grating (compare the thick and thin traces). In addition, the response to the chromatic grating is considerably larger than the sum of the responses to the red and green components presented in isolation. Furthermore, the chromatic response remains large when the balance between red and green luminances is varied slightly on either side of the equiluminant point. We conclude that this red-green response cannot be explained as a luminance artifact, and must be regarded as a genuine response to chromatic contrast. Additional supporting evidence is that the way in which response amplitude depends on spatial frequency is quite different for responses to chromatic contrast and luminance contrast.

In order to compare the source locations of responses to chromatic contrast ans luminance contrast, we have recorded from up to 54 scalp locations while stimulating one visual field quadrant with the 4 x 4 deg stimulus grating. Data have been collected for all four individual quadrants, for chromatic and luminance gratings, and for three subjects. These data are being analysed. A paper is in preparation (Ref 238), and an abstract will be submitted for ARVO 1993.

Department of Psychology

UNIVERSITÉ YORK UNIVERSITY

FACULTY OF ARTS

4700 KEELE STREET • NORTH YORK • ONTARIO • CANADA • M3J 1P3

3.15 Recognition and detection of texture-defined letters (long-term aims 1.1.1 and psychophysical backup for experiment 3.9 above)

It is well known that the ability to see (i.e. detect) an object can be supported by texture contrast alone, and there is considerable literature on the detection of texture-defined form (also called "texture segregation"). Little is known, however, about spatial discriminations for texture-defined (TD) form. This psychophysical study complements the neuromagnetic study 3.9 above. It is aimed to compare detection and discrimination for TD form, and to use the resulting data to compare physiologically-based models of the processing of TD form.

As a spatial discrimination task we chose reading performance for letters that were rendered visible by a texture difference (TD letters), and we compared letter recognition scores with letter detection scores. The reasons for choosing a letter reading task was as follows: (1) to expediate future research aimed to find whether there are different brain mechanisms that handle processing of texture-defined form, motion-defined form and luminance-defined form by investigating patients with brain lesions. This future project would follow the logic of our previous study on motion-defined letters in which we found that recognition of MD letters could be lost while recognition of LD letters was spared (3.2 above); (2) to ensure compatability with our data on MD form obtained using MD letters.

The texture is composed of short lines scattered pseudo-randomly. Lines within the letter are vertical, while lines outside the letter are horizontal. The visibility of the letter can be progressively degraded by adding randomly located "noise" dots to the pattern. A completely new pattern can be generated at up to 70 times per sec. There are 10 different letters. Letter recognition and letter detection is plotted versus the number of noise dots per texture line.

Over the last year we have completed the data collection for 4 subjects. Fig. 43 illustrates how percent correct reading accuracy falls off as the number of noise dots is progressively

Department of Psychology

UNIVERSITÉ
YORK
UNIVERSITY

FACULTY OF ARTS

4700 KEELE STREET • NORTH YORK • ONTARIO • CANADA • M3J 1P3

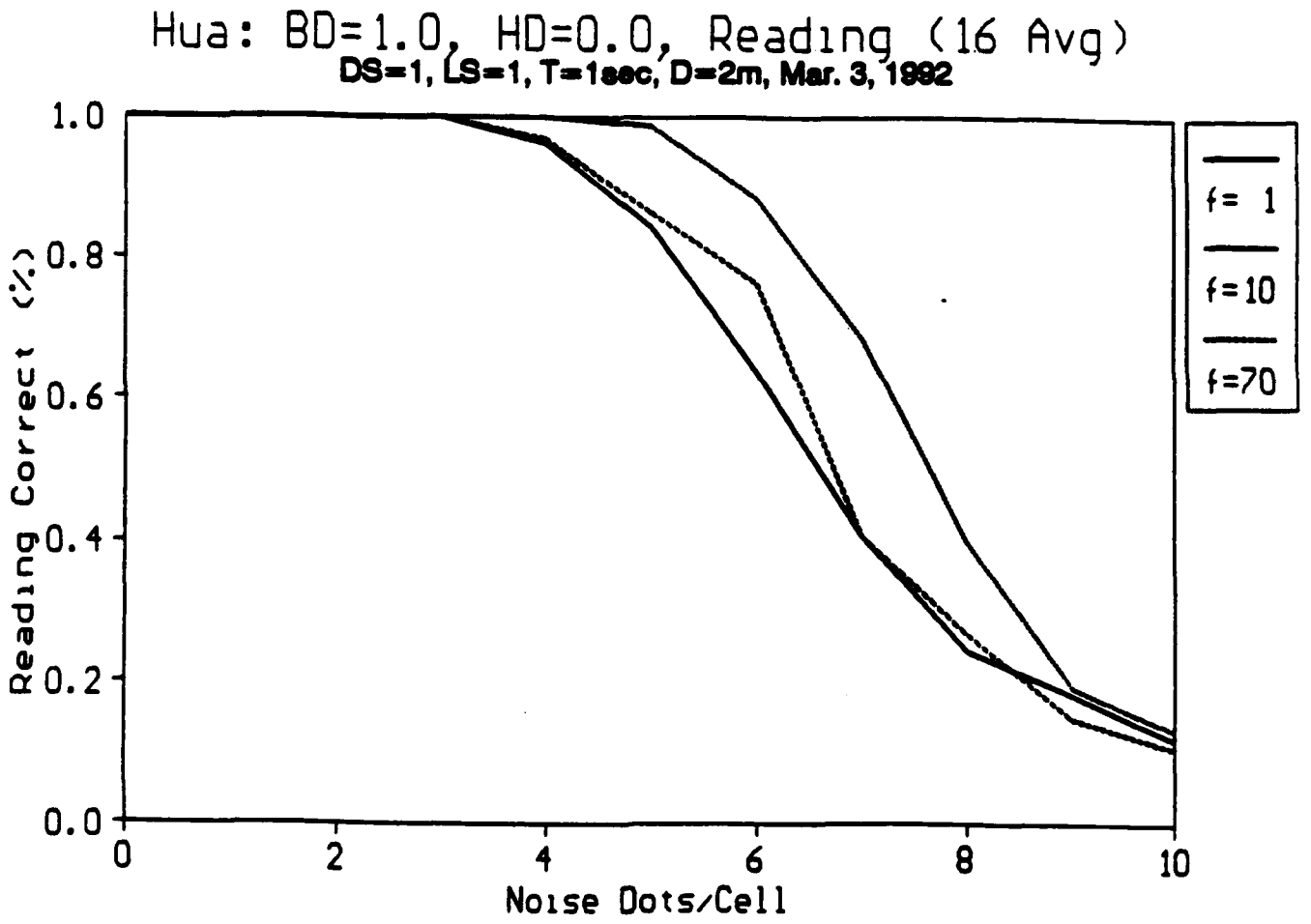

Figure 43. Texture-defined letter recognition. Ordinate: percent correct reading accuracy. Abscissa: number of noise dots per texture line. Reading accuracy falls off as the texture contrast is progressively degraded.

Department of Psychology

UNIVERSITÉ YORK UNIVERSITY

FACULTY OF ARTS

4700 KEELE STREET • NORTH YORK • ONTARIO • CANADA • M3J 1P3

increased. Presentation was 1.0 sec for all three curves and data are shown only when a single pattern was presented during the 1.0 sec (f=1), when 10 different patterns weere presented in 1.0 sec (f=10), and when 70 different patterns were presented in 1.0 sec (f=70).

We have attempted to describe these data using two physiologically-plausible models. Rather than comparing global statistical properties of the two textures we follow the bulk of current literature in using a multi-channel approach to specify the boundary between the textures. The first stage of both models is conventional: local analysis by a bank of parallel linear filters tuned to different orientations and spatial frequencies and with difference-of-gaussian profiles. The second stage of both models is nonlinear, and in particular, rectification. The two models differ at stage 3. One model involves nonlinear lateral facititation between responses to different orientations. The other model involves nonlinear orientation-specific inhibition within a single receptive field. Both models include a quantitative treatment of spatial variability within the textures as a limiting factor in texture segregation.

The models have been implemented on computer to generate predictions that compare directly with data of the kind shown in Fig. 43. We have also generated displays illustrating how the letters appear after passing through the several stages of the models. This work is currently being written up for publication (Ref 239).

3.16 Disassociation of chromatic and achromatic processing of spatial form (Long-term aim 1.1.1 and specific aim 1.2.1).

This experiment is concerned with the breaking of camouflage by chromatic contrast, i.e. with the perception of color-defined form. This psychophysical experiment complements our neuromagnetic study on color-defined form (3.14 above).

We addressed the assumption that equiluminance uncovers the chromatic contrast

Department of Psychology

UNIVERSITÉ YORK UNIVERSITY

FACULTY OF ARTS

4700 KEELE STREET • NORTH YORK • ONTARIO • CANADA • M3J 1P3

subsystem. A simple point is that CIE equiluminance will not be the same as biological equiluminance, because individual subjects differ from the CIE standard observer. But even for sensation luminance (measured by heterochromatic flicker photometry) there is little or no direct evidence to demonstrate that the achromatic subsystem is silenced at equiluminance, and the chromatic system uncovered. Indeed there is some evidence that this is not necessarily the case. For example, Gordon and Shapley found that detection of an edge or sinewave grating below 10 c/deg follows the $V\lambda$ curve, while for lower spatial frequencies the relevent spectral sensitivity curve deviates (Invest. Ophthalmol. and Vis. Sci. Suppl. 30, 128, 1989).

In our study we measured detection threshold for sinewave gratings that were made by superimposing an equiluminant red-green grating (Fig. 44A) on a yellow luminance grating (Fig. 44B) to give the grating shown in Fig. 44C. The luminance grating could be either 0 deg (Fig. 44A-C) or 180 deg (Fig. 44D-F) spatial phase relation with the red component of the chromatic grating. Subjects were provided with a control that increased or decreased the values of m_a and m_c in a yoked manner while leaving constant the ratio m_a/m_c (m_a and m_c are, respectively, the peak-to-peak luminance modulation of the achromatic and chromatic components of the grating, see Fig. 44). Subjects were instructed to set the control so that the grating was just visible. The setting was repeated for a series of values of m_a/m_c.

Our findings can be understood in terms of Fig. 45 where contrast detection threshold (ordinate) is plotted versus m_a/m_c. At 0.0 on the abscissa, the stimulus grating is a pure equiluminant red-green grating, the luminance component of the grating having zero modualation (m_a=0). As we move away from 0.0 on the abscissa, progressively more luminance contrast is "titrated" into the grating. If contrast detection threshold is unaffected by the added luminance contrast (flat line in Fig. 45), detection is entirely determined by the chromatic contrast subsystem. At the other extreme, if threshold progressively rises to a peak (broken line, Fig. 45) we have no

Department of Psychology

UNIVERSITÉ
YORK
UNIVERSITY

FACULTY OF ARTS

4700 KEELE STREET • NORTH YORK • ONTARIO • CANADA • M3J 1P3

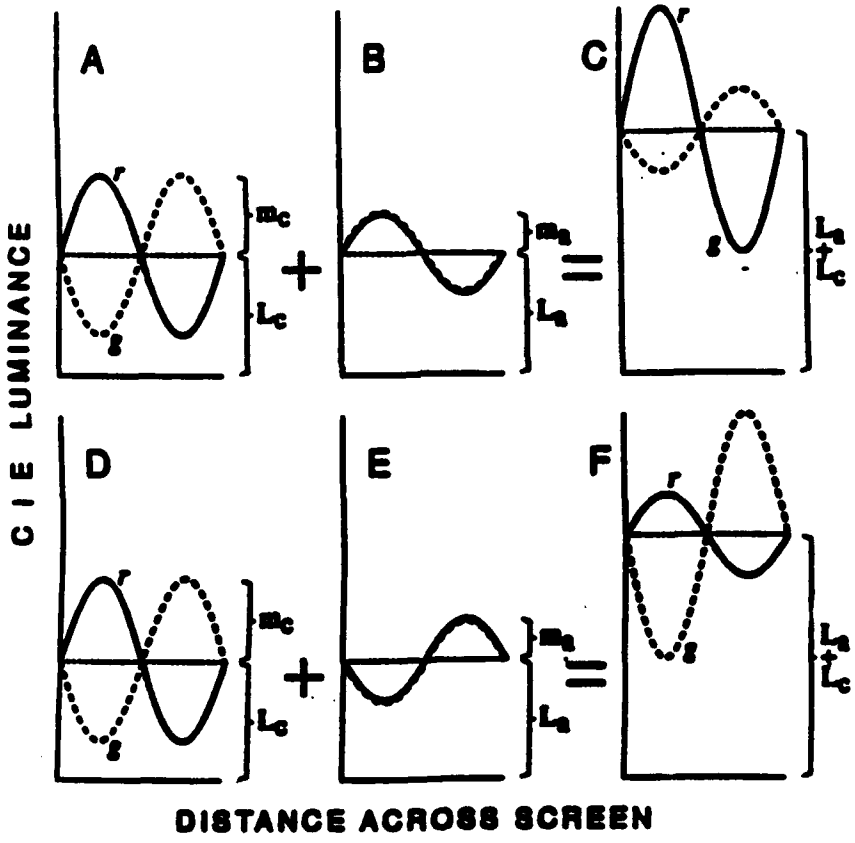

Figure 44. The stimulus grating comprised the linear sum of a chromatic contrast component of fixed mean luminance (L_c) and a luminance contrast component of fixed mean luminance (L_a). In our experiment $L_c = L_a$. In some cases the red modulations of the chromatic (A) and luminance (B) components were inphase, so that in the stimulus grating (C) the red modulation was stronger than the green modulation. In other cases the red modulations of the chromatic (D) and luminance (E) components were in antiphase, so that in the stimulus grating (F) the red modulations was weaker than the green modulation. The (luminance modulation)/(chromatic modulation) ratio was equal to (m_a/m_c). Grating detection threshold for any given (m_a/m_b) ratio was set by adjusting the values of m_a and m_c in a yoked manner, keeping the ratio m_a/m_b constant.

Department of Psychology

UNIVERSITÉ
YORK
UNIVERSITY

FACULTY OF ARTS

4700 KEELE STREET • NORTH YORK • ONTARIO • CANADA • M3J 1P3

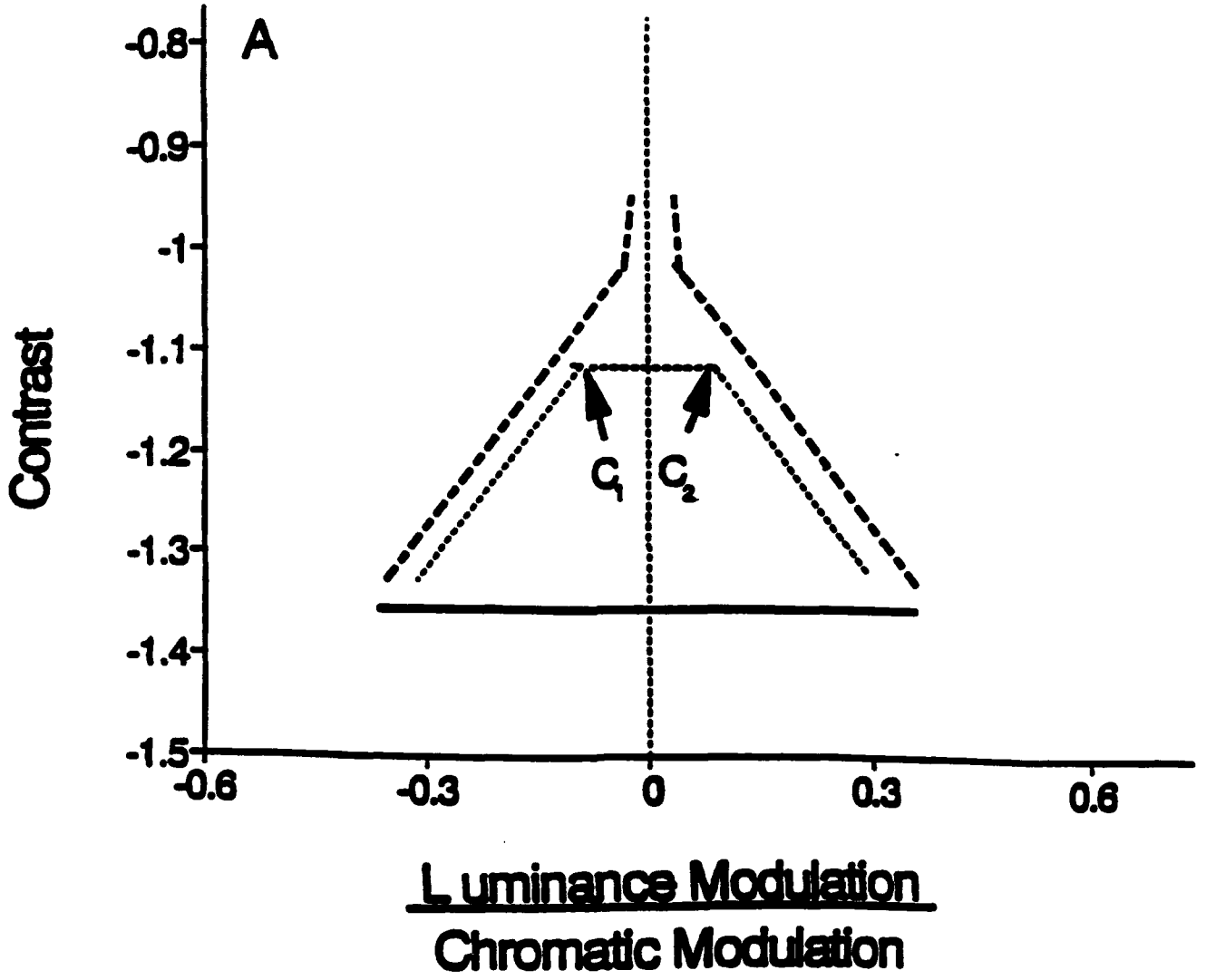

Figure 45. Rationale of the spatial titration method. Grating threshold, expressed as the contrast of the chromatic contrast component of the grating, is plotted as ordinate on a log axis in arbitrary units. The ratio of luminance modulation to chromatic modulation (i.e. m_a/m_c in Fig. 2) is plotted as abscissa on a linear axis. Positive and negative values indicate that the red modulations in the luminance and chromatic contrast components of the stimulus grating were, respectively, inphase and in antiphase (see Fig. 44). See text for details.

Department of Psychology

UNIVERSITÉ
YORK
UNIVERSITY

FACULTY OF ARTS

4700 KEELE STREET • NORTH YORK • ONTARIO • CANADA • M3J 1P3

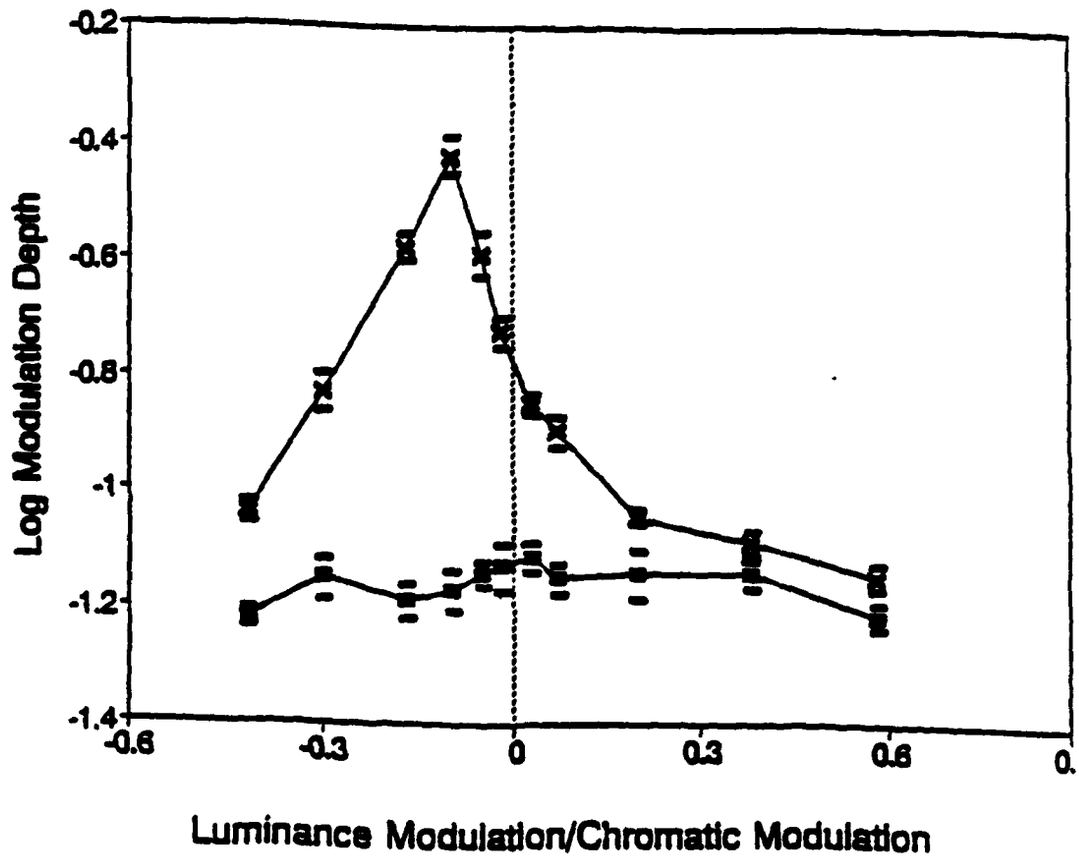

Figure 46. *Empirical examples of inverted-V and flat curve. The short horizontal bars indicate ±1 SE.*

Department of Psychology

UNIVERSITÉ YORK UNIVERSITY

FACULTY OF ARTS

4700 KEELE STREET • NORTH YORK • ONTARIO • CANADA • M3J 1P3

evidence that the chromatic contrast subsystem is ever uncovered. The intermediate case (dotted line, Fig. 45) has a flattened region between C_1 and C_2. We assume that the chromatic contrast system determines threshold from C_1 to C_2, and that the luminance contrast subsystem determines threshold outside the flattened region. If, as illustrated, the flattened region is centred over 0.0 on the abscissa, then biological equiluminance coincides with physical equiluminance. Fig. 46 shows empirical examples of the inverted-V curve and flat curve just described.

Results on our four subjects led us to conclude that an equiluminant pattern does not stimulate the physiological achromatic contrast subsystem at least from 2 to 8 c/deg. We add that the adequacy of an achromatising lens in cancelling ocular chromatic aberration at any given spatial frequency and accomodative state can be precisely verified using our titration method. Also that the titration method shows when the chromatic contrast subsystem has been uncovered, and when it has not. This work has been submitted for publication (Ref 226).

3.17 A comparison of the 40 Hz response in man and the properties of macaque ganglion cells (long term aim 1.1.2)

Summary

In the recent vision literature there has been much discussion of possible correlates in human vision of the parvocellular/magnocellular distinction in the monkey visual system. Here we report evidence that the properties of magnocellular-pathway neurons in macaque are closely similar to the properties of the human 40 Hz visual evoked potential (VEP). A paper is in press (Ref 217). In contrast, the properties of parvocellular-pathway neurons in macaque are quite different from the properties of the human 40 Hz VEP, and in several respects resemble the properties of the human 16 Hz VEP.

In 1990 Merigan and Maunsell [35] reported that lesions of the magnocellular portion of

Department of Psychology

UNIVERSITÉ YORK UNIVERSITY

FACULTY OF ARTS

4700 KEELE STREET • NORTH YORK • ONTARIO • CANADA • M3J 1P3

macaque lateral geniculate nucleus severely reduced the monkey's psychophysical ability to detect fast flicker of a very low spatial frequency stimulus (a gaussian blob of about 4 deg diameter). They concluded that the perception of high-frequency flicker for a stimulus of very low spatial frequency is mediated by the magnocellular pathway. Several years previously (in 1968) [36] I had reported that a resonant-like evoked potential response near 40 Hz is generated in human by a stimulus of very low spatial frequency that is modulated at a high temporal rate. Fig. 47 illustrates this 40 Hz VEP and shows how it can be generated as a 40 Hz response to 20 Hz flicker. In subsequent studies I described the colour properties of the 40 Hz response and also the properties of a second resonant-like response at 16 Hz. [37-39]

Lee has recently replicated the stimulus conditions that I used in the human studies while he recorded from macaque retinal ganglion cells in the magnocellular and parvocellular pathways. Lee and I have compared the human and monkey electrophysical data with human psychophysical data. The same stimuli were used to generate the psychophysical and electrophysical data. We found that the 40 Hz evoked potential data were in close agreement with the magnocellular-pathway data in all four respects investigated.

Fig. 48 shows how both the 40 Hz VEP (left panel) and the firing rate of the magnocellular-pathway cells fell to near-zero at the point of zero subjective flicker (arrowed) using the variable-modulation heterochromatic flicker photometry technique described earlier. [37,39] Similar findings were obtained using classical heterochromatic flicker photometry. This correlation between electrophysical minima and minimum subjective flicker held for wavelengths throughout the spectrum and, therefore, allowed us to estimate a spectral sensitivity curve. Fig. 49 shows spectral sensitivity estimated from the human 40 Hz VEP, from magnocellular-pathway cells (N=21) and psychophysically. The line is the CIE human V_λ curve (standard observer). The fit between 40 Hz VEP, magnocellular data and psychophysics is very close. We conclude that both

Department of Psychology

UNIVERSITÉ
YORK
UNIVERSITY

FACULTY OF ARTS

4700 KEELE STREET • NORTH YORK • ONTARIO • CANADA • M3J 1P3

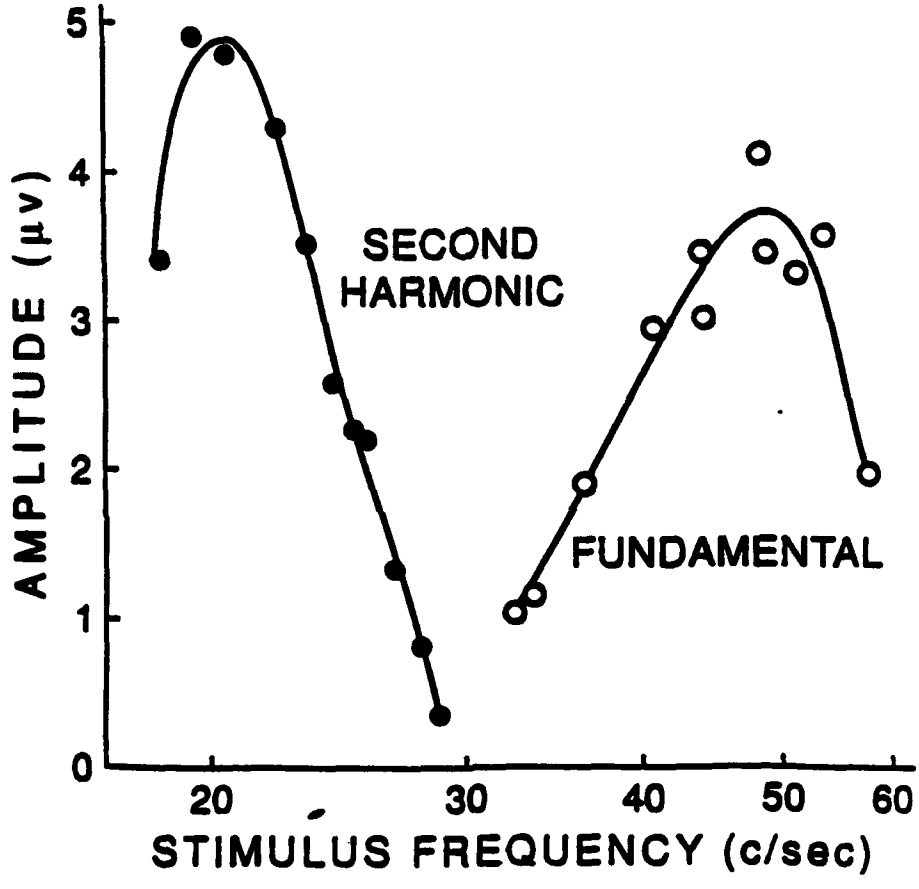

Figure 47. The human 40Hz response. Open circles plot the amplitudes of the fundamental component of the evoked potential that peaks at about 40 Hz. A similar 40 Hz response can be obtained as a second harmonic while viewing flicker of about 20 Hz (filled circles).

Department of Psychology

UNIVERSITÉ
YORK
UNIVERSITY

FACULTY OF ARTS

4700 KEELE STREET • NORTH YORK • ONTARIO • CANADA • M3J 1P3

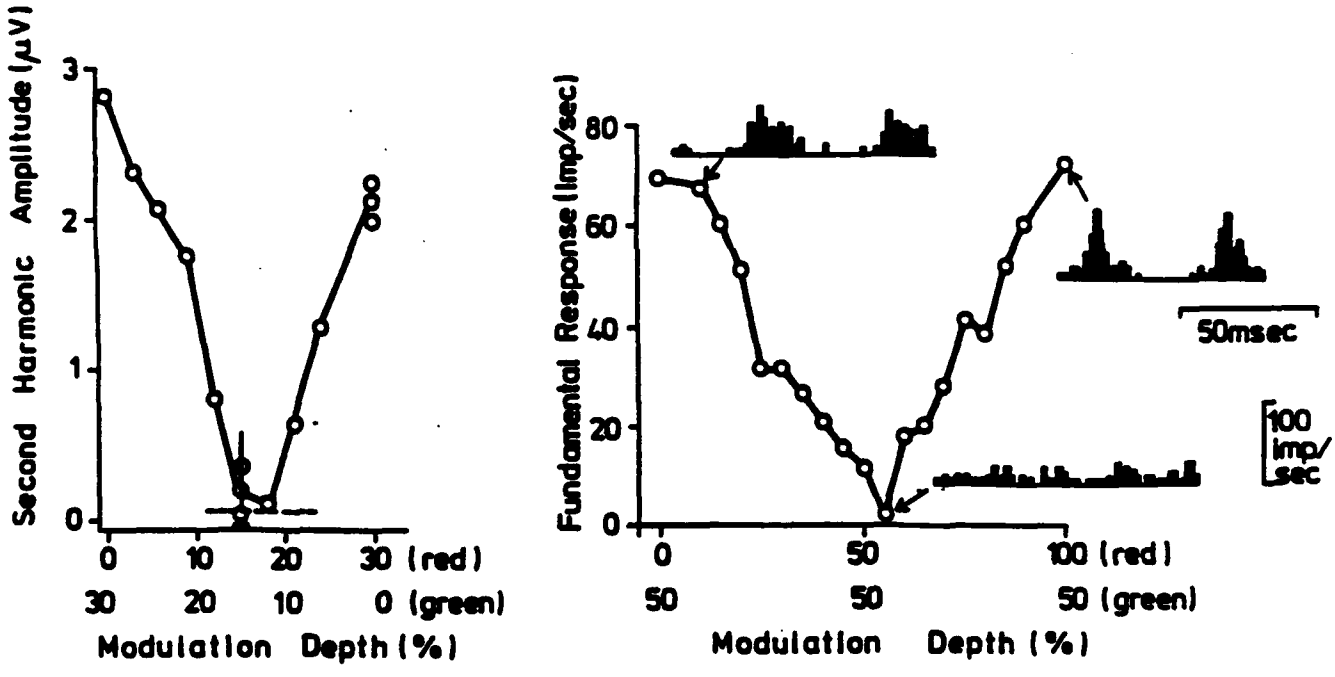

Figure 48. Open circles in left panel plot data obtained using variable-modulation heterochromatic flicker photometry (VMHFP) for the 40 Hz response in human. Monochromatic red (630 nm) and green (544 nm) fields of constant mean luminance were superimposed and modulated in antiphase at 24 Hz, and the relative modulation depth was varied. The modulation depth of the red and the stimulus lights are plotted linearly along the abscissa. The upper and lower sets of numbers indicate the modulation depths of the red and green respectively. The point of minimum subjective flicker is indicated by the short vertical line just over the abscissa, and the range of 6 settings is indicated by the bar. The dotted horizontal line at about 0.1 microvolts amplitude is the noise level recorded with flicker modulation depth set to zero. The subject centrally fixated a homogeneous field of 15 deg diameter which had a steady annular white surround extending to 30 deg diameter. Open cir les in right-hand panel show responses of a MC-pathway cell in monkey obtained using VMHFP. Monochromatic red (638 nm) and green (554 nm) fields (4 deg diameter) were used, modulated in antiphase at 19.8 Hz. Binwidth was 1.6 msec, and approximately 6 sec of activity was averaged for each condition. Retinal illuminance was 200 td. Response (first-harmonic) amplitude was derived from Fourier analysis of the histograms. The amplitude of the fundamental component is plotted against the modulation depth of the red and green stimulus lights. The minimum of the fundamental was close to the psychophysical flicker minimum for human observers.

Department of Psychology

UNIVERSITÉ
YORK
UNIVERSITY

FACULTY OF ARTS

4700 KEELE STREET • NORTH YORK • ONTARIO • CANADA • M3J 1P3

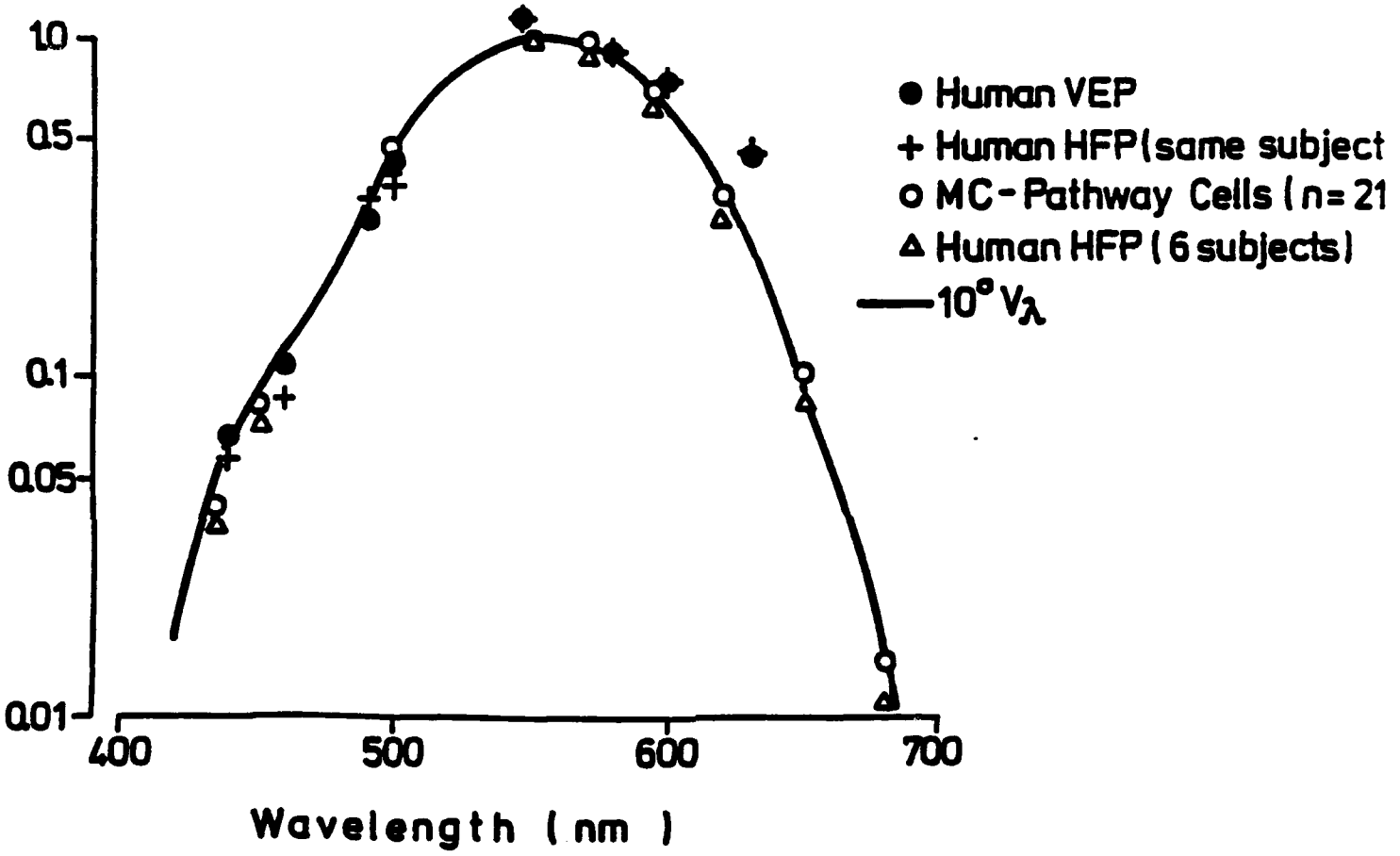

Figure 49. Estimates of the eye's spectral sensitivity curve obtained from the 40 Hz. VEP in human, from magnocellular-pathway retinal ganglion cells in monkey, and psychophysically in human.

Department of Psychology

UNIVERSITÉ
YORK
UNIVERSITY

FACULTY OF ARTS

4700 KEELE STREET • NORTH YORK • ONTARIO • CANADA • M3J 1P3

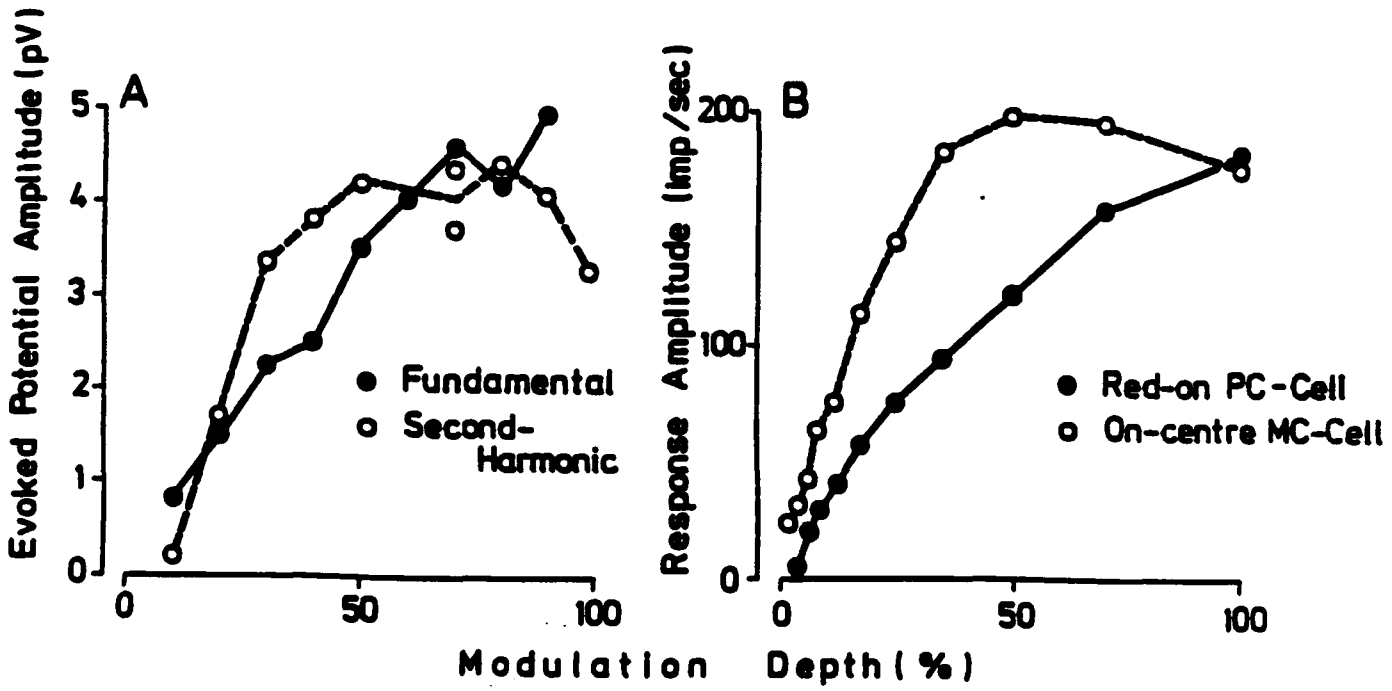

Figure 50. Saturation behaviour for human VEP (A) and monkey ganglion cell firing response (B). A shows the amplitude of the so-called 40 Hz. (open symbols) and 16 Hz. (filled symbols) responses to flicker stimulation. B shows the firing response of typical magnocellular-pathway (open symbols) and parvocellular-pathway (filled symbols) retinal ganglion cells in macaque.

Department of Psychology

UNIVERSITÉ YORK UNIVERSITY

FACULTY OF ARTS

4700 KEELE STREET • NORTH YORK • ONTARIO • CANADA • M3J 1P3

the 40 Hz VEP and magnocellular firing encode luminance.

We then alternated red with green light and varied the relative phase. Both the 40 Hz and the magnocellular-pathway firing fell to a sharp minimum red and green modulations were in antiphase.

The fourth correlation was obtained by comparing the saturation curves for the 40 Hz VEP and for magnocellular-pathway neurons. These curves, shown by the dashed lines in Fig. 50, are similar. Both saturate at low modulation depth (about 20-40%).

It is more difficult to assign specific features of the human VEP to parvocellular-pathway activity. However, in addition to the 40 Hz response, subjects also show a strong resonant-like response in the 15-30 Hz range (the so-called 16 Hz response). [38] In heterochromatic flicker photometry, the 16 Hz response does not show a minimum near minimum subjective flicker. Indeed the 16 Hz response can be largest at minimum subjective flicker so that, unlike the 40 Hz response, the 16 Hz response is generated by pure chromatic flicker. In this respect the 16 Hz response differs markedly from magnocellular-pathway activity, and resembles parvocellular-pathway activity. A further similarity between the human 16 Hz response and parvocellular activity is in the saturation behaviour. The continuous lines (filled circles) in Fig. 50 bring out the similarity.

Department of Psychology

UNIVERSITÉ
YORK
UNIVERSITY

FACULTY OF ARTS

4700 KEELE STREET • NORTH YORK • ONTARIO • CANADA • M3J 1P3

3.18 References

1. Julesz B (1971) *Foundations of Cyclopean Perception*. Chicago: Univ. of Chicago Press.
2. Gray CM, Konig P, Engel AK & Singer W (1990) Oscillatory responses in cat visual cortex exhibit inter-columnar synchronization which reflects global stimulus properties. *Nature* 338, 334-337.
3. Thurston SE, Leigh RJ, Crawford T, Thompson A & Kennard C (1988) Two distinct deficits of visual tracking caused by unilateral lesions of cerebral cortex in humans. *Ann Neurol* 23, 266-273.
4. Morrow MJ & Sharpe JA (1990) Cerebral hemispheric localization of smooth pursuit asymmetry. *Neurology*, in press.
5. Zihl JD, Von Cramon D & Mai N (1983) Selective disturbance of movement vision after bilateral brain damage. *Brain* 106, 313-340.
6. Van Essen DC (1985) Functional organization of primate visual cortex. In Peters A, Jones EG (eds) *Cerebral Cortex*. New York: Plenum, vol 3, pp. 259-330.
7. Campbell FW & Kulikowski JJ (1966) Orientation selectivity of the human visual system. *J Physiol* 187, 437-445.
8. Blakemore C & Nachmias J (1971) The orientation specificity of two visual aftereffects. *J Physiol* 213, 157-174.
9. Movshon JA & Blakemore C (1973) Orientation specificity and spatial selectivity in human vision. *Perception* 2, 53-60.
10. Thomas J & Gille J (1979) Bandwidths of orientation channels in human vision. *J Opt Soc Am* 69, 652-660.
11. De Valois RL, Yund EW & Hepler N (1982) The orientation and direction selectivity of cells in macaque visual cortex. *Vision Res* 22, 531-544.
12. Wilson HR (1991). Psychophysical models of spatial vision and hyperacuity. In D Regan (Ed) *Spatial Vision*. London: Macmillan.
13. Wilson HR & Gelb DJ (1984) Modified line element theory. *J Opt Soc Am* A1, 124-131.
14. Wilson HR & Regan D (1985) Spatial frequency adaptation and grating discrimination: predictions of a line element model. *J Opt Soc Am* A1, 1091-1096.
15. Wyszecki G & Stiles WS (1967) *Colour Science, Concepts and Methods: Quantitative Data and Formulas*. New York: Wiley.
16. Banton T & Levi DM (1990) Vernier localization in the motion system. *Invest Ophthalmol Vis Sci* (Suppl. 31). (ARVO Abstr.), 443.

Department of Psychology

UNIVERSITÉ YORK UNIVERSITY

FACULTY OF ARTS

4700 KEELE STREET • NORTH YORK • ONTARIO • CANADA • M3J 1P3

17. Lee DN (1976) A theory of visual control of braking based on information about time-to-collision. *Perception* 5, 437-459.
18. Lee DN & Lishman JR (1977) Visual control of locomotion. *Scand J Psychol* 18, 224-230.
19. Lee DN, Lishman JR & Thomson JA (1982) Visual regulation of gait in long jumping. *J Exp Psychol: Hum Percept Perform* 8, 448-459.
20. Warren WH, Young DS, & Lee DN (1986) Visual control of step length during running over irregular terrain. *J Exp Psychol: Hum Percept Perform* 12, 259-266.
21. Bootsma RJ & van Wieringen PCW (1990) Timing an attacking forehand drive in table tennis. *J Exp Psychol: Hum Percept Perform* 16, 21-29.
22. Savelsbergh GJP, Whiting HTA & Bootsma RJ (1991) Grasping 'Tau'. *J Exp Psychol: Hum Percept Perform*, in press.
23. Blakemore C & Campbell FW (1971) On the existence of neurons within the human visual system selectively sensitive to the orientation and size of retinal images. *J Physiol (Lond)* 213, 157-174.
24. DeValois RL & DeValois KK (1980) Spatial vision. *Ann Rev Psychol* 31, 309-341.
25. Wilson HR (1991) Psychophysical models of spatial vision and hyperacuity. In D Regan (Ed) *Spatial Vision*. London: Macmillan.
26. Wilson HR, McFarlane DK & Phillips GC (1983) Spatial frequency tuning of orientation specific units estimated by oblique masking. *Vision Res* 23, 873-882.
27. Tanaka K, Fukada Y & Saito H (1989) Underlying mechanisms of the response specificity of expansion/contraction and rotation cells in the dorsal part of the medial superior temporal area of the macaque monkey. *J Neurophysiol* 62, 642-656.
28. Tanaka K & Saito H (1989) Analysis of motion in the visual field by direction, expansion/ contraction and rotation cells clustered in the dorsal part of the medial superior temporal area of the macaque monkey. *J Neurophysiol* 62, 626-641.
29. Zeki SM (1974) Functional organization of a visual area in the posterior bank of the superior temporal sulcus of the rhesus monkey. *J Physiol (Lond.)* 236, 549-573.
30. Ball K & Sekuler R (1980) Models of stimulus uncertainty in motion perception. *Psychol Rev* 87, 435-469.
31. Hoyle F (1957) *The Black Cloud*. London: Heinemann. Repr. Penguin Books, 1971, 26-27.
32. De Valois KK & Switkes E (1983) Simultaneous masking inteactions between chromatic and luminance gratings. *J Opt Soc Am* 73, 11-18.
33. Bradley A, Switkes E & De Valois KK (1988) Orientation and spatial frequency selectivity of adaptation to isoluminant color and luminance patterns. *Vision Res* 28, 841-856.

Department of Psychology

UNIVERSITÉ YORK UNIVERSITY

FACULTY OF ARTS

4700 KEELE STREET • NORTH YORK • ONTARIO • CANADA • M3J 1P3

34. Bodis-Wollner I, Marx MS, Mitra S, Bobak P, Mylin L & Yahr M (1987) Visual dysfunction in Parkinson's disease. *Brain* 110, 1675-1698.

35. Merigan WH & Maunsell JHR (1990) Macaque vision after magnocellular lateral geniculate lesions. Visual Neuroscience 5, 347-352.

36. Regan D (1968) A high frequency mechanism which underlies visual evoked potentials. Electroenceph. Clin. Neurophysiol. 25, 231-237.

37. Regan D (1970) Objective method of measuring the relative spectral-luminosity curve in man. J. Opt. Soc. Amer. 60, 856-859.

38. Regan D (1968) Chromatic adaptation and steady-state evoked potentials. Vision Research 8, 149-158.

39. Regan D (1970) Evoked potential and psychophysical correlates of changes in stimulus colour and intesity. Vision Research 10, 163-178.

Department of Psychology

UNIVERSITÉ YORK UNIVERSITY

FACULTY OF ARTS

4700 KEELE STREET • NORTH YORK • ONTARIO • CANADA • M3J 1P3

4 CUMULATIVE LIST OF PUBLICATIONS

4.1 Books

1. Regan D (1972) Evoked potentials in psychology, sensory physiology and clinical medicine. London: Chapman & Hall; New York: Wiley, 328 pp, rpt 1975.
2. Regan D (1989) *Human brain electrophysiology: Evoked potentials and evoked magnetic fields in science and medicine*. New York: Elsevier, 672 pp.
3. Regan D, Shapley RM & Spekreijse H (Eds) (1985) *Systems approach in vision*. New York: Pergamon, 219 pp.
4. Regan D (Ed) (1991) *Binocular Vision* (Vol 9, "Vision and visual dysfunction" series). London: Macmillan.
5. Regan D (Ed) (1991) *Spatial Vision* (Vol 10, "Vision and visual dysfunction" series). London: Macmillan.

4.2 Papers

1966

1. Regan D (1966) Some characteristics of average steady-state and transient responses evoked by modulated light. *Electroenceph clin Neurophysiol* 20, 238-48.
2. Regan D (1966) An apparatus for the correlation of evoked potentials and repetitive stimuli. *Med Biol Engng* 4, 168-77.
3. Regan D (1966) An effect of stimulus colour on average steady-state potentials evoked in man. *Nature* 210, 1056-7.

1968

4. Regan D (1968) A high frequency mechanism which underlies visual evoked potentials. *Electroenceph clin Neurophysiol* 25, 231-7.
5. Regan D (1968) Chromatic adaptation and steady-state evoked potentials. *Vision Res* 8, 149-58.
6. Regan D (1968) Evoked potentials and sensation. *Percept Psychophys* 4, 347-50.

1969

7. Regan D (1969) Evoked potentials and colour vision. *7th ISCERG Symp*, Istanbul. Univ of Istanbul, 37-50.
8. Regan D (1969) Chapters 3 & 4 in DM MacKay (Ed), Evoked potentials and Psychophysics. *Neurosci Res Bull* 7, N° 3.
9. Regan D & Heron JR (1969) Clinical investigation of lesions of the visual pathway: a new objective technique. *J Neurol Neurosurg Psychiat* 32, 479-83.
10. Tweel LH van der, Regan D & Spekreijse H (1969) Some aspects of potentials evoked by changes in spatial brightness contrast. *7th ISCERG Symp*, Istanbul. Univ of Istanbul, 1-11.

1970

11. Regan D (1970) Evoked potentials and psychophysical correlates of changes in stimulus colour and intensity. *Vision Res* 10, 163-78.

Department of Psychology

UNIVERSITÉ YORK UNIVERSITY

FACULTY OF ARTS

4700 KEELE STREET • NORTH YORK • ONTARIO • CANADA • M3J 1P3

12. Regan D (1970) Objective method of measuring the relative spectral luminosity curve in man. *J Opt Soc Am* 60, 856-9.

13. Regan D & Heron JE (1970) Simultaneous recording of visual evoked potentials from the left and right hemispheres in migraine. In AL Cochrane (Ed), *Background to migraine*. London: Heinemann, 66-77.

14. Regan D & Cartwright RF (1970) A method of measuring the potentials evoked by simultaneous stimulation of different retinal regions. *Electroenceph clin Neurophysiol* 28, 314-9.

15. Regan D & Spekreijse H (1970) Electrophysiological correlate of binocular depth perception in man. *Nature* 255, 92-4.

1971

16. Regan D & Sperling HG (1971) A method of evoking contour-specific scalp potentials by chromatic checkerboard patterns. *Vision Res* 11, 173-6.

17. Regan D & Tyler CW (1971) Wavelength-modulated light generator. *Vision Res* 11, 43-56.

18. Regan D & Tyler CW (1971) Some dynamic features of colour vision. *Vision Res* 11, 1307-24.

19. Regan D & Tyler CW (1971) Temporal summation and its limit for wavelength changes: an analog of Bloch's law for color vision. *J Opt Soc Am* 61, 1414-21.

20. Regan D & Richards W (1971) Independence of evoked potentials and apparent size. *Vision Res* 11, 679-84.

1972

21. Regan D (1972) Evoked potentials to changes in the chromatic contrast and luminance contrast of checkerboard stimulus patterns. In GB Arden (Ed), *The visual system*. New York: Plenum, 171-87.

22. Regan D (1972) Evoked potentials to changes in chromatic contrast. Proc GAIN symp on EPs to spatial contrast. *Trace* 6, 20-8.

23. Regan D (1972) Cortical evoked potentials. *Adv Behav Biol* 5, 177-92.

24. Spekreijse H, van der Tweel LH & Regan D (1972) Interocular sustained suppression: correlations with evoked potential amplitude and distribution. *Vision Res* 12, 521-6.

25. Milner BA, Regan D & Heron JR (1972) Theoretical models of the generation of steady-state evoked potentials, their relation to neuroanatomy and their relevance to certain clinical problems. *Adv Med Biol* 24, 157-69.

1973

26. Regan D (1973) Parallel and sequential processing of visual information in man: investigation by evoked potential recording. In *Photophysiology*, Vol 8. New York: Academic, 185-208.

27. Regan D (1973) An evoked potential correlate of colour: evoked potential findings and single-cell speculations. *Vision Res* 13, 1933-41.

28. Regan D (1973) Evoked potentials specific to spatial patterns of luminance and colour. *Vision Res* 13, 2381-2402.

29. Regan D (1973) Rapid objective refraction using evoked brain potentials. *Invest Ophthalmol* 12, 669-79.

30. Regan D & Richards W (1973) Brightness contrast and evoked potentials. *J Opt Soc Am* 63, 606-11.

31. Regan D & Beverley KI (1973) Disparity detectors in human depth perception: evidence for directional

Department of Psychology

UNIVERSITÉ YORK UNIVERSITY

FACULTY OF ARTS

4700 KEELE STREET • NORTH YORK • ONTARIO • CANADA • M3J 1P3

selectivity. *Science* 18, 877-9.

32. Regan D & Beverley KI (1973) Some dynamic features of depth perception. *Vision Res* 13, 2369-79.

33. Regan D & Beverley KI (1973) The dissociation of sideways movements from movements in depth: psychophysics. *Vision Res* 13, 2403-15.

34. Beverley KI & Regan D (1973) Evidence for the existence of neural mechanisms selectively sensitive to the direction of movement in space. *J Physiol* 235, 17-29.

34a. Beverley KI & Regan D (1973) Selective adaptation in stereoscopic depth perception. *J Physiol* 232, 40-41P.

35. Regan D & Beverley KI (1973) Relation between the magnitude of flicker sensation and evoked potential amplitude in man. *Perception* 2, 61-5.

36. Regan D & Beverley KI (1973) Electrophysiological evidence for the existence of neurones sensitive to the direction of depth movement. *Nature* 246, 504-6.

37. Richards W & Regan D (1973) A stereo field map with implications for disparity processing. *Invest Ophthalmol* 12, 904-9.

1974

38. Cartwright RF & Regan D (1974) Semi-automatic, multi-channel Fourier analyser for evoked potential analysis. *Electroenceph clin Neurophysiol* 36, 547-50.

39. Regan D (1974) Electrophysiological evidence for colour channels in human pattern vision. *Nature* 250, 437-49.

40. Regan D & Spekreijse H (1974) Evoked potential indications of colour blindness. *Vision Res* 14, 89-95.

41. Heron JR, Regan D & Milner BA (1974) Delay in visual perception in unilateral optic atrophy after retrobulbar neurities. *Brain* 97, 69-78.

42. Beverley KI & Regan D (1974) Temporal integration of disparity information in stereoscopic perception. *Exp Brain Res* 19, 228-32.

43. Beverley KI & Regan D (1974) Visual sensitivity to disparity pulses: evidence for directional selectivity. *Vision Res* 14, 357-61.

44. Regan D (1974) Visually evoked potential methods with clinical application. Proc 11th ISCERG Symp, Bad Neuheim (1973). *Docum Ophthal Proc Series* 4, 285-301.

45. Milner BA, Regan D & Heron JR (1974) Differential diagnosis of multiple sclerosis by visual evoked potential recording. *Brain* 97, 755-72.

1975

46. Regan D (1975) Colour coding of pattern responses in man investigated by evoked potential feedback and direct plot techniques. *Vision Res* 15, 175-83.

47. Heron JR, Milner BA & Regan D (1975) Measurement of acuity variations within the central visual field caused by neurological lesions. *J Neurol Neurosurg Psychiat* 38, 356-62.

48. Regan D, Schellart NAM, Spekreijse H & van den Berg TJTP (1975) Photometry in goldfish by electrophysiological recording: comparison of criterion response method with heterochromatic flicker photometry. *Vision Res* 15, 799-807.

49. Beverley KI & Regan D (1975) The relation between discrimination and sensitivity in the perception of

Department of Psychology

UNIVERSITÉ YORK UNIVERSITY

FACULTY OF ARTS

4700 KEELE STREET • NORTH YORK • ONTARIO • CANADA • M3J 1P3

motion in depth. *J Physiol* 249, 387-98.

50. Regan D (1975) Recent advances in electrical recording from the human brain. *Nature* 253, 401-07.

1976

51. Regan D, Milner BA & Heron JR (1976) Delayed visual perception and delayed visual evoked potentials in the spinal form of multiple sclerosis and in retrobulbar neuritis. *Brain* 99, 43-66.

52. Regan D, Varney P, Purdy J & Kraty N (1976) Visual field analyser: assessment of delay and temporal resolution of vision. *Med Biol Engng* 14, 8-14.

53. Regan D (1976) Latencies of evoked potentials to flicker and to pattern speedily estimated by simultaneous stimulation method. *Electroenceph clin Neurophysiol* 40, 654-60.

54. Galvin RJ, Regan D & Heron JR (1976) A possible means of monitoring the progress of demyelination in multiple sclerosis: effect of body temperature on visual perception of double light flashes. *J Neurol Neurosurg Psychiat* 39, 861-65.

55. Galvin RJ, Regan D & Heron JR (1976) Impaired temporal resolution of vision after acute retrobulbar neuritis. *Brain* 99, 255-68.

1977

56. Regan D (1977) Fourier analysis of evoked potentials: some methods based on Fourier analysis. In JE Desmedt (Ed), *Visual evoked potentials in man: new developments*. Oxford: Oxford Univ Press, 110-17.

57. Regan D (1977) Rapid methods for refracting the eye and for assessing visual acuity in amblyopia, using steady-state visual evoked potentials. In JE Desmedt (Ed), *Visual evoked potentials in man: new developments*. Oxford: Oxford Univ Press, 418-26.

58. Regan D (1977) Evoked potential indications of the processing of pattern, colour, and depth information. In JE Desmedt (Ed), *Visual evoked potentials in man: new developments*. Oxford: Oxford Univ Press, 234-49.

59. Regan D, Milner BA & Heron JR (1977) Slowing of visual signals in multiple sclerosis, measured psychophysically and by steady-state evoked potentials. In JE Desmedt (Ed), *Visual evoked potentials in man: new developments*. Oxford: Oxford Univ Press, 461-69.

60. Regan D (1977) Speedy assessment of visual acuity in amblyopia by the evoked potential method. *Ophthalmologica* 175, 159-64.

61. Regan D & Spekreijse H (1977) Auditory-visual interactions and the correspondence between perceived auditory space and perceived visual space. *Perception* 6, 133-38.

62. Galvin RJ, Heron JR & Regan D (1977) Subclinical optic neuropathy in multiple sclerosis. *Arch Neurol* 34, 666-70.

63. Regan D (1977) Steady state evoked potentials. Proc Symp Electrophysiological Techniques in Man. *J Opt Soc Am* 67, 1475-89.

64. Regan D, Silver R & Murray TJ (1977) Visual acuity and contrast sensitivity in multiple sclerosis - hidden visual loss. *Brain* 100, 563-79.

65. Regan D, Murray TJ & Silver R (1977) Effect of body temperature on visual evoked potential delay and visual perception in multiple sclerosis. *J Neurol Neurosurg Psychiat* 40, 1083-91.

66. Arden GB, Bodis-Wollner I, Halliday AM, Jeffreys A, Kulikowski JJ, Spekreijse H & Regan D (1977) Methodology of patterned visual stimulation. In JE Desmedt (Ed), *Visual evoked potentials in man: new*

Department of Psychology

UNIVERSITÉ YORK UNIVERSITY

FACULTY OF ARTS

4700 KEELE STREET • NORTH YORK • ONTARIO • CANADA • M3J 1P3

developments. Oxford: Oxford Univ Press, 3-15.

67. Regan D (1977) Visual evoked potentials and visual perception in multiple sclerosis. *Proc San Diego Biomed Symp*, Vol 16. New York: Academic, 87-95.

68. Regan D (1977) New methods for neurological assessment: overview. *Proc San Diego Biomed Symp*, Vol 16. New York: Academic, 55-62.

69. Regan D (1977) Evoked potentials in basic and clinical research. In A Rémond (Ed), *EEG informatics: a didactic review of methods and applications of EEG data processing*. Amsterdam: Elsevier, 319-46.

70. Regan D (1977) Colour and contrast. In H Spekreijse & LH van der Tweel (Eds), *Spatial contrast: report of a workshop*. Publ for Netherlands Royal Academy of Sciences. Amsterdam: North-Holland, 75-9.

1978

71. Regan D & Milner BA (1978) Objective perimetry by evoked potential recording: limitations. *Electroenceph clin Neurophysiol* 44, 393-7.

72. Regan D & Beverley KI (1978) Looming detectors in the human visual pathway. *Vision Res* 18, 415-21.

73. Cynader M & Regan D (1978) Neurones in cat parastriate cortex sensitive to the direction of motion in three-dimensional space. *J Physiol* 274, 549-69.

74. Regan D & Beverley KI (1978) Illusory motion in depth: aftereffect of adaptation to changing size. *Vision Res* 18, 209-12.

75. Hillyard SA, Picton TW & Regan D (1978) Sensation, perception and attention: analysis using ERPs. In E Callaway, P Tueting & SH Koslow (Eds), *Event-related brain potentials in man*. New York: Academic, 223-321.

76. Regan D (1978) Assessment of visual acuity by evoked potential recording: ambiguity caused by temporal dependence of spatial frequency selectivity. *Vision Res* 18, 439-45.

77. Regan D (1978) Investigations of normal and defective colour vision by evoked potential recording. *Mod Probl Ophthal* 19, 19-28.

78. Regan D, Beverley KI & Cynader M (1978) Stereoscopic depth channels for position and for motion. In SJ Cool & EL Smith (Eds), *Frontiers in visual science*. New York: Springer, 351-72.

1979

79. Regan D, Beverley KI & Cynader M (1979) Stereoscopic subsystems for position in depth and for motion in depth. *Proc R Soc Lond* B 204, 485-501.

80. Regan D & Tansley BW (1979) Selective adaptation to frequency-modulated tones: evidence for an information-processing channel selectively sensitive to frequency changes. *J Acoust Soc Am* 65, 1249-57.

81. Regan D & Beverley KI (1979) Visually guided locomotion: psychophysical evidence for a neural mechanism sensitive to flow patterns. *Science* 205, 311-13.

82. Beverley KI & Regan D (1979) Separable aftereffects of changing-size and motion-in-depth: different neural mechanisms? *Vision Res* 19, 727-32.

83. Beverley KI & Regan D (1979) Visual perception of changing-size: the effect of object size. *Vision Res* 19, 1093-1104.

84. Regan D & Cynader M (1979) Neurons in area 18 of cat visual cortex selectively sensitive to changing size:

Department of Psychology

UNIVERSITÉ YORK UNIVERSITY

FACULTY OF ARTS

4700 KEELE STREET • NORTH YORK • ONTARIO • CANADA • M3J 1P3

nonlinear interactions between responses to two edges. *Vision Res* 19, 699-711.

85. Regan D & Beverley KI (1979) Binocular and monocular stimuli for motion in depth: changing-disparity and changing-size feed the same motion-in-depth stage. *Vision Res* 19, 1331-42.

86. Regan D, Beverley KI & Cynader M (1979) The visual perception of motion in depth. *Scient Am* 241, 136-51.

87. Tansley BW & Regan D (1979) Separate auditory channels for unidirectional frequency modulation and unidirectional amplitude modulation. *Sensory Proc* 3, 132-40.

88. Regan D (1979) Electrical responses evoked from the human brain. *Scient Am* 241, 134-46.

1980

89. Regan D, Whitlock J, Murray TJ & Beverley KI (1980) Orientation-specific losses of contrast sensitivity in multiple sclerosis. *Invest Ophthalmol Vis Sci* 19, 324-28.

90. Regan D & Beverley KI (1980) Visual responses to changing size and to sideways motion for different directions of motion in depth: linearization of visual responses. *J Opt Soc Am* 11, 1289-96.

91. Beverley KI & Regan D (1980) Temporal selectivity of changing-size channels. *J Opt Soc Am* 11, 1375-77.

92. Beverley KI & Regan D (1980) Visual sensitivity to the shape and size of a moving object: implications for models of object perception. *Perception* 9, 151-60.

93. Beverley KI & Regan D (1980) Device for measuring the precision of eye-hand coordination while tracking changing size. *Aviat Space Environ Med* 51, 688-93.

94. Regan D (1980) Speedy evoked potential methods for assessing vision in normal and amblyopic eyes: pros and cons. *Vision Res* 20, 265-69.

95. Regan D (1980) New visual tests in multiple sclerosis. In HS Thompson (Ed), *Topics in neuro-ophthalmology*. Baltimore: Williams & Wilkins, 219-42.

96. Regan D (1980) Detection and quantification of neuroophthalmological abnormalities using psychophysical measures of visual delay and temporal resolution. In S Sokol (Ed), *Electrophysiology and psychophysics: their use in ophthalmic diagnosis*. Intl Ophthal Clinics. Boston: Little, Brown, 185-204.

97. Regan D (1980) Control system and physiological monitoring applications of steady-state evoked potentials. In FE Gomer (Ed), *Biocybernetic applications for military systems*. DARPA Conf, Chicago (1978). St Louis: McDonnell-Douglas. Report MDC E2191, 175-202.

1981

98. Regan D & Beverley KI (1981) Motion sensitivity measured by a psychophysical linearizing technique. *J Opt Soc Am* 71, 958-65.

99. Raymond J, Regan D & Murray TJ (1981) Abnormal adaptation of visual contrast sensitivity in multiple sclerosis patients. *Can J Neurol Sci* 8, 221-34.

100. Noseworthy J, Miller J, Murray TJ & Regan D (1981) Auditory brainstem responses in postconcussion syndrome. *Arch Neurol* 38, 275-78.

101. Regan D, Raymond J, Ginsburg A & Murray TJ (1981) Contrast sensitivity, visual acuity and the discrimination of Snellen letters in multiple sclerosis. *Brain* 104, 333-50.

102. Petersik JT, Beverley KI & Regan D (1981) Contrast sensitivity of the changing-size channel. *Vision Res*

Department of Psychology

UNIVERSITÉ YORK UNIVERSITY

FACULTY OF ARTS

4700 KEELE STREET • NORTH YORK • ONTARIO • CANADA • M3J 1P3

21, 829-32.

103. Regan D (1981) Psychophysical tests of vision and hearing in patients with multiple sclerosis. In SG Waxman & JM Ritchie (Eds), *Demyelinating disease: basic and clinical electrophysiology*. Proc Vail Conf MS Soc of USA. New York: Raven, 217-37.

104. Kruk R, Regan D, Beverley KI & Longridge T (1981) Correlations between visual test results and flying performance on the Advanced Simulator for Pilot Training (ASPT). *Aviat Space Environ Med* 52, 455-60.

105. Regan D (1981) Visual psychophysical tests in multiple sclerosis as an aid to diagnosis, localization of pathology, and assessment of experimental therapy. In *Clinical applications of visual psychophysics* (Proc NAS/NRC Symp). New York: Cambridge Univ Press.

106. Regan D (1981) Electrophysiology and psychophysics of motion in depth. Proc 18th ISCERG Symp, Amsterdam (1981). *Docum Ophthal Proc Series* 27, 271-81.

107. Regan D (1981) Evoked potential studies of visual perception. *Can J Psychol* 35, 77-112.

108. Regan D, Kruk R, Beverley KI & Longridge T (1981) The relevance of channel theory for the design of simulator imagery. *Proc Image II conf*, Arizona, 307-44.

1982

109. Regan D (1982) Comparison of transient and steady-state methods. *Proc NY Acad Sci* 388, 46-71.

110. Beverley KI & Regan D (1982) Adaptation to incomplete flow patterns: no evidence for "filling in" the perception of flow patterns. *Perception* 11, 275-78.

111. Cynader M & Regan D (1982) Neurons in cat visual cortex tuned to the direction of motion in depth: effect of positional disparity. *Vision Res* 22, 967-82.

112. Regan D & Cynader M (1982) Neurons in cat visual cortex tuned to the direction of motion in depth: effect of stimulus speed. *Invest Ophthalmol Vis Sci* 22, 535-50.

113. Tansley BW, Regan D & Suffield JB (1982) Measurement of the sensitivities of information-processing channels for frequency change and for amplitude change by a titration method. *Can J Psychol* 36, 723-30.

114. Regan D & Beverley KI (1982) How do we avoid confounding the direction we are looking with the direction we are moving? *Science* 215, 194-96.

115. Regan D (1982) Visual information channeling in normal and disordered vision. *Psychol Rev* 89, 407-44.

116. Regan D, Regal DM & Tibbles JAR (1982) Evoked potentials during recovery from blindness recorded serially from an infant and his normally sighted twin. *Electroenceph clin Neurophysiol* 54, 465-68.

117. Regan D, Bartol S, Murray TJ & Beverley KI (1982) Spatial frequency discrimination in normal vision and in patients with multiple sclerosis. *Brain* 105, 735-54.

118. Regan D (1982) Visual sensory aspects of simulation. In W Richards & K Dismukes (Eds), *Vision research for flight simulator*. Washington: National Academy Press, 65-71.

1983

119. Kruk R, Regan D, Beverley KI & Longridge T (1983) Flying performance on the Advanced Simulator for Pilot Training and laboratory tests of vision. *Human Factors* 25, 457-66.

120. Regan D (1983) Visual psychophysical tests in demyelinating disease. *Bull Soc Belge Ophtal* 208-I, 303-21.

121. Regan D & Beverley KI (1983) Visual fields described by contrast sensitivity, by acuity and by relative

Department of Psychology

UNIVERSITÉ YORK UNIVERSITY

FACULTY OF ARTS

4700 KEELE STREET • NORTH YORK • ONTARIO • CANADA • M3J 1P3

sensitivity to different orientations. *Invest Ophthalmol Vis Sci* 24, 754-59.

122. Regan D & Beverley KI (1983) Visual fields for frontal plane motion and for changing size. *Vision Res* 23, 673-76.

123. Regan D (1983) Spatial frequency mechanisms in human vision investigated by evoked potential recording. *Vision Res* 23, 1401-08.

124. Quine DB, Regan D & Murray TJ (1983) Delayed auditory tone perception in multiple sclerosis. *Can J Neurol Sci* 10, 183-86.

125. Beverley KI & Regan D (1983) Texture changes versus size changes as stimuli for motion in depth. *Vision Res* 23, 1387-1400.

126. Kruk R & Regan D (1983) Visual test results compared with flying performance in telemetry-tracked aircraft. *Aviat Space Environ Med* 54, 906-11.

127. Burbeck CA & Regan D (1983) Independence of orientation and size in spatial discriminations. *J Opt Soc Am* 73, 1691-94.

128. Regan D & Beverley KI (1983) Spatial frequency discrimination and detection: comparison of postadaptation thresholds. *J Opt Soc Am* 73, 1684-90.

129. Regan D & Neima D (1983) Low-contrast letter charts as a test of visual function. *Ophthalmology* 90, 1192-1200.

1984

130. Regan D & Beverley KI (1984) Figure-ground segregation by motion contrast and by luminance contrast. *J Opt Soc Am* 1, 433-42.

131. Quine DB, Regan D, Beverley KI & Murray TJ (1984) Patients with multiple sclerosis experience hearing loss specifically for shifts of tone frequency. *Arch Neurol* 41, 506-08.

132. Quine DB, Regan D & Murray TJ (1984) Degraded discrimination between speech-like sounds by patients with multiple sclerosis and Friedreich's ataxia. *Brain* 107, 1113-22.

133. Neima D & Regan D (1984) Pattern visual evoked potentials and spatial vision in retrobulbar neuritis and multiple sclerosis. *Arch Neurol* 41, 198-201.

134. Neima D, LeBlanc R & Regan D (1984) Visual field defects in ocular hypertension and glaucoma. *Arch Ophthalmol* 102, 1042-45.

135. Regan D & Neima D (1984) Visual fatigue and VEPs in multiple sclerosis, glaucoma, ocular hypertension and Parkinson's disease. *J Neurol Neurosurg Psychiat* 47, 673-78.

136. Wilson HR & Regan D (1984) Spatial frequency adaptation and grating discrimination predictions of a line-element model. *J Opt Soc Am* A 1, 1091-96.

137. Regan D & Neima D (1984) Balance between pattern and flicker sensitivities in the visual fields of ophthalmological patients. *Br J Ophthalmol* 68, 310-15.

138. Regan D & Neima D (1984) Low contrast letter charts in early diabetic retinopathy, ocular hypertension, glaucoma and Parkinson's disease. *Br J Ophthalmol* 68, 885-89.

Department of Psychology

UNIVERSITÉ YORK UNIVERSITY

FACULTY OF ARTS

4700 KEELE STREET • NORTH YORK • ONTARIO • CANADA • M3J 1P3

139. Regan D (1984) Visual psychophysical tests in the diagnosis of multiple sclerosis. In CM Poser (Ed), *The diagnosis of multiple sclerosis*. New York: Thieme-Stratton, 64-75.

140. Regan D (1984) Chapters 11 & 12 in E Donchin (Ed), Cognitive psychophysiology. Hillsdale, NJ: Erlbaum, 303-38.

141. Regan D & Beverley KI (1984) Psychophysics of visual flow patterns and motion in depth. In L Spillman & BR Wooten (Eds), *Sensory experience, adaptation and perception*. Hillsdale, NJ: Erlbaum, 215-40.

142. Regan D (1984) Visual factors in flying performance. Proc TARP, NAMRL Monograph 33, 3-10.

143. Regan D, Beverley KI & Macpherson H (1984) Pattern visual evoked potentials in amblyopic children. In RH Nodar & C Barber (Eds) *Evoked potentials II*. Boston: Butterworth, 293-301.

144. Regan D (1984). Spatial vision: VEP evidence for mechanisms tuned to spatial frequency. In RH Nodar & C Barber (Eds) *Evoked potentials II*. Boston: Butterworth, 287-89.

1985

145. Regan D & Beverley KI (1985) Postadaptation orientation discrimination. *J Opt Soc Am* A 2, 147-55.

146. Regan D (1985) Visual flow and direction of locomotion.*Science* 227, 1063-65.

147. Regan D & Beverley KI (1985) Visual responses to vorticity and the neural analysis of optic flow. *J Opt Soc Am* A 2, 280-83.

148. Regan D (1985) Evoked potentials in diagnosis. In M Swash & C Kennard (Eds), *Scientific basis of clinical neurology*. Edinburgh: Churchill Livingstone.

149. Regan D (1985) Masking of spatial frequency discrimination. *J Opt Soc Am* A 2, 1153-59.

150. Regan D (1985) Storage of spatial-frequency information and spatial-frequency discrimination. *J Opt Soc Am* A 2, 619-21.

151. Regan D (1985) Evoked potentials and their application to neuro-ophthalmology. *Neuro-ophthalmology* 5, 73-108.

152. Regan D (1985) New visual sensory tests in neurology and ophthalmology. In A Starr (Ed), *Proc 7th evoked potential workshop*, Univ of California, Irvine (1984). Milan: Amplifon, 101-19.

153. Spekreijse H, Dangelie G, Maier J & Regan D (1985) Flicker and movement constituents of the pattern reversal response. *Vision Res* 25, 1297-1304.

1986

154. Regan D (1986) Visual processing of four kinds of relative motion. *Vision Res* 26, 127-45.

155. Regan D & Price P (1986) Periodicity in orientation discrimination and the unconfounding of visual information. *Vision Res* 26, 1299-1302.

156. Regan D & Spekreijse H (1986) Evoked potentials in vision research: 1961-1985. *Vision Res* 26, 1461-80.

157. Regan D (1986) Form from motion parallax and form from luminance contrast: vernier discrimination. *Spatial Vision* 1, 305-18.

158. Regan D, Collewijn H & Erkelens CJ (1986) Necessary conditions for the perception of motion in depth . *Invest Ophthalmol Vis Sci* 27, 584-97.

159. Regan D, Erkelens CJ & Collewijn H (1986) Visual field defects for vergence eye movements and for

Department of Psychology

UNIVERSITÉ YORK UNIVERSITY

FACULTY OF ARTS

4700 KEELE STREET • NORTH YORK • ONTARIO • CANADA • M3J 1P3

stereomotion perception. *Invest Ophthalmol Vis Sci* 27, 806-19.

160. Regan D & Maxner C (1986) Orientation-dependent loss of contrast sensitivity for pattern and flicker in multiple sclerosis. *Clin Vision Sci* 1, 1-23.

161. Erkelens CJ & Regan D (1986) Human ocular vergence movements induced by changing size and disparity. *J Physiol* 379, 145-69.

162. Collewijn H, Erkelens CJ & Regan D (1986) Absolute and relative disparity: a re-evaluation of their significance in perception and oculomotor control. In E Keller & DS Zee (Eds), *Adaptive processes in visual and oculomotor systems*. Pergamon.

163. Regan D (1986) The eye in ballgames: hitting and catching. *Sport en zien*. Haarlem: De Vrieseborch, pp 7-32.

164. Regan D. , Kaufman, L. and Lincoln, J (1986) Motion in depth and visual acceleration. In KR Boff, L. Kaufman & JP Thomas (Eds) *Handbook of perception and human performance*. New York: Wiley, pp.19-1 to 19-46.

165. Regan D (1986) Binocular vision. In *Encyclopaedia of physics in medicine and biology*. Pergamon, pp 33-4.

1987

166. Regan D & Maxner C (1987) Orientation-selective visual loss in patients with Parkinson's disease. *Brain* 110, 239-71.

167. Regan D & Regan MP (1987) Nonlinearity in human visual responses to two-dimensional patterns and a limitation of Fourier methods. *Vision Res* 27, 2181-83.

168. Regan D (1987) Human visual evoked potentials. In T Picton (Ed), *Human event-related potentials*. Amsterdam: Elsevier, pp 159-243.

169. Regan D (1987) Evoked potentials and color-defined categories. In S Harnad (Ed), *Categorical perception*. New York: Cambridge Univ Press, 443-51.

170. Regan D & Regan MP (1987) Spatial frequency tuning, orientation tuning and spatial discrimination investigated by nonlinear analysis of pattern evoked potentials. In C Barber & T Blum (Eds) *Evoked potentials III*. Stoneham, MA: Butterworths.

171. Morgan MJ & Regan D (1987) Opponent model for line interval discrimination: interval and vernier performance compared. *Vision Res* 27, 107-18.

172. Apkarian P, Tijssen R, Spekreijse H & Regan D (1987) Origin of notches in CSF: optical or neural? *Invest Ophthalmol Vis Sci* 28, 607-12.

173. Regan D & Regan MP (1987) "Dissecting" the visual and auditory pathways by means of the two-input technique. Proc Conf on Electric and Magnetic Activity of the Central Nervous System, Trondheim, Norway. AGARD Conf Proc. 432, 6, 1-9.

174. Regan D & Neima D (1987) Relation between VEP and visual function in lesions of the optic nerve and visual pathway. Proc Conf on Electric and Magnetic Activity of the Central Nervous System, Trondheim, Norway. AGARD Conf. Proc. 432, 38, 1-8.

1988

175. Regan D (1988) Low contrast letter charts and sinewave grating tests in ophthalmological and neurological disorders. *Clin Vision Sci* 2, 235-50.

Department of Psychology

UNIVERSITÉ YORK UNIVERSITY

FACULTY OF ARTS

4700 KEELE STREET • NORTH YORK • ONTARIO • CANADA • M3J 1P3

176. Regan D (1988) Low-contrast visual acuity test for paediatric use. *Can J Ophthalmol* 23, 224-27.

177. Regan D & Regan MP (1988) The transducer characteristic of hair cells in the human ear: a possible objective measure. *Brain Res* 438, 363-65.

178. Regan D & Regan MP (1988) Objective evidence for phase-independent spatial frequency analysis in the human visual pathway. *Vision Res* 28, 187-91.

179. Regan MP & Regan D (1988) A frequency domain technique for characterizing nonlinearities in biological systems. *J Theoret Biol* 133, 293-317.

180. Regan D (1988) Visual sensory loss in patients with Parkinson's disease. In I Bodis-Wollner & M Piccolino (Eds), *Dopaminergic mechanisms in vision*. Neurology & Neurobiology 43. New York: AR Liss, pp 221-26.

1989

181. Hong X & Regan D (1989) Visual field defects for unidirectional and oscillatory motion in depth. *Vision Res* 29, 809-19.

182. Regan D (1989) Orientation discrimination for objects defined by relative motion and objects defined by luminance contrast. *Vision Res* 29, 1389-1400.

183. Regan MP & Regan D (1989) Objective investigation of visual function using a nondestructive zoom-FFT technique for evoked potential analysis. *Can J Neurol Sci* 16, 168-79.

184. Regan D (1989) Magnetic fields generated by the human brain. *Can Res* 22, 11-15.

185. Regan D (1989) To what extent can visual defects caused by multiple sclerosis be understood in terms of parallel processing? In B Cohen (Ed), *Vision and the brain: The organization of the central visual system*. New York: Raven, 317-29.

186. Regan D (1989) Acute spatial discriminations and the unconfounding of visual information. In JJ Kulikowski (Ed), *Seeing contour and colour*, 333-339.

187. Regan MP & Regan D (1989) Evoked potential investigation of nonlinear processing stages in human spatial vision. In JJ Kulikowski (Ed), *Seeing contour and colour*, 513-18.

188. Regan D & Regan MP (1989) Ultra-high resolution analysis of auditory and visual brain responses using zoom-FFT. In SJ Williamson, M Hoke, G Stroink & M Kotani (Eds), *Advances in biomagnetism*. New York: Plenum, 205-07.

189. Regan MP & Regan D (1989) A frequency domain technique for using evoked magnetic fields to test multi-stage models of sensory processing. In SJ Williamson, M Hoke, G Stroink & M Kotani (Eds), *Advances in biomagnetism*. New York: Plenum, 201-04.

1990

190. Regan D & Hong X (1990) Visual acuity for optotypes made visible by relative motion. *Optom & Vision Science* 67, 49-55.

191. Kothe A. & Regan D (1990) The component of gaze selection/control in the development of visual acuity in children. *Optom & Vision Science* 67, 770-778.

192. Kothe AC & Regan D (1990) Crowding depends on contrast. *Optom & Vis Sci* 4, 283-86.

193. Regan D (1990) High and low contrast acuity. *Optom & Vis Sci* 67, 650-53.

Department of Psychology

UNIVERSITÉ YORK UNIVERSITY

FACULTY OF ARTS

4700 KEELE STREET • NORTH YORK • ONTARIO • CANADA • M3J 1P3

194. Regan D, Frisby J, Poggio G, Schor C & Tyler CW (1990) The perception of stereodepth and stereomotion. In L Spillman and JS Werner (Eds), *Neurophysiological foundations of visual perception*. Academic, 317-47.

1991

195. Regan D (1991) Specific tests and specific blindness: keys, locks and parallel processing. Prentice Medal Lecture. *Optom & Vis Sci* 68, 489-512.

196. Regan D & Hamstra S (1991) Shape discrimination for motion-defined and contrast-defined form: Squareness is special. *Perception* 20, 315-36.

197. Regan D, Kothe AC & Sharpe JA (1991) Recognition of motion-defined shapes in patients with multiple sclerosis and optic neuritis. *Brain* 114, 1129-55.

198. Regan D (1991) Do letter charts measure contrast sensitivity? *Clin Vis Science* 6, 401-08.

199. Regan D (1991) A brief review of some of the stimuli and analysis methods used in spatiotemporal vision research. In D Regan (Ed), *Spatial vision*. London: Macmillan, 1-42.

200. Regan D (1991) Spatiotemporal abnormalities of vision in patients with multiple sclerosis. In D Regan (Ed), *Spatial vision*. London: Macmillan, 239-49.

201. Regan D. (1991) Detection and spatial discriminations for objects defined by colour contrast, binocular disparity and motion parallax. In D Regan (Ed), *Spatial vision*. London: Macmillan, 135-78.

202. Bodis-Wollner I & Regan D (1991) Spatiotemporal contrast vision in Parkinson's disease and MPTP treated monkeys: the role of dopamine. In D Regan (Ed), *Spatial vision*. London: Macmillan, 250-60.

203. Regan D (1991) Depth from motion and motion in depth. In D Regan (Ed), *Binocular vision*. London: Macmillan, 37-69.

204 Collewjjn H, Steinman RM, Erkelens CJ & Regan D (1991) Binocular fusion, stereopsis and stereoacuity with a moving head. In D Regan (Ed.) *Binocular vision*. London, Macmillan, 121-36.

205. Regan D & Hong XH (1991) Motion-defined letter reading test. *Opt Soc of Amer Tech Digest*.

206. Regan D (1991) A sensitive method for quantifying functional loss caused by veiling glare in patients and in elderly nonpatients. *Opt Soc of Amer Tech Digest*.

207. Regan D, Hong XH & Hamstra (1991) Visual sensitivity to camouflaged motion-defined objects and the limits of safety in nap-of-the-Earth helicopter navigation. In Proc. Symp. on *Aeromedical Aspects of Vision*, Toronto, 161-66.

208. Regan D (1991) Procedures for establishing low-contrast vision and glare susceptibility standards for pilots and drivers, and the selection of personnel for visual search and surveillance. In Proc. Symp. on *Aeromedical Aspects of Vision*, Toronto, 34-56.

209. Karnavas WJ, Bahill AT and Regan D (1991) Sensitivity analysis of a model for the rising fastball and breaking curveball. *Proc IEEE Syst Man & Cybernet*, Los Angeles.

1992

210. Regan D & Hamstra S (1992) Dissociation of orientation discrimination from form detection for motion-defined bars and luminance-defined bars: effects of dot lifetime and presentation duration. *Vision Res.*,32,1655-1666.

Department of Psychology

UNIVERSITÉ YORK UNIVERSITY

FACULTY OF ARTS

4700 KEELE STREET • NORTH YORK • ONTARIO • CANADA • M3J 1P3

211. Regan D & Hamstra S (1992) Shape discrimination and the judgement of perfect symmetry: dissociation of shape from size. *Vision Res.* 32,1845-1864.

212. Regan D, Hamstra S (1992) Dissociation of discrimination thresholds for time to contact and for rate of angular expansion *Vision Res.*,in press.

213. Regan D, Giaschi D, Sharpe JA & Hong XH (1992) Visual processing of motion-defined form: selective failure in patients with parieto-temporal lesions. *J. Neurosci.*, 12, 2198-2210.

214. Giaschi D, Regan D, Kothe AC, Hong XH & Sharpe JA (1992) Motion-defined letter detection and recognition in patients with multiple sclerosis. *Ann. Neurol.* 31, 621-628.

215. Giaschi D, Regan D, Kraft S & Hong XH (1992) Defective processing of motion in the fellow eye of unilateral amblyopes. *Invest Ophthal. Vis. Sci.*, 33, 2483-2489.

216. Regan D, Giaschi D, Kraft S & Kothe AC (1992) A method for identifying amblyopes whose reduced line acuity is caused by defective selection and/or control of gaze. *Opthalmic & Physiological Optics.* in press.

217. Regan D & Lee BB (1992) A comparison of the human 40 Hz response with the properties of macaque ganglion cells. *Visual Neuroscience*, in press.

218. Regan D (1992) Visual judgements and misjudgements in cricket, and the art of flight. *Perception.* 21, 91-115.

219. Regan D (1992) Nonlinearities in psychophysical models of the processing of spatial form and motion. In R. Pinter (Ed) *Nonlinearities in Visual Processing.* pp 293-307

220. Regan D (1992) Detection and discrimination of motion-defined and luminance-defined two-dimensional form.In L.Harris and M.Jenkins(Eds.)*Spatial Vision in Humans and Robots*,Cambridge Univ.Press.

221. Regan MP & Regan D (1992) A frequency domain method for testing nonlinear multi-neuron models against data. In R. Pinter (Ed) *Nonlinearities in Visual Processing*..pp 265-291

222. Regan.D.(1992) Detection and discrimination of spatial form in patients with eye or visual pathway disorders.Fifth Annual Retina Research Foundation Symposium. *Contrast Sensitivity:From Receptors to Clinic*, M.I.T.Press, In Press.

223. Regan D, Hamstra S & Kaushal S (1992) Visual factors in the avoidance of front-to-rear end highway collisions. *Proc. Human Factors Soc. 36th Annual meeting.*

224. Regan D.(1992) Spatial vision in children and adults: A tribute to Russel Harter *Internat.J.Neurosci.* in press.

Articles Submitted

225. Regan D, Giaschi D & Fresco B (1992) Measurement of glare sensitivity in cataract patients using low-contrast letter charts. *Ophthalmic & Physiological Optics* submitted.

226. Regan D.,Kaiser P.K. & Nakano Y.(1992) Dissociation of chromatic and achromatic processing of spatial form by the titration method. *J. Opt. Soc. Amer.* submitted.

227. Regan D, Giaschi D & Fresco B (1992) Measurement of glare sensitivity in cataract patients using low-contrast letter charts. *Ophthalmic & Physiological Optics* submitted.

228. Giaschi D & Regan D (1991) Spatial discrimination for motion-defined form and for contrast-defined form: dissociated development in children. *J. Exp. Psychol.*, submitted.

229. Giaschi D, Regan D, Kraft S & Kothe AC (1992) Crowding and contrast in amblyopia. *Optom. Vis. Sci.*.

Department of Psychology

UNIVERSITÉ YORK UNIVERSITY

FACULTY OF ARTS

4700 KEELE STREET • NORTH YORK • ONTARIO • CANADA • M3J 1P3

Submitted.

230. Giaschi D, Lang A, Kierens C, Hong XH & Regan D (1992) Motion and contrast processing in the "on" and "off" periods in Parkinson's disease. *J. Neurology, Neurosurgery & Psychiatry*. Submitted..

231. Regan MP & Regan D (1992) Nonlinear terms produced by passing amplitude-modulated sinusoids through Corey & Hudspeth's hair cell transducer function.*Journal of the Acoustical Society of America* submitted

232. Regan D & Hamstra S (1992) Shape discrimination for objects defined by relative motion: effects of presentation duration. *Vision Res* . Submitted.

233. Regan D, Giaschi D, Trope G, Kothe AC & Hong XH (1992) Visual sensitivity to motion-defined letters in patients with primary open angle glaucoma and ocular hypertension. *Invest. Ophthalmol. & Vis. Sci*, submitted.

234. Regan D, Giaschi D, Kothe, A & Hong XH (1992) Detection and discrimination of motion-defined and luminance-defined form in visual pathway disorders. *J. Opt. Soc. Amer*, submitted.

Articles in Preparation

235. Regan D ,Kaushal S (1992) Monocular judgement of the direction of motion in depth. *Vision Res*..in preparation

236. Regan D & He P (1992) Comparison of visual responses to texture-defined form and to luminance-defined form by neuromagnetic recording. *J Neurosci*.,in preparation.

237. Regan D & He P (1992) Comparison of visual responses to colour-defined form and to luminance-defined form by neuromagnetic recording. *J. Physiol*.,in preparation.

238. Regan D.& Hong X.H.(1992) Recognition and detection of texture-defined letters. *Vision Res*. in preparation

239. Regan D & Hong XH (1992) Visual resolution, contour interaction and contrast. *J Opt Soc Amer*. in preparation

240. He P (1992) Magnetic brain responses evoked by pattern, motion and flicker. Electroenceph. Clin. Neurophysiol. in preparation.

241. Regan MP, He P, Hong, XH & Regan D (1992) Neuromagnetic identification of an audio-visual convergence area in the human brain. Exp. Brain Res. in preparation.

Abstracts and Book Reviews

About 150–200 (not listed)

Patents

Regan D & Parr N. "Improvement in paramedical instrumentation" (Joule-Thomson effect cataract surgery probe). U.K. patent application 4964 (1972). Wilkinson Sword Research.

Regan D. "Improvements in paramedical instrumentation" (visual acuity measurement). U.K. patent application 4866 (1972). Accepted in U.K. , U.S.A., Germany, E. Europe, Japan. Wilkinson Sword Research.

Regan D. "Improvements in paramedical instrumentation" (multiple sclerosis diagnosis). U.K. patent application 4865(1972). U.S.A. patent N° 3,837,734; West German Patent N° 2,304,808. Wilkinson Sword Research.

Regan D. "Improvements in signal analysis". U.K. patent application 59921 (1972).

Department of Psychology

UNIVERSITÉ YORK UNIVERSITY

FACULTY OF ARTS

4700 KEELE STREET • NORTH YORK • ONTARIO • CANADA • M3J 1P3

Regan D. "Improved apparatus and methods for optometry" (1972). U.K. patent application 15246/72, 49241/72, 9934/73. U.S.A., E. Europe, W. Germany, U.K. National Research Development Corporation.

Regan D. "Paramedical apparatus and method" (multiple sclerosis diagnosis). U.K. patent application 25,532 (1964). Wilkinson Sword Research.

Regan D & Beverley KI. "Methods and apparatus for measuring hand-eye coordination while tracking a changing-size image". U.S. patent N° 4,325,697 (1982). U.S. Air Force.

Regan D. "Paramedical apparatus and method" (eye test chart). U.K. provisional patent 8521775 (1985).

Department of Psychology

UNIVERSITÉ YORK UNIVERSITY

FACULTY OF ARTS

4700 KEELE STREET • NORTH YORK • ONTARIO • CANADA • M3J 1P3

5 PARTICIPATING PROFESSIONALS, DEGREES AND HONORS

5.1 Participating professionals

D. Regan, Ph.D., D.Sc., F.R.S.C. Professor of Ophthalmology, University of Toronto (Cross Appts. Depts. of Medicine, Biomedical Engineering, and Psychology). Professor of Psychology, York University (Cross Appts. Depts of Biology and Physics). Co-Director, Human Performance in Space Laboratory, Institute for Space & Terrestrial Science.

D. Giaschi, Ph.D.

P. He, Ph.D.

X. H. Hong, Ph.D.

M. P. Regan, Ph.D.

T. Simpson, Ph.D.

S. Hamstra, M.A.

S. Kaushal, B.A.

5.2 Degrees and honors

Awarded to the PI: At the November 1991 Convocation, York University awarded the degree *honoris causa* and title of Distinguished Research Professor. The Prentice Medal of the American Academy of Optometry was awarded at the December 1990 Annual Meeting. Elected a Fellow of the Optical Society of America. Awarded a Killam Senior Fellowship.

6 INTERACTIONS

6.1 Scientific visitors

Professor H. Spekreijse, Director of the Inter-University Eye Institute (I.O.I.) of the Netherlands and Belgium, visited for two weeks in April 1991 to carry out joint research with the PI and Dr. He on visually-evoked magnetic brain responses. By invitation, Dr. He paid a return

Department of Psychology

UNIVERSITÉ YORK UNIVERSITY

FACULTY OF ARTS

4700 KEELE STREET • NORTH YORK • ONTARIO • CANADA • M3J 1P3

visit to the I.O.I. (funded by York University).

Professor J. Victor (Cornell University) visited for two weeks in July 1991 to carry out joint research on magnetic and electrical brain responses to non-Fourier motion with the PI, Dr. He and Dr. M. P. Regan (visit funded by York University and Cornell University).

Professor J. Daugman (Harvard University) visited for one week to carry out joint research on the visual processing of motion (visit funded by York University).

6.2 Meetings organized

Co-organized (with Dr. I. Howard) an international meeting on Spatial Vision at York University, August 1991. This was funded by York University and the Natural Sciences and Engineering Research Council of Canada. The speakers were Drs. Ballard, Bergen, Cavanagh, Daugman, De Valois, Heeger, Hinton, Julesz, Klein, Nakayama, Penland, Poggio, Regan, Richards, Szeliski, Tsotsos, Wilson, Yuille and Zucker. In addition to the invited speakers, there were poster presentations (submitted). About 200 attended.An international meeting on visual flow and stereopsis is planned to be held at York in June 1993.

6.3 Papers presented at meetings, conferences, seminars, etc.

6.3.1 *Formal Lectures*

The Charles F. Prentice Award Lecture. "Specific tests and specific blindnesses: keys, locks and parallel processing".

The Medical Research Council of Canada Lecture. "Selective visual loss in patients and super-sight in athletes: two ends of a continuum".

Distinguished Speaker Series, York University. "Visual processing of motion and form in normally-sighted individuals and in neurological patients".

Association for Research in Vision and Ophthalmology (ARVO) (1991). Regan D, Hamstra S.

Department of Psychology

UNIVERSITÉ YORK UNIVERSITY

FACULTY OF ARTS

4700 KEELE STREET • NORTH YORK • ONTARIO • CANADA • M3J 1P3

"Shape discrimination and the judgement of perfect symmetry," *Invest Ophthalmol Vis Sci* Suppl. 32, 1271.

Association for Research in Vision and Ophthalmology (ARVO) (1991). Hamstra S, Regan D. "Dot lifetime and presentation duration have little effect on orientation discrimination for equally detectable motion-defined and contrast-defined bars," *Invest Ophthal Vis Sci* Suppl. 32, 1270.

Association for Research in Vision and Ophthalmology (ARVO) (1991). Fresco B, Giaschi D, Regan D. "Sensitive measurement of glare susceptibility in cataract patients and nonpatients," *Invest Ophthalmol Vis Sci* Suppl. 32, 1084.

Association for Research in Vision and Ophthalmology (ARVO) (1991). Giaschi D, Regan D, Kothe A, Hong XH, Sharpe J. "Multiple sclerosis can degrade detection and/or discrimination of motion-defined form while sparing motion sensitivity," *Invest Ophthalmol Vis Sci* Supp. 32, 1282.

Air Standardization Coordinating Committee (USA/Canada/Australia/New Zealand/UK) WP61 (1991). Regan D. "Procedures for establishing low-contrast vision and glare susceptibility standards for pilots and drivers, and the selection of personnel for visual search and surveillance".

Air Standardization Coordinating Committee (USA/Canada/Australia/New Zealand/UK) WP61 (1991). Regan D, Hong XH, Hamstra S. "Visual sensitivity to camouflaged motion-defined objects and the limits of safety in nap-of-the-Earth helicopter navigation".

Optical Society of America meeting on Noninvasive Assessment of the Visual System, Santa Fe. (1991). Regan D. "A sensitive method for quantifying functional loss caused by veiling glare in patients and elderly nonpatients".

Optical Society of America meeting on Noninvasive Assessment of the Visual System, Santa Fe. (1991). Regan D, Hong XH. "Motion-defined letter reading test". Invited Demonstration.

Department of Psychology

UNIVERSITÉ YORK UNIVERSITY

FACULTY OF ARTS

4700 KEELE STREET • NORTH YORK • ONTARIO • CANADA • M3J 1P3

International Conference on Spatial Vision in Humans and Robots, York University (1991). Regan D. "Spatial vision for motion-defined form".

International Conference on Spatial Vision in Humans and Robots, York University (1991). Hong XH, Regan D. "Motion blindness for unilateral and oscillatory motion in depth".

IEEE, Los Angeles (1991). Bahill AT, Karnavas WJ, Regan D. "The perceptual illusion of the rising fastball and breaking curveball".

Annual Meeting, American Academy of Optometry (1991). Kothe AC, Regan D, Sharpe J. "A motion-defined letter test to detect visual dysfunction in patients with optic neuritis and MS".

Sixth International Conference on Event Perception and Action, Amsterdam (1991). Regan D, Hamstra S. "Dissociation of time-to-contact (T) and rate of increase of angular size ($d\theta/dt$)".

Sixth International Conference on Event Perception and Action, Amsterdam (1991). Regan D, Hamstra S, Hong XH, Beverley KI, Giaschi D. "Spatial discrimination for motion-defined form".

Fifth Annual Retina Research Symposium, Houston (1992). "Detection and discrimination of spatial form in patients with eye or visual pathway disorders".

Annual Research Day, Department of Ophthalmology, University of Toronto (1992). Regan D, Kraft SP, Giaschi D. "A functional subclassification of amblyopia and implications for patient management".

Annual Research Day, Department of Ophthalmology, University of Toronto (1992). Francis C, Rootman DS, Regan D. "Contrast acuity testing in aphakic pateints with epikeratophakia or contact lens".

Association for Research in Vision and Ophthalmology (ARVO) (1992). He P, Regan D. "Magnetic responses of the brain to texture-defined form: dissociation of responses to form and to texture".

Department of Psychology

UNIVERSITÉ YORK UNIVERSITY

FACULTY OF ARTS

4700 KEELE STREET • NORTH YORK • ONTARIO • CANADA • M3J 1P3

Association for Research in Vision and Ophthalmology (ARVO) (1992). Giaschi D, Regan D, Sharpe J, Hong, XH, Bernstein M. "Visual processing of motion-defined form: selective failure in patients with parieto-temporal lesions".

Association for Research in Vision and Ophthalmology (ARVO) (1992). Regan D, Hamstra, S. "Dissociation of discrimination thresholds for time to contact and for rate of angular expansion".

Association for Research in Vision and Ophthalmology (ARVO) (1992). Hong XH, Giaschi D, Kraft S, Regan D. "Defective processing of motion defined form in the fellow eye of unilateral amblyopes".

Workshop on Functional Imaging, Virginia (1992). Regan D, "The use of MEG and EEG in studying parallel processing in human vision".

International Meeting on Parallel Processing in Vision, Dalhousie University (1992). Regan D, "Psychophysical and electrophysical evidence for parallel processing".

6.3.2 *Seminars*

Massachusetts Institute of Technology (Cognitive Sciences and A.I.). "Spatial vision for motion-defined form". (1991).

Johns Hopkins University (Dept. of Neuroscience). "Processing of shape and motion: human vision and visual physiology". (1991).

Rochester University (Center for Visual Science). "Spatial vision for motion-defined form". (1991).

University of Toronto (Dept. of Biomedical Engineering). "Human vision investigated by functional methods and by magnetic brain recording". (1991).

University of Aston (Dept. of Optometry). "Disorders of motion, form and contrast processing in

Department of Psychology

UNIVERSITÉ YORK UNIVERSITY

FACULTY OF ARTS

4700 KEELE STREET • NORTH YORK • ONTARIO • CANADA • M3J 1P3

patients with amblyopia, glaucoma and multiple sclerosis". (1991).

University of Toronto (Dept. of Psychology). Selective visual loss in patients and super-sight in athletes: opposite ends of a continuum?". (1991).

Dalhousie University (Dept. of Ophthalmology). "Subclassification of amblyopia; assessment of intraocular lenses; vision in multiple sclerosis". (1991).

Dalhousie University (Neurology, Ophthalmology and Pediatrics Residents). "Implications of current research for future clinical practice". (1991).

University of Houston (School of Optometry). "Visual processing of motion-defined form". (1992).

University of Montreal (School of Optometry). "Processing of motion-defined form and luminance-defined form in normals and in patients". (1992).

University of Maryland (Department of Psychology). "Specific tests and specific blindnesses: keys, locks and parallel processing". (1992).

Dalhousie University, Residents in Ophthalmology, Neurology and Pediatrics. "Recent research on amblyopia, cataract and multiple sclerosis". (1992).

University of Otago (Department of Psychology). "Visual processing of form and motion". (1992).

University of Otago (Department of Ophthalmology). "Processing of form and motion in amblyopia and multiple sclerosis". (1992).

University of Auckland (Department of Psychology). "Parallel processing of different kinds of spatial form". (1992).

University of Melbourne (Department of Psychology). "Parallel processing in human vision". (1992).

University of New South Wales (Department of Psychology). "Spatial vision". (1992).

Department of Psychology

UNIVERSITÉ YORK UNIVERSITY

FACULTY OF ARTS

4700 KEELE STREET • NORTH YORK • ONTARIO • CANADA • M3J 1P3

University of Sydney (Department of Psychology). "Seeing objects and judging their trajectories". (1992).

7 STATEMENTS: INFORMATION FOR ATTENTION OF AFOSR PROGRAM MANAGER

Results and techniques that are of immediate selection and operational, or medical relevance are as follows.

7.1 Selection and operational

Our GLARE SUSCEPTIBILITY TEST (Section 3.13 above) is immediately relevant to selection of aircrew for fixed wing and rotary wing vehicles who must fly in high glare (e.g. midday, desert conditions, low sun) and/or low-contrast conditions (e.g. high Arctic).

Our MOTION-DEFINED LETTER TEST (Sections 3.3 & 3.12 and Refs 190, 195, 213) assesses quantitatively intersubject differences in the ability to process relative motion and, in particular, to recognize camouflaged objects defined by relative motion. This ability is presumably important for terrain avoidance and flight safety in nap-of-the-Earth helicopter flight in either naked-eye conditions or when using night vision goggles. This is because many terrain features (e.g. grassy protuberance with grassy surround) and objects (e.g. a tree against a background of trees) are partly camouflaged when hovering, and clearly visible only when moving.

We have developed software for this test that runs on a standard IBM PC or true clone with "Wonder Plus" graphics card. On receipt of a blank floppy disk we will supply the test gratis to vision researchers. The software cites AFOSR sponsorship and instructions for use are supplied. Six copies of the disk are enclosed with this report.

Our technique for measuring discrimination thresholds for (θ/ $\dot{\theta}$) in the absence of other

Department of Psychology

UNIVERSITÉ YORK UNIVERSITY

FACULTY OF ARTS

4700 KEELE STREET • NORTH YORK • ONTARIO • CANADA • M3J 1P3

cues (Section 3.4 above and Ref 216) may help to predict intersubject differences in discriminating TIME TO COLLISION, and these intersubject differences may be important for flying safety (terrain avoidance) in low-level flight in fixed-wing vehicles and nap-of-the-Earth flight in rotary-wing vehicles.

7.2 Medical

Our GLARE SUSCEPTIBILITY TEST assesses the effect of early cataract on visual disability sensitivity. The results are quantitative and expressed in a way that is intuitively simple to relate to performance in specific real-world tasks.

Our MOTION-DEFINED LETTER TEST sensitively picks up visual damage hidden to the Snellen test, contrast sensitivity tests and motion sensitivity tests in the following diseases: ocular hypertension and glaucoma; amblyopia; multiple sclerosis; brain lesions involving a specific region of white matter (Section 3.12 above and Refs 198, 209, 219, 220, 221, 224, 230).